Investigating the Thermosensitivity of Cancer Cell Division Dynamics: Toward Cancer Thermotherapies?

Christopher James Steel

September 2020

A thesis submitted to Lancaster University in fulfilment of the requirements for the degree of Masters by Research.

This thesis is entirely my own work and has not been submitted in full or in part for the award of a higher degree at any other educational institution. No sections of this thesis have been published

Abstract

The application of heat to treat disease can be dated back over 5000 years. Ancient Egyptian papyrus records describe heated instruments being used to cauterise breast tumours. In recent times, hyperthermia range temperatures are increasingly routinely used to treat cancer. Heating tumours alongside conventional therapies and pre-heating aqueous drug suspensions prior to administration are both commonplace in oncology clinics. Despite this, the mechanisms which underpin the efficacy of hyperthermia therapy in cancer treatment remain poorly understood. In particular, the impact of temperature on cancer cell cycle dynamics is under explored. We set out to investigate these mechanisms. We employed time lapse confocal microscopy and fluorescence ubiquitin-based cell cycle indicator expressing cancer cell lines to interrogate the effects of temperature on the cell cycle. To complement our investigation, we utilised the open source cancer genomics platforms cBioPortal and XenaBrowser to explore potential molecular determinants of cancer thermosensitivity. Through tracking the breast cancer cell line MCF-7 we observed hyperthermia to result in increased instances of endoreplication and mitotic catastrophe induced cell death. We also highlight components of the T complex protein ring complex as playing a potential role in testicular cancer. These findings will guide design of future cancer thermosensitivity study and may contribute towards novel adjuvant therapeutic cancer strategies.

Table of Contents

1. Introduction

1.1. Cancer as a disease

1.1.1. The burden of cancer

Cancer is the second leading cause of death globally with an estimated 9.6 million deaths worldwide in 2018 (Ferlay et al., 2019). The high mortality rate, significant morbidity, and complexities involved in the treatment of cancer carry with it an economic burden of £7.6 billion per year in the UK alone (Smith, 2020). These statistics emphasise the need for advancement in our understanding of cancer in order to aid in the development of novel therapeutic avenues to alleviate the diseases economic burden and impact on public health.

1.1.2. The biology of cancer

The developed human body consists of approximately 3.72×10^{13} cells (Bianconi *et al.*, 2013). The vast majority reside either terminally differentiated, or in a dormant state known as quiescence (Potten and Loeffler, 1990). Many cells, however, divide and differentiate in order to facilitate growth and maintain life (Kaneko and Yomo, 1994). Evolution has led to the development of complex multi-layered biochemical signalling networks which transmit information within and between cells in order to regulate a proper balance of proliferation, differentiation, quiescence, and programmed cell death (Sever and Brugge, 2015). It is a dysregulation of these processes which leads to cancer. An imbalance in the complex network of growth and death signals promotes aberrant proliferation. After multiple generations these cells present as a neoplasm; literally a new growth (Hanahan and Weinberg, 2011). Almost every cell type in the body has the capacity to dysregulate cell cycling in this way. Thus, cancer shouldn't be thought of as an individual disease, but rather a family of diseases (Hoadley *et al.*, 2018). To add further complexity, the major genes responsible for oncogenesis, tumour suppressor genes and proto-oncogenes, often differ in their mutational profile between individuals (Muir and Nunney, 2015). This variability in genetic signature can result in vastly different phenotypic profiles between patients whose cancers share the same tissue of origin. This inter-individual heterogeneity leads to complications in designing therapeutic regimens (Kittaneh *et al.*, 2013).

Cells usually proliferate in a highly regulated manner, progressing through defined phases collectively known as the cell cycle (Vermeulen *et al.*, 2003). A disruption in cell cycle regulation can lead to reduced DNA replication fidelity, promoting genomic instability and thus

increasing mutational burden promoting neoplasms to select for new characteristics (Hanahan and Weinberg, 2011). Just as Darwinian evolution dictates for the selection of randomly occurring mutations which confer organismal fitness, cancerous cells select for mutations which confer fitness at the cellular level, promoting proliferation and survival (Little, 2010). For example, once a tumour outgrows its local microenvironment, selection pressure is placed on cells to acquire the capability to break through extracellular matrices and travel through blood and lymphatic vessels in order to inhabit new compartments within the body (Seyfried and Huysentruyt, 2013). This process, known as metastasis, is strongly correlated with poor prognosis due to pathophysiological accumulation of neoplastic cells in multiple sites and subsequent complexities involved in treatment (Riihimäki *et al.*, 2013). Furthermore, the interaction between non-neoplastic cells and cancer cells within the tumour microenvironment play an important role in cancer pathogenesis. For example, it is widely accepted that tumour-associated-macrophages are obligate partners for tumour invasion and metastasis (Condeelis and Pollard, 2006). It is evident that oncogenesis is a complex process involving multiple dysregulated molecular and cellular components; at the centre of the disease however, is aberrant cell cycle regulation (Knox, 2010).

1.2. Cancer and the cell cycle

1.2.1. Cell cycle phases

The cell cycle is primarily characterised by four consecutive phases. In the first phase, G_1, cells undergo increased growth and synthesize the components needed for DNA replication (Donjerkovic and Scott, 2000). Following G_1 cells enter S phase, otherwise known as synthesis phase, where DNA and chromosomes undergo duplication (Bertoli *et al.*, 2013). Subsequently, a further growth phase coined G_2 commences where the cell increases protein synthesis in order to generate the machinery needed for the next phase, mitosis, where the cell divides (see figure 1.1)(Murray, 1993). The phases either side of M phase, where most cells generally reside, are collectively known as interphase (Vorsanova *et al.*, 2010). Cells have evolved a multitude of mechanisms to drive cycling through these defined phases in a highly regulated manner. Signalling networks regulate the cycle ensuring phase directionality and provide checkpoints that act as a surveillance system to monitor the integrity and fidelity of cell cycle events. In cancer these mechanisms go awry, checkpoints become ignored, and the cell cycle is uncontrollably driven (Hanahan and Weinberg, 2011).

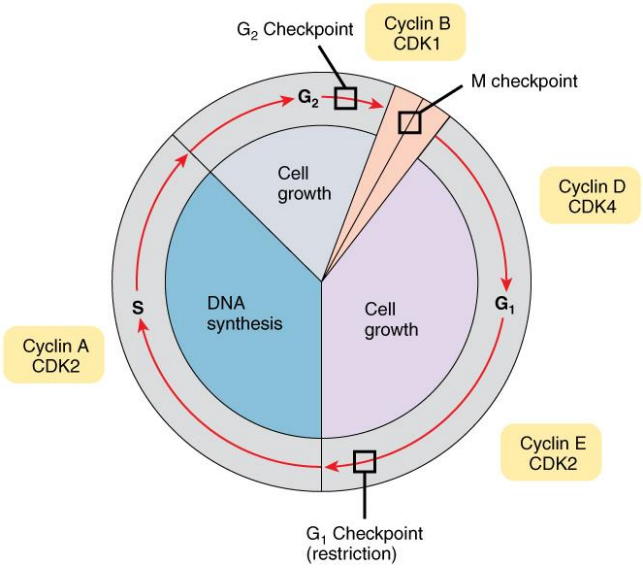

Figure 1. Cell cycle phases. Dividing cells pass through consecutive phases collectively known as the cell cycle. **Growth 1 (G_1)** cells undergo metabolic changes in order prepare the cell for DNA synthesis. **Synthesis phase (S)** refers to the stage in which the cell replicates its chromosomes in preparation for providing progeny with equal genomic material. **Growth 2 (G_2)** phase represents further growth and massive upregulation of protein synthesis in order to generate the machinery needed for cell division. **Mitosis (M)** the cell segregates its chromosomes and divides (Bartee et al., 2017).

1.2.2. DNA damage response checkpoints

It is estimated that the human body suffers tens of thousands of DNA lesions per day (Lindahl and Barnes, 2000). This damage, if not repaired, or repaired incorrectly, can lead to cell heritable mutations which can disrupt cell cycle regulation and promote tumorigenesis. Some lesions arise through physiological processes such as DNA replication base-pair mismatching, and others due to exposure of exogenous toxic substances such as those found in tobacco smoke (Furrukh, 2013; Umar and Kunkel, 1997). To combat these degenerative changes, cells have evolved surveillance mechanisms which scan the genome and halt the cell cycle in order facilitate the repair of damage or signal for the destruction of the cell (Zhou and Elledge, 2000). These mechanisms act to avoid producing progeny with aberrant genetic lesions which may promote dysregulated cycling.

These processes are collectively known as the DNA damage response (DDR). The DDR is active throughout the entirety of the cell cycle and may alter the cycle at any given phase. Individual checkpoints are generally defined by the phase in which is the cell stalled (Houtgraaf *et al.*, 2006). Although distinct molecular pathways have been demonstrated to act at specific phases, DDR proteins are often shared between phase checkpoints (Zhou and Elledge, 2000).

The response can be thought of as consisting of three core components; damage sensors and signal transducers, mediators, and effectors. Sensors act to initiate the signalling response to incorrect DNA structures (McGowan and Russell, 2004). The best understood of these is proliferating cell nuclear antigen (PCNA). PCNA is an essential processing factor in DNA replication and acts as a scaffold for the recruitment of factors needed for base mismatch repair (Umar *et al.*, 1996; Majka and Burgers, 2004). Two master DDR signal transducers are the conserved and related serine/threonine kinases ataxia-telangiectasia mutated (ATM) and ataxia telangiectasia and Rad3-related protein (ATR). Following DNA damage hundreds of proteins are phosphorylated in an ATM or ATR dependent manner (Bensimon *et al.*, 2010). ATM is activated predominantly by DNA double-strand breaks and ATR more generally in response to DNA damage (Maréchal and Zou, 2013). Inherited dysfunctional ATM is responsible for the neurodegenerative syndrome ataxia telangiectasia, which not surprisingly predisposes individuals to a range of cancers (Savitsky *et al.*, 1995). Although there are distinct substrates between the two, there is also a considerable overlap. An important overlapping substrate is the tumour suppressor p53, often referred to as the guardian of the genome (Kim *et al.*, 1999; Toufektchan and Toledo, 2018).

Checkpoint kinase 1 (CHK1) and checkpoint kinase 2 (CHK2), also serine/threonine kinases, act as DDR effectors, phosphorylating downstream targets and halting the cell cycle. In mammals, CHK1 and CHK2 play an important role in all checkpoint DDR signalling pathways. RAD53 and CDS1, CHK2 yeast homologs, respond to replication blocks and DNA damage, whereas yeast CHK1 seems to act only in cell cycle arrest in response to damage (Brown *et al.*, 1999; Matsuoka *et al.*, 1998). CHK1 and CHK2 are activated via phosphorylation and transduced interchangeably by ATM or ATR depending on the specific damage scenario (Liu et al., 2000,p.1; Melchionna et al., 2000). These proteins then go onto mediate cell cycle arrest through phosphorylation and inactivation of proteins involved in driving the cell cycle.

Specific DDR signalling generally depends of the type of DNA damage (Jackson and Bartek, 2009). The G1/S checkpoint can be mediated through the phosphorylation and deactivation of dual specificity phosphatase cell division cycle protein 25A (CDC25A) by CHK1 or CHK2. CDC25A promotes entry past the G1/S transition through the desphosphorylation and activation of cyclin dependent kinase 2 (CDK2)(Hoffmann *et al.*, 1994). Two well understood pathways are known to regulate an intra-S-phase checkpoint. The first, mediated by ATM and ATR, is similar to the G1/S checkpoint, arresting cycle progression through CDC25A inactivation (Sørensen *et al.*, 2003, p.1). The second involves NBS1, the culprit responsible for the chromosomal instability disorder Nijmen Breakage syndrome (NBS) which predisposes individuals to a plethora of cancers. NBS1 in complex with p95 binds to hRAD50 and hMRE11

following their recognition of DNA double strand breakages and signals for p53 dependent cycle arrest (Jongmans *et al.*, 1997). The G2/M checkpoint prevents the cell from entering mitosis. As is the case with previous checkpoints, the specific DNA lesion dictates the signalling pathway activated. ATM/ATR-CHK1/2-CDC25 pathways previously described are activated in response to double strand breaks and lesions which arise from UV damage (Matsuoka *et al.*, 1998; Blasina *et al.*, 1999). An important kinase required specifically for this checkpoint is Wee1, known as the gatekeeper G2/M. CHK1 signals through WEE1 which phosphorylates and inactivates CDK1, a key driver of mitosis (O'Connell *et al.*, 1997). WEE1 is over expressed in many cancers allowing for the repair of otherwise fatal DNA aberrations in the absence of p53, which is commonly dysfunctional in cancer cells. It has been hypothesised that this represents a potential Achilles heel in cancer, with much current interest in WEE1 as a potential therapeutic target (Do *et al.*, 2013; Matheson *et al.*, 2016; Bukhari *et al.*, 2019). These DDR checkpoint signalling pathways have evolved into order to prevent the transmission of aberrant genetic information, therefore, it is little wonder that the dysregulation of these components is associated with cancer.

1.2.3. The restriction point

The point at which cells no longer require growth factor signalling to progress in cycling is the restriction point, or R point, which resides in late G_1 (fig. 1). In cell culture the removal of growth factors prior to the R point will prevent the progression into S-phase (Pardee, 1974). Once past this point, cells are irreversibly committed to DNA synthesis and thus no longer require mitogenic signalling for cell cycle progression. The molecular mechanisms regulating this checkpoint are incompletely understood. However, members of the retinoblastoma (RB) family and associated proteins are indicated to be important regulators which will be discussed further in section 1.2.6 (Chi et al., 2017, p.3; Sage et al., 2000). Naturally, loss of R-point signalling is thought to be critical in cancer, as dysregulation would permit cells to proliferate in the absence of mitogenic signal (DelSal *et al.*, 1996).

1.2.4. Spindle checkpoint

Undoubtably the most visually remarkable phase of the cell cycle is mitosis, the phase in which chromosomes can be observed aligning and segregating under a microscope (Salmon *et al.*, 1994). The spindle checkpoint acts to ensure proper chromosomal alignment before the segregation of chromosomes during anaphase. The mitotic spindle is a complex and dynamic bipolar network of protein filaments which operate as the machinery needed to separate chromosomes during mitosis (Musacchio and Hardwick, 2002). Mitosis can be subdivided into well-defined individual sequential phases; prophase, metaphase (sometimes subdivided into

prometaphase and metaphase), anaphase, and telophase (Walczak *et al.*, 2010). In prophase, chromosomes condense, replicated centrosomes move towards opposite poles, and breakdown of the nuclear envelope initiates. The central alignment of chromosomes takes place in metaphase and prometaphase. In anaphase, sister chromatids separate at the centromere and begin to move apart, and in telophase, the final stage, chromatids have reached poles and individual nuclear envelopes begin to form (See figure 2)(Cooper, 2000b). Finally, the physical separation of cells proceeds, known as cytokinesis.

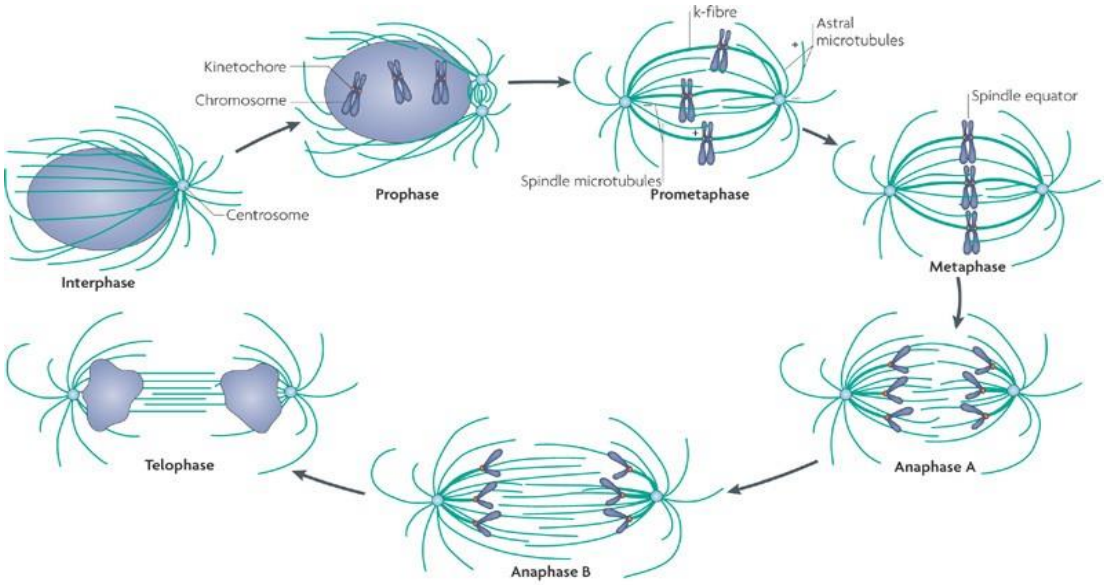

Figure 2. Mitotic phases. During interphase chromatin is mostly decondensed, conversely, in prophase, chromatin becomes highly compact and the nucleolar envelope begins to break down. In prometaphase, the nuclear envelope is fully broken down, allowing bundles of microtubules (K-fibres) to connect the kinetochore of chromosomes to the spindle. Chromosomes are then uniformly oriented along the equator of the cell, defining metaphase. In anaphase A, kinetochore microtubules shorten, pulling chromatids apart towards poles, followed by anaphase B where interpolar and astral microtubules provide force that separates the poles. In the final phase, telophase, the nuclear envelope begins to reform, and chromatin begins to decondense. The cytoplasm and nuclei are then divided into individual daughter cells, constituting cytokinesis (Walczak et al., 2010)**.**

Improper chromosomal segregation during mitosis can promote aneuploidy and genetic instability (Rajagopalan and Lengauer, 2004). Cells therefore must tightly regulate segregation in order to prevent instability. The spindle assembly checkpoint (SAC) consists of machinery which ensures the correct attachment of microtubules to all chromosomes prior to anaphase onset. Chromosomes attach to microtubules via the kinetochore, a proteinaceous platform associated with the centromere, the structure connecting sister chromatids (McKinley and Cheeseman, 2016). The process of microtubule attachment to the

kinetochore during prometaphase is a stochastic process in which microtubules extend and retract until two kinetochores of a sister chromatid pair attach to opposite poles (Cleveland *et al.*, 2003). It is critical that cells ensure segregation of chromosomes ensues only once proper metaphase plate orientation is achieved. The core components of this checkpoint complex, first elucidated in *Schizosaccharomyces pombe,* are Mad, Bub and Cdc20 (Overlack *et al.*, 2014). Importantly, Cdc20 is also a core component of the anaphase promoting complex (APC/C), which when active, targets the destruction of securin (Thornton and Toczyski, 2003). Securin is an inhibitor of separase, which initiates anaphase onset through the cleavage Scc1, a key protein involved in the complex which holds sister chromatids together, cohesin. Fundamentally the checkpoint seems to act through the quenching of the cytoplasmic pool of Cdc20 by unattached kinetochores, thus inhibiting APC/C function and downstream signalling (Yu, 2002; Cleveland *et al.*, 2003). It is inherent that defects in this network sensitise cells to improper chromosomal segregation and genetic instability. Indeed, such components, when defective, have been shown to predispose individuals to cancer and contribute to tumorigenesis (Bharadwaj and Yu, 2004; Ryan *et al.*, 2012; Hanks *et al.*, 2004).

1.2.5. Cytoskeletal changes

The cytoskeleton is a group of filamentous proteins which, (1) organise spatial arrangement within the cell, (2) generate the physical forces which facilitate changes in cell morphology, and, (3) biochemically and physically link the cell to the external environment (Fletcher and Mullins, 2010). This web-like network is a dynamic and adaptive set of structures, constantly rearranging during the lifetime of a cell. Polymers of specific proteins form three main distinct structures. These are microtubules, actin filaments and intermediate filaments (Hohmann and Dehghani, 2019).

Microtubules are stiff tube-like protein filaments made up of αβ-tubulin polymers. These structures function as a network for intracellular transport, support cellular shape, and facilitate the segregation of chromosomes during mitosis (Roostalu and Surrey, 2017). Microtubules are highly active structures, constantly undergoing dynamic polymerisation and depolymerisation (Brouhard and Rice, 2018). This dynamic instability is essential to their function in capturing chromosomes during mitosis (Sacristan *et al.*, 2018). Moreover, the mechanisms which underpin microtubule organisation, and thus mitosis, have been long recognised to display high sensitivity to changes in temperature (Engelborghs *et al.*, 1976; Grzanka *et al.*, 2008). The organisational centre of microtubule assembly during the cell cycle is the centrosome, which consists of two cylindrical centrioles surrounded by a mass of

proteins collectively known as the pericentriolar material (PCM). The PCM is responsible for the de novo formation of microtubules, known as microtubule nucleation (Job *et al.*, 2003). Microtubule nucleation is critical in cell migration, division, maintenance of cell shape, and cilia formation (Job *et al.*, 2003). During S-phase the centrosome duplicates exactly once in preparation for division. As cells enter mitosis, microtubule nucleation initiates from these complexes forming an antiparallel structure which is pushed apart by kinesin motor proteins to form the mitotic spindle (Wordeman, 2010). It's not surprising that these structures are normally tightly regulated, and that aberrant centrosome amplification is often observed cancer. Indeed, work in *drosophila melanogaster* has demonstrated amplification can contribute to tumorigenesis (Basto *et al.*, 2008). On the other hand, whether centrosome amplification is a cause or consequence of cancer in mammals is controversial. It is clear that amplification does cause oncogenic traits such as aneuploidy, invasion, and metastasis (Ganem *et al.*, 2009; Godinho *et al.*, 2014). A recent study from (Levine *et al.*, 2017) provides compelling evidence that centrosome amplification can indeed drive cancer formation in mammals. The study implemented a murine model in which centrosome number could be amplified in the absence of additional genetic alterations and demonstrated the spontaneous development of tumours in multiple tissues.

Intermediate filaments make up the major morphological framework in a cell and undergo drastic reorganisation during the cell cycle. As their name suggests, these diverse cytoskeletal structures are intermediate in their size relative to microtubules and actin filaments. They are encoded by over 65 genes (Herrmann *et al.*, 2002). Mutation in subunit components therefore is generally better tolerated than in microtubules and actin filaments, which consist solely of tubulin and actin, respectively (Klymkowsky, 2019). Moreover, intermediate filaments are not directly involved in cell motility, rather playing a structural role in tissues and cells (Cooper, 2000a). Naturally the breakdown of these foundations is essential during mitosis. An example of such is the deconstruction of the architectural network of the nuclear lamina. The nuclear lamina is a thick fibrous network associated with the nuclear envelope made up of lamin proteins which assemble into V-type intermediate filaments. Nuclear lamina disassembly is triggered by the activation of mitotic kinases such as CDK1 through the direct phosphorylation of lamin filament subunits. This mechanism was eloquently elucidated through *in vitro* catalysis assays and phospho-dead mutants blocking lamina disassembly during mitosis (Heald and McKeon, 1990; Peter *et al.*, 1990).

Actin filaments are the thinnest of the trio and are often crosslinked into complex networks (Blanchoin *et al.*, 2014). These filaments have an extremely diverse array of physiological functions, often involving myosin motor proteins which move along actin filaments in an ATP-

dependent reaction which strikingly resembles walking (Kodera and Ando, 2014). Actin-myosin chemistry generates the mechanical force needed for muscle contraction, vesicle transport, and cytokinesis to just name a few processes. During cytokinesis, the cytoplasm is divided in two by a complex meshwork of these filaments and associated proteins known as the cell cortex (Reichl *et al.*, 2008). Furthermore, the actin filament cytoskeletal network plays a defining role in cell cycle progression past the G1 checkpoint through linking extra cellular matrix (ECM) signal transduction (Forgacs *et al.*, 2004).

Regulation of the cell cycle is tightly linked to the adhesive interactions of cells with the ECM. Integrin transmembrane receptors and proteoglycans mediate this communication at specific lipid raft areas, known as focal adhesions sites, which directly link to the actin cytoskeleton (Burridge *et al.*, 1990). Multiple components of mitogenic signal transduction networks have been demonstrated to directly link to this actin cytoskeleton, prime examples include phospholipase C and phosphatidylinositol kinase (Payrastre *et al.*, 1991). Indeed, pharmacological aberration of actin structure leads to G1 cell cycle arrest in multiple cell types (Huang and Ingber, 2002; Lohez *et al.*, 2003). Furthermore, actin cytoskeletal dynamics are tightly linked with metastasis. The epithelial to mesenchymal transition (EMT) is a tissue remodelling cellular programme initiated during development. During EMT, actin cytoskeleton cell-cell junction linkages in epithelium break down, allowing cells to migrate. Cancer cells hijack this physiological process in order to promote metastasis, in which actin plays a critical role. This is reflected by regular presence of upregulated actin-associated proteins during cancer EMT (Lamouille *et al.*, 2014).

1.2.6. Cyclins and cyclin dependent kinases

The master regulators of eukaryotic cell cycle progression are cyclin dependent serine-threonine kinases. The CDK catalysed phosphorylation of key substrates is central in ensuring major events are correctly orchestrated (Morgan, 1995). CDKs act as information processing nodes which integrate intracellular and extracellular signalling networks (Malumbres and Barbacid, 2009). CDK catalytic capacity requires their regulatory subunits; the cyclins, which are aptly named after their ability to drive cell cycling (Morgan, 1997). CDKs undergo constitutive expression, whereas specific cyclins oscillate at different cell cycle phases to activate their partner CDKs (Wright *et al.*, 2019). Cyclins can be broadly divided into four classes, G_1/S, S, M and G_1 cyclins. G_1 cyclins regulate entry into the cell cycle (Bertoli *et al.*, 2013). The Cyclin E family are expressed at the G_1/S transition, Cyclin A in S phase and G_2 phase, and cyclin B in M phase (fig. 3)(Musgrove, 2006). D type cyclins pay a key role in G_1 phase initiation and are tightly regulated. Activation is complex and can occur at both the

transcriptional and post-transcriptional level (Blagosklonny and Pardee, 2002). Classically, cyclin D1 is transcriptionally activated via the Ras-Raf-MEK-ERK cascade in response to mitogenic signalling (Lavoie *et al.*, 1996). Cyclin D is then available to bind with CDK4/6 and phosphorylate a number of downstream substrates. A key target of this complex is RB, a tumour suppressor commonly dysfunctional in many cancers (Dunn *et al.*, 1988). The evolved complexity of signalling and tight regulation around this node of cell cycle initiation is pertinent given aberrant cell cycle entry promotes oncogenesis (Malumbres and Barbacid, 2009). Further highlighting importance of tight regulation, cyclin D mutation and overexpression is commonly seen in a range of cancers (Musgrove *et al.*, 2011).

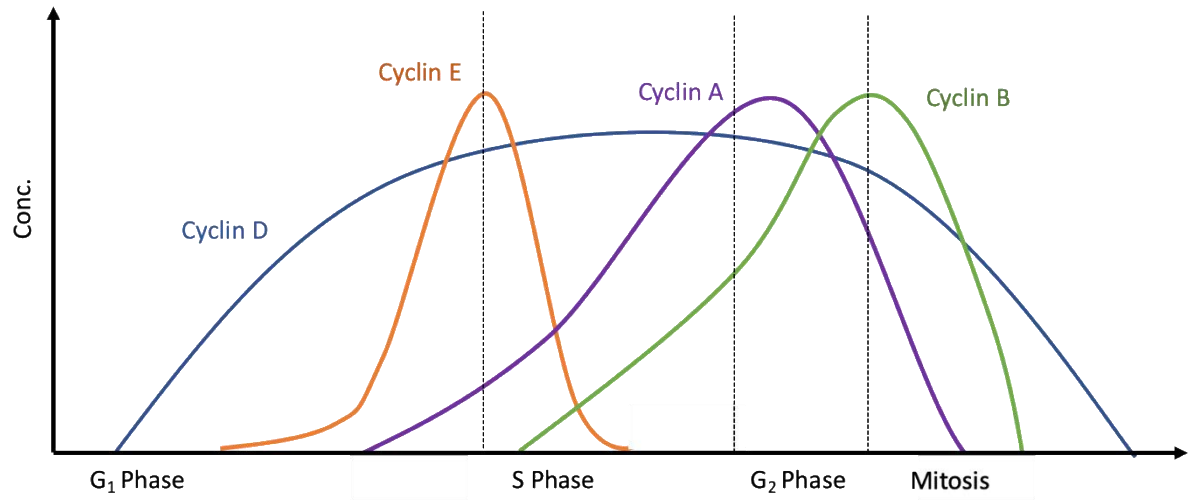

Figure 3. Schematic representation of cyclin concentration over the course of the cell cycle (figure adapted from Morgan and Roberts, 2002).

Provided mitogenic signalling is sustained, CyclinD-CDK4/6 remains catalytically active and phosphorylates RB (Rubin, 2013). In the absence of phosphorylation, RB inhibits E2F, a key transcription factor that upregulates a plethora of genes involved in DNA synthesis and nucleotide metabolism and thus licences cycle progression into S phase (Lundberg and Weinberg, 1998). RB phosphorylation releases E2F, which is then free to bind to its target promoters and upregulate key genes, an important one to note being cyclin E. Once synthesised, cyclin E then binds and activates CDK-2 which phosphorylates a number of substrates, one being RB, thus forming a feedback loop (Rubin, 2013). Sequential phosphorylation of RB by cyclinD-CDK4/6 and cyclinE-CDK-2 is required for complete hyperphosphorylation of RB and cell cycle progression past the restriction point (Lundberg and Weinberg, 1998). Once past the restriction point, the cell is irreversibly committed to DNA replication and cell cycle progression (Blagosklonny and Pardee, 2002). It is no surprise therefore that restriction point signalling components are commonly mutated and dysfunctional in cancer (Malumbres and Barbacid, 2001). In late G_1 phase cyclin A concentration increases

playing essential role in S phase initiation, causing phosphorylation of key DNA replication components by activating CDK2. These levels rise and don't start decline until mid G_2 phase (Erlandsson *et al.*, 2000). Interestingly, cyclin A functions in both S and M phase by associating with functionally distinct CDKs 1 and 2 (Pagano *et al.*, 1992). In G_2 A type cyclins are degraded and cyclin B is actively expressed activating CDK1 which phosphorylates a number of substrates involved in driving M phase processes such as chromosomal condensation and nuclear lamina breakdown (McHugh and Heck, 2003; Gavet and Pines, 2010).

1.2.7. Ubiquitin and the cell cycle

Selective and orderly protein degradation via the ubiquitin-proteasome system ensures correct cell cycle event timing and directionality. Ubiquitin is a small, highly conserved, ubiquitously expressed 76 amino acid protein that post-translationally marks proteins, either as a single ubiquitin moiety or as polyubiquitin chains (Cappadocia and Lima, 2018). Ubiquitination of proteins can mediate cellular localisation, function and stability (Pickart, 2001). Ubiquitin is covalently attached to lysine residues on a target protein and itself contains seven lysine residues, each of which serves as a potential linkage site for ubiquitin chain polymerisation. The linear and branching linkage possibilities provide immense structural diversity for effector protein recognition (Deol *et al.*, 2019). For example, K11 or K48 linkages adopt a compact conformation and usually lead to proteasomal degradation. In contrast, K63/M1 linkages specify a more open configuration and are involved in proteasome-independent functions such as DNA damage repair signalling (Belzile *et al.*, 2010; Metcalf *et al.*, 2014).

The tagging of target proteins with ubiquitin is a highly ordered process orchestrated by the sequential action of three enzymes. The process begins with E1 activating enzymes which activate ubiquitin in an ATP-dependent two-step reaction. E1 forms a thiol ester with the G76 carboxyl of ubiquitin priming the C terminus for nucleophilic attack (Cappadocia and Lima, 2018). E2 conjugating enzyme then transiently carries activated ubiquitin as a thioester and E3 ligase facilitates the addition of ubiquitin to a given substrate, most commonly forming an isopeptide bond between the substrate and ubiquitin (fig. 4)(Pickart, 2001). This process can be repeated, leading to poly-ubiquitylation, although a further novel E4 ubiquitylation factor may be required for certain linkages (Hoppe, 2005). Whilst E1 and E2 are generally involved in activating and carrying ubiquitin, E3 ligases are considered responsible for substrate specificity. Over 600 E3 domain proteins have been characterised in the human genome (Deshaies and Joazeiro, 2009). The majority of which form multi-subunit complexes, facilitating substrate recognition via complexed binding domains, representing a further layer of ubiquitin signalling complexity (Berndsen and Wolberger, 2014).

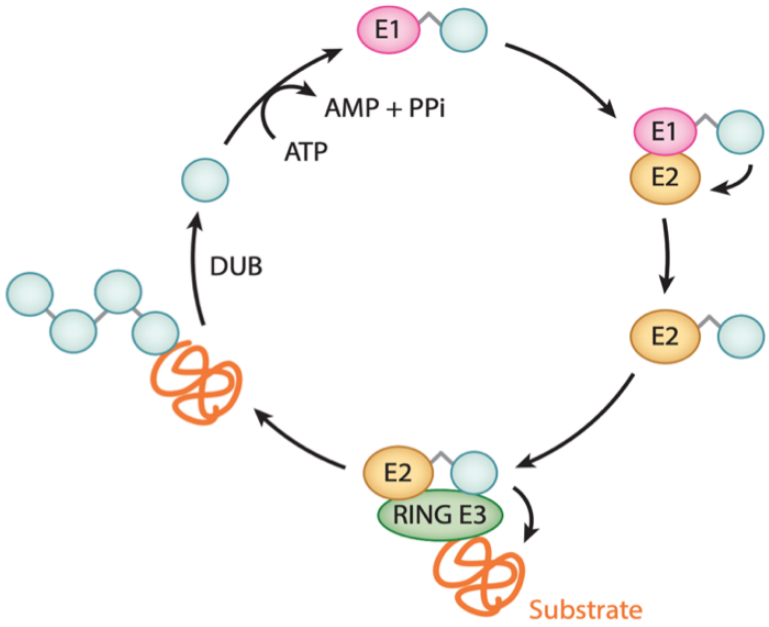

Figure 4. The ubiquitin cycle ubiquitylation is carried out by the sequential action of ubiquitin activating (E1), conjugating (E2) and ligating (E3) enzymes. Ubiquitin can be removed by deubiquitylases (labelled DUB). E3s can be subdivided into categories based on their structure and catalytic chemistry (RING E3 displayed). Blue circles represent ubiquitin (Figure adapted from Borg and Dixit, 2017).

The dysregulation of this system is often seen in cancer. A key example is the overexpression of S-phase kinase associated protein 2 (SKP2). SKP2 is a core component of the SKP1-CUL1-F-box (SCF^{SKP2}) E3 ligase complex involved in the recognition and ubiquitin mediated proteasomal degradation of the G1 phase checkpoint protein p27 (Nakayama and Nakayama, 2005). p27 is essential in G1 cell cycle arrest in response to DNA damage (Cuadrado *et al.*, 2009). It is pertinent therefore that many cancers select for overexpression of this component, promoting proliferation and genomic instability (Harper *et al.*, 2002). SCF plays a central role in cell cycle control signalling. Dynamic interplay between ubiquitylation and phosphorylation form regulatory mechanisms and feedback loops (Swaney *et al.*, 2013). Cyclin D is an example of phosphorylation dependent ubiquitylation directed proteasomal degradation, and contains a so called phosphodegron (O. *et al.*, 2009). DNA damage activates MAP kinases which phosphorylate cyclin D facilitating SCF^{SKP2} recognition and subsequent ubiquitylation and degradation (Santra *et al.*, 2009; Shan *et al.*, 2009). The SCF core complex is in part regulated through variable substrate recognition subunits. SKP2 is the most well understood of these subunits with maximal expression seen at S and G2 phases. In addition to p27, SKP2

targets other related cyclin kinase inhibitors and cyclins, promoting progression through these phases (Nakayama and Nakayama, 2005).

A further important E3 ligase involved cell cycle regulation is the anaphase promoting complex/cyclosome (APC/C). APC consists of ~12 subunits and is regulated through activating subunits cell division cycle protein 20 (CDC20) and APC activator protein CDH1 (CDH1), each conferring diverse substrate specificities (Harper *et al.*, 2002). Shortly before mitosis, CDC20 is phosphorylated by CDK1, which in part facilitates its interaction with the core APC complex (Kramer *et al.*, 2000). Once all chromosomes are successfully attached to the bipolar mitotic spindle, the spindle assembly checkpoint, described earlier, is satisfied and CDC20 binding to APC induces the recognition and ubiquitin mediated degradation of cyclin B and securin thus promoting anaphase. Moreover, activation of APC through CDH1 binding plays a pivotal role in G1 phase cycle progression by maintaining low CDK activity, in addition to, regulating the transition from G1 phase to S phase via the degradation of DNA replication origin regulation factors geminin and CDC6 (Petersen *et al.*, 2000; McGarry and Kirschner, 1998). Both APC activators play significant distinct roles in tumorigenesis. CDC20 is commonly upregulated in cancers and inhibition has been shown to reduce tumour growth (Manchado *et al.*, 2010). Conversely, a reduction in CDH1 expression is common in many cancers suggesting a tumour suppressor role (Fujita *et al.*, 2008b, 2008a).

1.3. Monitoring the cell cycle

In order to investigate cancer cell cycle regulation it is essential to have a means of monitoring cell cycle state (Price *et al.*, 2016). Early studies of cell division involved observing morphological changes of cells, such as chromatin state changes during mitosis, thus limiting phase discrimination to interphase and mitosis (Nurse, 2000). Since then a myriad of techniques has emerged, each with their caveats and nuances (Schorl and Sedivy, 2007). Current monitoring technology can be divided into two categories; snapshot-type approaches and continuous live monitoring methods. Snapshot methods generally require cell synchronisation and/or fixation and provide limited temporal information (Davis *et al.*, 2001). These include techniques which quantify DNA synthesis or content and immunohistochemical staining of cell cycle markers. Although flawed by their inability to monitor live cells, these classic methods are an important spanner in the investigative toolkit. The second category, live cell continuous monitoring methods, allow for the observation of dynamic changes in cell behaviour (Jensen, 2013).

1.3.1. Cell stains

Treating fixed cells with dyes and stains were among the earliest innovations used to analyse cell cycle state. A prominent early example is Feuglen stain (Biesterfeld *et al.*, 2011). In 1924 German physiologist Robert Feulgen developed an assay which would lead to repeated fundamental discoveries in biology over the coming years. The assay used HCl hydrolysis to generate free aldehyde groups in DNA backbones followed by the staining of these groups in a coloured reaction developed over 50 years earlier (Schiff, 1866). This reaction then went on to aid in the establishment of the DNA/chromosome 1:1 relationship, DNA content doubling during mitosis, and provided a basis for early flow cytometry (Reviewed by Chieco and Derenzini, 1999, pp.345–358). Further advancement in cell cycle analysis came following the development of fluorescent DNA-intercalating dyes and deoxyribonucleotide analogs such as Hoechst and bromodeoxyuridine (BrdU) respectively. Hoechst's low toxicity allowed for DNA staining of live cells and the incorporation of BrdU with the DNA of S-phases cells later provided a means of DNA replication temporal quantification through pulse-chase labelling (Humphreys, 2015; Latt, 1974). Shortly thereafter, the development of a BrdU specific antibody resulted in a more efficient means of BrdU incorporation detection (Gratzner *et al.*, 1975). In recent years cell staining's have evolved considerably. There are now vast catalogues of cell-permeable organelle specific fluorescent dyes, allowing one to analyse multiple subcellular structures with live-continuous microscopy methods. Important to note however, that imaging of these molecules can lead to highly cytotoxic breakdown products, thus limiting application (Ettinger and Wittmann, 2014).

1.3.2. Cell counting

Accurately counting the number of cells in a sample is of importance to a diverse array of disciplines. From colony counting microbes in an agar dish, to the quantification of leukocytes in a blood sample, cell counting's applications span the breadth of the life sciences. Furthermore, the quantitative analysis of cell proliferation through cell counting is a corner stone of both cancer biology and pharmacological screening (Romar *et al.*, 2016). Counting cancer cells before and after a perturbation of interest, hypoxic exposure or drug treatment for example, can provide an important and economical initial outlook of the impact of the specific perturbation on proliferation rate (Fujimoto-Ouchi *et al.*, 2007; Morten *et al.*, 2016). The haemocytometer is one of the most rudimentary tools used to count cells. The instrument consists of two glass slides with precise markings which allow the user to manually count the number of cells in a predefined volume of solution under a microscope, thus producing a cell/ml approximation (Absher, 1973). Given its low-cost and ease of use the haemocytometer has earned its place as the cornerstone method of cell counting. Despite it being over 100

years since its invention, one can be found in the draw of practically every cell biologists lab across the globe (Vembadi *et al.*, 2019). This method is relatively low throughput however, thus automated cell counting methods have evolved and become popular in modern life sciences.

There are three main automated cell counting methods used to count cells. These are coulter counting, flow cytometry, and digital imaging combined with automated cell counting (Vembadi *et al.*, 2019). The coulter counter is used most prevalently in clinical haematology (Mei *et al.*, 2012). The device works by individually passing cells through an orifice and measuring electrical impedance. This provides direct information on cell size, and thus is able to discriminate between lymphocytes and erythrocytes. From a cell cycle biologists perspective, Coulter counting has proven useful in investigating changes in mass, volume and density of cells during the cycle (Bryan *et al.*, 2010; Ondracka *et al.*, 2018). The counter is limited in cell cycle biology, however, as is unable to accurately differentiate between cell cycle phases.

In flow cytometry cells are passed individually through an aperture in a similar way to Coulter counting. Although rather than measuring impedance, flow cytometers use laser beams to gather information on cell characteristics (McKinnon, 2018). As a cell passes through the aperture, laser light is scattered and gathered by a detector (Ormerod and Imrie, 1990). In addition to analysing cellular parameters, many cytometry systems also have the capability to physically separate cells based on their optical output, so called fluorescent activated cell sorting (Sergent-Tanguy *et al.*, 2003). Moreover, the multiparametric capabilities of flow cytometry deliver considerable advantages over coulter counting. Moderns systems are able to analyse up to 20 parameters through laser scattering and the excitation/emission of fluorescent probes (Vembadi *et al.*, 2019). In cell cycle investigations Hoechst DNA staining is often used alongside flow cytometry to discriminate between cells in G1 and S/G2 phases (Kim and Sederstrom, 2015). Standard flow cytometry methods are unable to provide dynamic cell cycle phase resolution or visualise cell morphology. However, automated image analysis of real-time confocal microscopy time lapse imaging can over-come such limitations (Ford *et al.*, 2018). As such, this method of counting will be employed in this study.

1.3.3. Fucci

Fluorescence microscopy underwent a resurgence following the purification and characterisation of jelly fish green fluorescent protein (GFP) (Morise *et al.*, 1974). Years later, in 1992, Prasher and colleagues went on to successfully genetically engineer GFP into living cells, demonstrating the transgenic expression of a fluorescent probe for the first time (Prasher

et al., 1992). This advancement blew open the possibilities of fluorescence microscopy by allowing almost any protein to be fluorescently tagged and imaged with fine temporal and submicrometer spatial resolution (Thorn, 2017). Furthermore, through protein engineering, the palette of colours available has expanded to almost any colour imaginable, allowing multiple labels to be imaged simultaneously (Greenwald *et al.*, 2018). Despite this range, certain constraints must be considered when designing an imaging pipeline. When imaging multiple fluorochromes simultaneously, the experiment must be designed to avoid excitation and emission peak spectral overlap, otherwise one fluorochrome may be detected in another's channel (North, 2006). This generally limits scanning laser confocal imaging to 4 colours at once. Although with careful fluorochrome selection and specialist set-ups, 6 colour is possible without the need for deconvolution (Eissing *et al.*, 2014).

Cell cycle biologists took advantage of this capability to fluorescently tag almost any gene and designed the fluorescent ubiquitination-based cell cycle indicator (Fucci). Asako Sakaue-Sawano and colleagues (2008) linked orange fluorescent protein mKO2, and green mAG, to Cdt1 and geminin respectively. As aforementioned, these proteins oscillate reciprocally during the cell cycle due to timed and co-ordinated proteasomal degradation catalysed by E3 ligases SCF and APC (fig. 5A). Geminin levels are highest during S, G2 and M phases, and Cdt1 is highest during G1. Thus, Fucci can accurately and reproducibly discriminate between cells in G1 and S/G2/M phases (See fig 5B) (Sakaue-Sawano *et al.*, 2008).

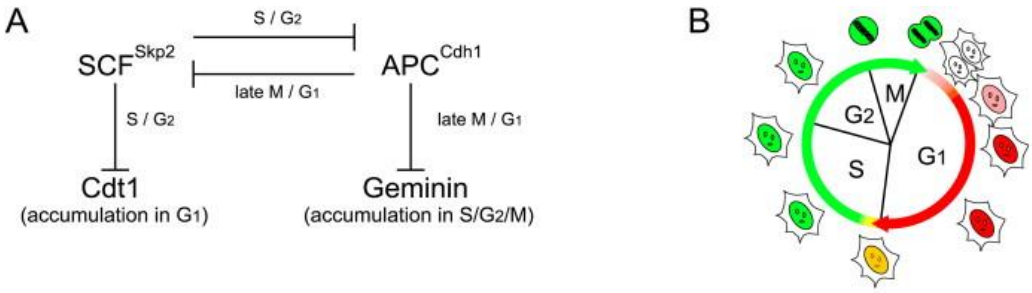

Figure 5. Fucci (a) Cell cycle regulation by oscillating E3 ligases SCF and APC results in Cdt1 and Geminin bistability between G1 and S/G_2/M phases. **(b)** Fluorescent probes label G_1 phase cells in red, and S/G_2/M phase cells in green.

Since its creation, Fucci has been repeatedly modified and upgraded. Notable adaptations include Fucci2, which replaced previous fluorochromes with mCherry and mVenus resulting in better colour contrast (Abe *et al.*, 2013). Fucci2a overcame issues with varied expression between probes by incorporating both into one polycistronic transcript by fusing the *Thosea asigna* virus 2A (T2A) self-cleaving peptide between probes (Mort *et al.*, 2014a). One of the more recent modifications to Fucci involved the redesign of the truncated Cdt1 probe to include

the PIP box motif and exclude Cy motif (fig 6A-B). By modifying Cdt1 in this way the probe is no longer recognised by SCF, but rather by the S-phase specific E3 ligase $CUL4^{Ddb1}$ (fig. 6A) (Sakaue-Sawano *et al.*, 2017). The resultant biosensor, coined Fucci(CA), produces a distinct tri-colour separation of G1, S and G2/M phases (see fig 6C). In this study we intend to modify and extend Fucci(CA) in order to facilitate novel time-lapse confocal cell cycle imaging pipelines. We will do this by incorporating additional fluorochrome linked reporters with Fucci(CA).

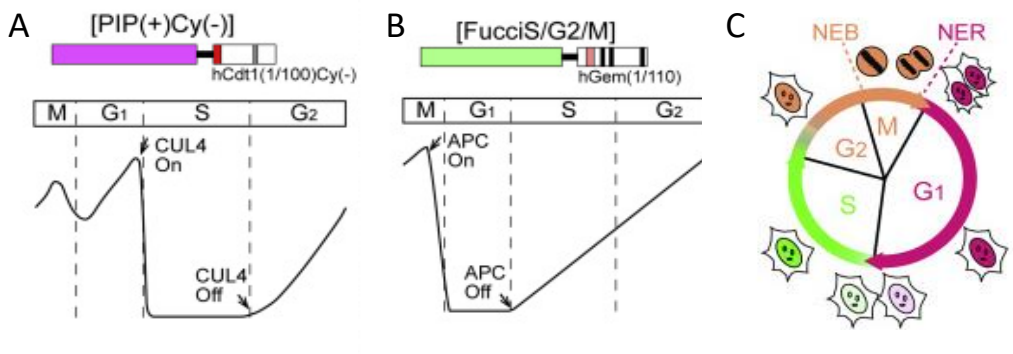

Figure 6. Fucci(CA) (a) CUL4 sensitive hCdt1 probe **(b)** APC sensitive hGeminin probe **(c)** modified probe provides tri-colour G1, S and G2/M phase discrimination.

1.4. Disrupting the cell cycle

Cancer treatment aims to rid the body of cancerous cells through their removal and/or destruction (Huang *et al.*, 2017). The efficacy of surgical removal on its own is limited. Removal of metastases and microscopic disease often present an unworkable surgical challenge and surgery can lead to an increased risk of micrometastatic growth (Tohme *et al.*, 2017). For curative treatment cancer destructive modalities are generally needed. The most prevalent systemic therapeutic strategies involve disrupting the cell proliferation or DNA synthesis thus leading to the destruction of cancer cells (Khanna, 2015).

1.4.1. Chemotherapy

During the 1st world war both sides engaged in the production and experimentation of poisonous gases. One notably effective agent, di-(2-chloroethyl)sulphide, otherwise known as mustard gas, was recognised to cause bone marrow aplasia and gastrointestinal tract aberrations (Brookes, 1990). This cytotoxic activity was later discovered to be due to the agent's DNA alkylating activity (Brookes and Lawley, 1961). This discovery serendipitously provided a basis for chemotherapeutic anti-cancer treatments and gave birth to the era of chemotherapy (Falzone *et al.*, 2018; Gilman, 1963).

Chemotherapeutic agents can broadly be split into two categories; cytotoxic and targeted therapies (Masui *et al.*, 2013). Cytotoxic drugs are the more traditional of the two therapies and generally act through disrupting DNA synthesis or microtubule regulation (Mitchison, 2012). It is thought that cytotoxic chemotherapies cancer killing specificity is due to preferential destruction of rapidly dividing cells (Brunton *et al.*, 2006). This is supported by a myriad of evidence, including the drug's effect on quickly dividing normal cell types, which can result in severe side effects such as alopecia, diarrhoea, vomiting, itchiness and cytopenia to name just a few (Liu *et al.*, 2015). Interestingly however, cytotoxic regimens have been shown to be effective in shrinking tumours with relatively low proliferation rates, contradicting what is understood to be cytotoxic chemotherapies specificity mechanism (reviewed by Mitchison, 2012).

Cytotoxic chemotherapy can further be broadly divided into alkylating agents, antimetabolites, anti-microtubule agents, topoisomerase inhibitors and cytotoxic antibiotics. Alkylating agents are the most common and earliest to be used to treat cancers and generally function by covalently crosslinking strands of DNA in cycling cells resulting in cell death (Ralhan and Kaur, 2007). Antimetabolites are molecules which structurally resemble purine and pyrimidine nucleotide bases and disrupt DNA synthesis by either inhibiting enzymes associated with DNA synthesis, or their incorporation into DNA resulting in dysfunction and cell death (Lind, 2008). Tubulin binding drugs, such as paclitaxel, prevent microtubule assembly or disassembly and thus disrupt chromosome separation and cell division (Weaver, 2014). Topoisomerases ameliorate topological DNA aberrations which occur during transcription, replication, recombination and chromatin remodelling by cleaving and re-joining DNA (Champoux, 2001). These enzymes are often upregulated in cancer and their inhibition can prevent cell cycling (Pommier, 2013). Cytotoxic antibiotics, such as anthracyclines, are thought to induce cell death through multiple mechanisms (Lind, 2008). The second broad category of drugs; targeted therapies, differ from traditional cytotoxic chemotherapy in that they inhibit specific molecular targets in cancer rather than broadly effecting cell division. These therapies include small molecule inhibitors, monoclonal antibodies and immunotherapy (Walter and Ahmed, 2018).

Chemotherapeutic regimens are predominantly designed to include a combination of drugs (Emil Frei and Eder, 2003). A single drug is often not a sufficient treatment due to acquired drug resistance (Pritchard *et al.*, 2012). Combinatorial therapy can be designed to modulate multiple signalling cascades in order to overcome acquired drug resistance and maximise patient response (Hu *et al.*, 2016). Moreover, when administering multiple drugs, the

therapeutic effect can by synergistic, whilst toxicity remain independent, allowing a higher cumulative dose of drug to be administered (Pritchard *et al.*, 2012). The vast catalogue of approved agents combined with neoplastic disease heterogeneity have resulted in chemotherapeutic regimen design becoming somewhat of an art form. Clinicians prescribe a complex variable cocktail of agents of a particular composition depending on tumour classification and a myriad of other clinical parameters (Ibrahim *et al.*, 2012). Despite such innovation and ingenuity systemic chemotherapy practically always leads to concerning side effects (Nurgali *et al.*, 2018). Therefore, there is drive much in the oncological science community to develop novel therapeutic modalities to reduce toxicity (Alexander *et al.*, 2017; Hedigan, 2010).

1.4.2. Radiotherapy

When Wilhelm Conrad Röntgen first discovered X-rays in 1895 the field of radiation oncology was born (Baskar *et al.*, 2012). Very shortly after this discovery the clinical effectiveness of X-rays was demonstrated by the treatment of a patient with breast cancer using radiation (Gianfaldoni *et al.*, 2017). Shortly thereafter, Marie Sklodowska-Curie and husband Pierre Curie discovered radium as a radiation source. The following work on the physiological effects of radium would later award Marie Curie a Nobel prize (Diamantis *et al.*, 2008). Radiation oncology has since developed into a vital wrench in the cancer treatment toolbox. Radiation therapy (RT) is used to treat >50% of cancers and is highly cost effective, incurring just ~5% of total cancer treatment cost (De Ruysscher *et al.*, 2019; Ringborg *et al.*, 2003).

RT functions by applying ionizing radiation to cancer cells in order to destroy them. Ionizing radiation deposits energy in the form of electrically charged particles in the tissues it passes through, damaging DNA, and inducing apoptosis or blocking cell division (Jackson and Bartek, 2009). RT high energy particles are damaging to both normal and cancer cells, however. Thus, the design of RT application aims to maximise the dose at the site of the tumour and minimise normal cell exposure (Baskar *et al.*, 2012). RT is generally administered in one of two ways. The most common method of administration is done by using high energy rays delivered into the body from an external source. Many methods of delivery of this category have been developed in order to maximise the dose to cancer cells and minimise the dose to normal cells. One such approach is intensity-modulated radiation therapy (IMRT). IMRT uses radiation beams from multiple angles focused to a precise point at the tumour. This approach maximises the dose at the tumour, whilst minimal dosage is delivered to the normal tissues, allowing deep tissue tumours to be treated effectively (fig. 7) (Baumann *et al.*, 2016).

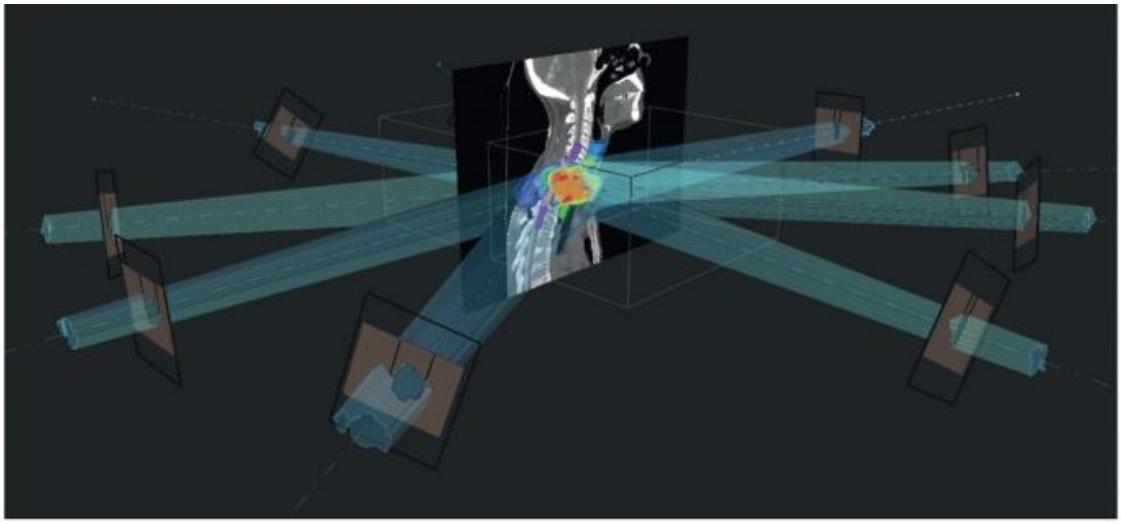

Figure 7. Intensity-modulated radiation therapy (IMRT) functions through the precise focusing of radiation from multiple beams meeting at the site of the tumour (Figure adapted from Baumann et al., 2016).

The second less common mode of administration is brachytherapy, which involves radioactive material being placed inside the body. This modality is predominantly used to treat gynaecological and prostate malignancies (Banerjee and Kamrava, 2014; Porter *et al.*, 1995).

Despite RT's modern technological advancements a substantial proportion of patients experience radiation resistance and cancer reoccurrence (Kim *et al.*, 2015). In radiation resistance, cancer cells adapt and are able to tolerate the molecular changes induced by RT. This process is complex and involves multiple factors and mechanisms (Tang *et al.*, 2018). Furthermore, despite advances in delivery, RT is often associated with toxicity and long-term side effects. Side effects generally depend on the site of administration. These include impairments to bone growth, hair loss, reproductive disorders, gastrointestinal damage, cardiac toxicity and secondary cancer to name a few (Reviewed by De Ruysscher et al., 2019). Thus, there is much interest and effort in the development of novel combinatorial therapies to improve the therapeutic ratio of RT in order to reduce toxicity and side effects (Baskar *et al.*, 2012).

1.4.3. Hyperthermia therapy

Hyperthermia therapy (HT) aims to raise the temperature of a specific tissue, or the whole body, to temperatures usually between 39 and 45 ^{o}C to treat cancer (Behrouzkia *et al.*, 2016). The application of heat to treat disease can be dated back as far as ancient Egypt. Papyrus scroll records describe the use of so called 'fire drills' used to treat breast cancer (Watmough and Ross, 1986). Moreover, records describe medical practitioners in ancient India and China

making use of hyperthermia range temperature treatments to treat tumours (Gas, 2017). In modern medicine, however, HT is predominantly used as an adjunctive and acts to increase the therapeutic ratio of conventional therapy. That is, combining HT with chemo or RT to increase the efficacy of a specific dose and reduce overall toxicity (Horsman and Overgaard, 2007). HT is commonly used in clinic, with a plethora of clinical trial outcomes being reported in recent years (Arjona-Sánchez *et al.*, 2018, 2018; Koole *et al.*, 2020; Ohguri *et al.*, 2018). Despite clinical application, the effect of HT on cancer cell cycle dynamics is poorly understood. Thus, an increased understanding of the parameters involved in HT may aid in the design of novel adjunctive therapeutic regimens.

Clinical application generally falls under three categories, whole body, regional or local (van der Zee, 2002). Whole body HT is used to treat metastatic disease. Treatment of this type typically involves patients being anaesthetised and incubated in a flexible infra-red chamber (Jia and Liu, 2010). In regional HT the goal is to heat a limb or a particular body cavity. Hyperthermic chemoperfusion is a regional therapy that has shown marked success in treating peritoneal metastases. This involves filling the abdominal cavity with pre-heated chemotherapeutic agents (Goodman *et al.*, 2016). Methods used for local therapy aim to specifically heat tumours and can be divided into superficial and deep tissue techniques. Superficial treatments are well developed and generally involve heating through the precise application of a microwave emitting contact medium at the skin surface (Maccarini *et al.*, 2004). Specifically heating a tumour deep within the body is more complicated task. Current methods used in clinic involve applying micro or ultrasound-waves from multiple sources focused to a point at the site of the tumour (Datta *et al.*, 2015). This method has proven limited however, due to heterogeneous heat distribution and difficulties with overheating. Currently there is much interest in the development of magnetic nanoparticles (MNP) as a means of delivering site specific heating (Giustini *et al.*, 2010; Hedayatnasab *et al.*, 2017). This approach aims to target magnetic nanoparticles, which is a key challenge of the approach, to tumour sites and uses an alternating magnetic current to raise the temperature of the particles thus heating the surrounding tumour. An interesting targeting approach to note, which has shown efficacy in animal models, functions through hijacking the propensity of phagocytes to engulf nanoparticles and infiltrate tumours as a novel delivery system (Toraya-Brown *et al.*, 2013).

Despite decades of investigation the effects of HT on tumours is not well understood. Selective tumour cytotoxicity *in vivo* is suggested to be in part to be due to differences between tumour and normal tissue physiology (van der Zee, 2002). Tumour vasculature is chaotic and unevenly distributed, which is attributed to the rate of angiogenesis often falling behind the

growth of rapidly proliferating neoplastic cells (Nagy *et al.*, 2009). Consequently, tumour vasculature displays high resistance, fragility, and reduced blood flow, which leads to areas of tumour deprived of oxygen and glucose (Hanahan and Weinberg, 2011). Many studies have shown that moderate HT (41.5-42.5 ^{o}C) can significantly increase perfusion in tumours, thus increasing pO_2 (reviewed by Song et al., 2001). This reduction in hypoxia is thought to be an important mechanism behind HT's dose lowering effects on RT, given molecular oxygen is a potent radiosensitiser (Rockwell *et al.*, 2009). Moreover, an increase in perfusion may lead to more efficient drug delivery, which is suggested to be partly responsible for HT's additive effects to chemotherapy (van der Zee, 2002).

In addition to these effects described above, HT can stimulate immunological attacks on tumours. The heat shock proteins (HSP) are a group of chaperone proteins that are induced in response to an array of physical and chemical cellular stresses. HSPs aid cell survival through chaperone activity and inhibition of caspase activation (Beere, 2004). The major orchestrater of HSP activation is transcription factor heat shock factor-1 (HSF-1). HSF-1 undergoes constitutive expression and exists sequestered in an inactive state in the cytoplasm of unstressed cells. Once cells are heated, proteins begin to misfold, which signals the activation of HSF-1 through the depletion of the chaperone involved in assembling the HSF-1 inhibitory complex (Shamovsky and Nudler, 2008). HSF-1 is then free to trimerise and upregulate the expression of a plethora of heat shock genes (Voellmy, 1994). In addition to assisting in protein folding, HSP complexes can directly elicit an anti-tumour immune response. Heat stressed tumour cells release heat shock protein 70 (HSP70) in complex with tumour-derived peptides into the extracellular space. These particles are then able to stimulate dendritic cell maturation and activation, which in turn prime and activate tumour specific cytotoxic T lymphocytes (fig. 5) (Frey *et al.*, 2012). Indeed, autologous administration of these tumour derived complexes has been shown to elicit a specific immunological response, thus posing a potential attractive vaccination strategy (Murshid *et al.*, 2011).

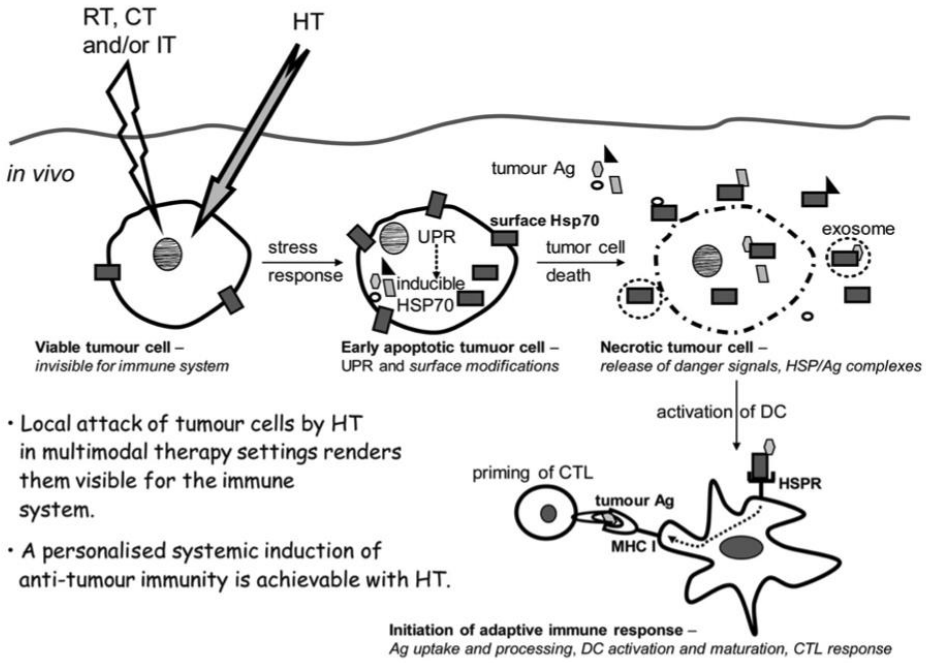

Figure 8. HT renders tumour cells immunogenic. Following hyperthermia treatment, protein aggregation and misfolding induces the unfolded protein response (UPR). In this response, heat shock protein 70 (Hsp70) is upregulated, leading to increased surface Hsp70. In addition, hyperthermia treatment increases intracellular tumour antigen (Ag) levels. Following a second stress signal from conventional therapy for example, tumour cell necrosis is induced, which releases Hsp70/Ag complexes into the extracellular space. Exosomal Hsp70/Ag complexes are also released. The exosome and free Hsp70/Ag complexes activate and attract dendritic cells (DC), which present tumour Ag and induce immunogenicity by priming cytotoxic T lymphocytes (Figure adapted from Frey et al., 2012).

Early studies investigating the basic principles of in vitro hyperthermic cellular death uncovered a dose and time dependent relationship between a range of 41 ^{o}C and 47 ^{o}C. Moreover, the ability of HT to induce cell death is markedly higher ≥ 43 ^{o}C (Hildebrandt and Wust, 2007). A further observation is the tendency of cells to develop a thermotolerance. If cells are cooled to 37 ^{o}C between heat treatments a reduction in cell killing is observed. This adaptation is not inherited, and is thought to be a result of heat shock proteins and other processes regulated through post-translational modification (Ohnishi, 2016). Another pioneering in vitro discovery was the propensity of HT to sensitise tumour cells to RT and chemotherapy. Although incompletely understood, this phenomena is thought to occur due to the inactivation of double-strand break repair machinery (Bolomey *et al.*, 1995; Zhu *et al.*, 2015).

The topic of differences in HT sensitivity between normal cells and cancer cells is one of complexity. The vast majority of studies aim to investigate intrinsic differences in HT sensitivity as an adjunctive with chemotherapy and/or RT. Differences in sensitivity to HT alone are somewhat controversial. Mixed data are available for both the support and contradiction of autonomous cellular sensitivity differences. A review Van der Zee and colleagues (2002) suggested the data point towards there being “no intrinsic differences between hyperthermia sensitivity of normal and tumour cells except for haematological malignancies”. Conversely, a review from Chi-Dug Kang and Sun-Hee Kim(Kang and Kim, 2016)stated “many preclinical and clinical studies have shown that cancer cells are more sensitive to moderate hyperthermia than normal cells”. Interestingly, both reviews lack cited literature to support their statements. Furthermore, Kanwal Ahmed and colleagues (2015) stated in their review of HT apoptosis induction in cancer that generally cancer cells and normal cells bear no intrinsic differences in HT sensitivity. Oddly, the study cited to support this claim contains no relevant data, only data from the analysis of various breast cancer cell lines (Brade *et al.*, 2003).

A recent bioinformatics study boldly states that it has been known for over three decades that tumour cells are significantly more sensitive to mild hyperthermia than normal cells (Amaya *et al.*, 2014). Although similarly, the literature cited to support this understanding contains no supporting data (Habash *et al.*, 2006a, 2006b), only a sweeping statement, cited by another study (Dickson and Calderwood, 1980), which cites an investigation that carried out HT cell survival assays of Chinese hamster ovary (CHO) cells at varying pH concentrations to mimic the acidic environment of tumour cells (Freeman *et al.*, 1977). As CHO cells do not represent true tumour cells this approach carries obvious limitations, thus, drawing a reasonable conclusion on the question of intrinsic differences could be considered unsuitable. A recent study demonstrated that immortalised keratinocytes are significantly more resistant to HT when compared with melanoma cells (Mantso *et al.*, 2018). Although whether this is a characteristic of differences in sensitivity between cell types or neoplasticity remains unanswered. It is clear therefore, that the question of differences in HT sensitivity between neoplastic and non-neoplastic cells is one that is poorly understood and warrants further investigation.

It’s been long recognised that cell cycle compartments vary in their sensitivity to hyperthermia. In the 1970s is was shown that cells in S-phase present a sensitivity to hyperthermia and the treatment therefore induces chromosomal irregularities (Dewey *et al.*, 1971). Cells in M phase display the highest sensitivity to hyperthermia, with M phase cells undergoing microscopically observable aberrant mitotic apparatus formation (Hildebrandt and Wust, 2007), and HT treated lung cancer cells undergo cell death via mitotic catastrophe (Pawlik *et al.*, 2013a).

Furthermore, it has been shown that cancer cells exposed to HT arrest in G2/M phase of the cell cycle, and given a sufficient temperature and treatment duration, will undergo apoptosis in a ATR-Chk1 dependent manner (Furusawa *et al.*, 2012). Further, Amaya and colleagues (2014) found that breast cancers cells, but not mammary epithelial cells, accumulated in G2/M phase following HT treatment. Despite intensive research it is not understood which of the three apoptosis pathways; intrinsic, extrinsic, or the nascently elucidated endoplasmic reticulum intrinsic pathway (Sankari *et al.*, 2012), are activated by hyperthermia (Reviewed by Ahmed et al., 2015).

Differences in cell cycle dynamics in response to HT between cell types are understudied and poorly understood. As mentioned earlier, various aspects of the cytoskeleton, particularly the polymerisation of microtubules and actin, are sensitive to changes in temperature. It was also described how microtubule and actin dynamics are key to cell cycle progression. In particular, the dynamic instability of microtubules is required for chromosome capture and therefore successful progress through mitosis. Moreover, it was detailed how the actin cytoskleleton is involved in the G1/S checkpoint and extensive remodelling of actin is required for mitosis and cytokinesis. We therefore hypothesize that a disruption of cytoskeletal dynamics by heat treatment will lead to cell cycle aberrations in G1/S and mitosis. These aberrations may lead to cancer-specific effects due to cancer cells generally cycling more rapidly, and therefore will be more susceptible to cell-cycle disruption. To investigate, we set out to design novel Fucci based biosensors and engineer them into a range of cell types before exposing these cells to HT relevant temperatures whilst simultaneously carrying out time-lapse confocal microscopy. Such analysis may uncover novel differences in cell cycle compartment sensitivity between cell types. Also, it is possible that the molecular components regulating microtubule and actin dynamics will be dysregulated in cancer cells, which may be responsible for their sensitivity to changes in temperature. In addition, the mitotic regulators previously described to show altered expression in response to HT by Amaya (2014) and colleagues may confer cancer vs normal and cancer type/subtype specific thermosensitivity. We therefore took interest in these mitotic regulators and a number of cytoskeletal associated genes (table 1). To investigate the role of these genes in cancer thermosensitivity we utilised the cancer genomics open platforms cBioPortal and Xenabrowser (Goldman *et al.*, 2020; Cerami *et al.*, 2012). We used these platforms to manipulate cancer genomic data sets in order to explore the expression of these genes in cancer and normal tissues. It is predicted that this analysis may elucidate potential molecular determinants of cancer specific sensitivity to HT. Elucidation of these mechanisms may aid in the design of adjunctive therapeutic cancer specific regimens and is thus of clinical importance.

Table 1. List of genes hypothesised to be involved in cancer specific thermosensitivity..

Genes	Function	Rationale	Refs
KIF11, STAG2, NEK2, CHUK, KPNA4, CENPF, NCAPG	Mitotic regulators	Breast cancer cells treated with HT displayed a reduction in expression of these genes when compared with epithelial control. Reduced function of these genes and their regulators may confer thermosensitivity.	(Amaya *et al.*, 2014)
CFL1, CFL2, DSTN	Actin binding proteins	Cofilin has been shown to thermally stabilise G-actin and stabilise F-actin.	(Levitsky *et al.*, 2008)
RAPH1, EVL	Cytoskeletal remodelling	Promotes actin assembly.	(Hansen and Mullins, 2015)
TCP1, CCT2, CCT3, CCT4, CCT5, CCT6A, CCT6B, CCT7, CCT8	T-complex protein ring complex (TRiC)	Major microtubule stability complex.	(Quintá *et al.*, 2011)

2. Materials and Methods

2.1. Materials

All custom oligo-nucleotide primers and cell culture media were sourced from ThermoFisher (Invitrogen).

All PCR kits and molecular biology reagents were sourced from New England Bio labs. Transfections carried out with Genejuice (Merck) transfection reagent.

Table 2. Oligo-nucleotide sequences used to form poly-linker insertion and primers used for NEB HiFi cloning.

Oligo name	Direction	Sequence 5' to 3'	Tm(°C)
Polylinker	Fwd	CCGGGCAATTGGCCGCCACCATGAC GCGTTCGCGAACCGGTTTCGAATTTA AACTC	-
Polylinker	Rev	GGCCGAGTTTAAATTCGAAACCGGTT CGCGAACGCGTCATGGTGGCGGCCA ATTGC	-
FP1(iRFP670-Qu)	Fwd	CACCACCAACGCTAAAGATCTGACGA GGTGGACTTCCAG	61 (last 24bp)
FP2(iRFP670-Qu)	Fwd	GATCCTGGACAGGCTGGCGGCCGCG ACTCTAGAT	61 (last 18bp)
RP1(iRFP670-Qu)	Rev	AGTCGCGGCCGCCAGCCTGTCCAGG ATCCACAGG	62 (last 22bp)
RP2(iRFP670-Qu)	Rev	TCCACCTCGTCAGATCTTTAGCGTTG GTGGTGGGCG	61 (last 19bp)

2.2. Methods

2.2.1. PCR

All PCR reactions carried out were done so under these conditions outlined in tables 3 and 4 with amplification verification carried out through gel electrophoresis.

Table 3. PCR cycling parameters (Touchdown)

Step	**Temperature (°C)**	**Time (s)**
Phase I (10 cycles)		
Initial denaturation	98	30
Denaturation	98	10
Anneal	Tm + 10	30
Elongate	72	60 (or more dependent on bp)
Phase II (20 cycles)		
Denaturation	98	10
Anneal	Tm - 5	30
Elongate	72	60 (or more dependent on bp)
Final elongation	72	5 mins
Hold	4	

Table 4. PCR reaction components**.**

Component	**Volume (µl)**
Forward primer (10 mM)	2.5
Reverse primer (10 mM)	2.5
Phusion Hot-Start II Flex master mix	25
DMSO	1.5
DNA	1 ng
dH_2O	X

2.2.2. Poly-linker synthesis

Oligomer sequences outlined in table 2 were resuspended in TE buffer according to manufacturer's specifications to produce a concentration of 1 µg/µl. 5 µl of each oligomer, 2.5 µl 5x ligase buffer and 35 µl dH_2O were mixed and incubated at 98 ^oC for 5 minutes in a PCR cycler.

2.2.3. NEB HiFi

PCR Amplified DNA was first treated with DpnI restriction enzyme (as outlined in table 6) to degrade template DNA. PCR amplified fragments were added at specific pmol ratios calculated using the formula (weight in ng) x 1,000 / (base pairs x 650 daltons). For insertions of fragments below 250 bp, a 1:6 vector/insert ratio was used. 10 µl NEB HiFi master mix and dH_2O was added to total 20 µl as outlined in table 5. Mixtures were incubated at 50^oC for 15 mins in a PCR cycler.

Table 5. NEB HiFi reaction components**.**

DNA ratio	**Vector/Insert 1:2**	**vol**
Total fragments	0.12/0.23 pmol	X
NEB HiFI master mix...		10 µl
Water…		Up to 20 µl

2.2.4. Restriction digests

All enzymes and buffers were supplied by NEB labs. Digests were set up dependent on desired enzymes. Constituents were set up and mixed as outlined in table 6 and incubated at 37 ^oC for one hour. Restriction enzymes used for screening, ligations and template degradation were: AgeI, NotI, PmeI, BamHI, SpeI, MluI, NruI, MfeI, DpnI.

Table 6. Restriction enzyme digestion reaction constituents

Component	**Single digest (µl)**	**Double digest (µl)**	**Triple digest**
DNA	2	2	2

Enzyme 1	1	1	1
Enzyme 2	-	1	1
Enzyme 3	-	-	1
Cutsmart 10x	2	2	2
dH_2O	15	14	13

2.2.5. Ligations

Table 7. Ligation reaction components. All ligation reactions were incubated at 4 ºC for 24 hours. Ligase and ligase buffer sourced from NEB labs.

Ligation	**1 (µl)**	**2 (µl)**	**3 (µl)**	**4 (µl)**
Recipient	1	1	1	1
Donor	2	3	4	-
10x T4 buffer	1	1	1	1
T4 ligase	1	1	1	1
dH_20	5	4	3	7

2.2.6. DNA purification

All Purification of PCR products was carried out using Purelink PCR purification kit (ThermoFisher). Manufacturers specifications were followed, expect for the case of elution, in which 30 µl elution buffer was used in order to generate a more concentrated sample. Briefly, 50 µl binding buffer was added to mixture and was loaded into the purification columns and centrifuged at >12,000 g for one minute. Elutant was then discarded and 600 µl wash buffer was added, before another three minutes of centrifugation at the same speed. Elutant was again discarded and 30 µl pre-warmed elution buffer was added to column and centrifuged at 12,000 g for two minutes. DNA concentration was measured using a Nano-drop instrument.

2.2.7. Mini preps

Mini preps were carried out with a ThermoFisher Scientific #K0502 kit according to manufacturer's specifications. Briefly, three ml of LB broth was inoculated with a single bacterial colony using a pipette tip. Cultures were then incubated shaking at 37 ºC for 24 hours. The resultant cultures were then centrifuged at 12,000 G for two minutes, supernatant

removed, and cell pellet resuspended in 250 µl resuspension buffer (Including RNAase A). 250 µl Lysis buffer was then added and incubated at RT for five minutes. 350 µl precipitation buffer was then added and mixed until homogenous before the mixture was centrifuged for 10 minutes at 12,000 G, the supernatant was then further centrifuged in a spin column at the same G for one minute. The flow through was then discarded, and 700 µl wash buffer was added columns then centrifuged for one minute at 12,000 G, flow through discarded and spun again for a further minute. Spin columns then put into a elution tube, 30 µl of TE buffer added to column and spun at 12,000 G for one minute before DNA concentration was determined using a NanoDrop Instrument.

2.2.8. Maxi preps

Maxi preps were carried out with a ThermoFisher PureLink kit with modifications the manufacturer's protocols as follows. A three ml miniprep starter culture was used to inoculate 200 ml of LB and was incubated at 37 ^{o}C shaking for 30 hours. This mixture was then split evenly, to within 0.01 gram, between two Nalgene PPCO 250 ml centrifuge containers and span at 4,000 G for 10 minutes at four degrees Celsius. Supernatant was then removed, and pellet resuspended in 20 ml resuspension buffer. 20 ml lysis buffer was then added and mixture incubated for five minutes at RT. 20 ml precipitation buffer was added and then centrifuged at 4,000 G for one hour at RT. Supernatant was then added to equilibrated column and left to drain for 20 minutes. 60 ml wash buffer then added to the column and left to drain for 30 minutes. Columns then placed in falcon tubes and 15 ml elution buffer added to columns and allowed to drain into falcons. 10.5 ml IPA was then added to elution tube and mixed. Falcons then centrifuged at 4000g for one hour 30 minutes at 4 ^{o}C. Supernatant then removed, and pellet resuspended in five ml 70% ethanol. Mixture was then centrifuged again for 15 minutes at 4,000 G at four degrees Celsius. The supernatant then removed and pellet allowed to air dry before being resuspended in 200 µl TE buffer and DNA quantified using a NanoDrop instrument.

2.2.9. Electrophoresis

All gel electrophoresis was carried out using a 0.5% w/v agarose, TBE (Tris/borate/EDTA) buffer gel with 1:20,000 SYBR safe stain (ThermoFisher) added for band visualisation. Gels were ran for one hour at 100 V using TBE as running buffer. 10x Sigma OG loading buffer was loaded with samples and seven µl of 1 Kb+ DNA fast ladder (ThermoFisher) used for band quantification.

2.2.10. Cell culture

RPMI/Glutamax 1640 was used for all cell lines with 10,000 UI/ml and 10,000 µg/ml Penicillin/streptomycin added. For MCF-7 and Melan-A media 50 ml foetal calf serum (FCS) was added to each bottle (10%). For B16F10, 25 ml (5%) was added. Melan-A media also included 200 µM TPA.

2.2.11. Cell passage

Media was aspirated off before the cells were washed with two ml trypsin (Gibco). This trypsin was then aspirated and one ml fresh trypsin added and cells incubated at 37^{o}C for five minutes to detach cells. Nine ml (complete as described) media was added to the flask and pipetted up and down to help detach cells. This trypsin/cell mixture was then added to a flask with desired ratio to fresh media. For MCF-7 cells this ratio was 1:5 trypsinate/media respectively.

2.2.12. Cell counting

Media was aspirated off before the cells were washed with two ml trypsin (Gibco). This trypsin was then aspirated and one ml fresh trypsin added and cell incubated for five minutes at 37^{o}C. Once cells had visibly detached, nine ml media was added to the cells and pipetted up and down to detach cells. 200 µl of the suspended cells were then added to a haemocytometer. Cells/ml were calculated by counting the number of cells in one large square, five times, and producing an average cell count per large square. The resultant value x10^{4} then produced our cell/ml value.

2.2.13. Transfections

All transfections were carried out with Genejuice (Merck) transfection reagent. Cells were seeded into 6-well plates at appropriate count (240,000 per well for MCF-7s). 24 hours later three µl Genejuice reagent and 100 µl Optimem reduced serum media were mixed and incubated at RT for five minutes. Varying quantities of DNA were then added to this mixture (as outlined in table 8) in order to find optimal molar ratio of PiggyBac and transposase plasmids (hybase) and incubated at RT for 20 minutes. Cell media was then replaced before transfection mixture was added dropwise to cells. 24 hours after cells were then split into 10 cm dishes. After a further 24 hours the appropriate antibiotic selection media was added to the dishes. Transfections were validated through confocal microscopy.

Table 8. Transfection plasmid ratios

Well	Plasmid 1 (ul) PiggyBac-Construct	Plasmid 2 (ul) Transposase (Hybase)
1	0	0
2	2	0
3	2	0.4
4	1	1

2.2.14. Transformations

Five ng plasmid DNA was mixed with 50 µl dH5α chemically competent *E. coli* (ThermoFisher), cells were then incubated on ice for 30 minutes. The cells were then heatshocked for 30 seconds at 42ºC, 950 µl of pre-warmed SOC media was added and then incubated at 37ºC for one hour. The cells were then spread onto LB agar plates containing appropriate antibiotic (100 µg/ml ampicillin or 50 µg/ml kanamycin).

2.2.15. cBioPortal and XenaBrowser

Analysis was carried out using the open source cancer genomics platform cBioPortal (https://www.cbioportal.org/). Genes outlined in table 1 were queried against TCGA Pan Cancer Studies consisting of 10967 samples from 32 studies. Genes were sorted into three catagories, mitotic regulators (KIF11, STAG2, NEK2, CHUK, KPNA4, CENPF, NCAPG), cytoskeletal associated genes (CFL1, CFL2, DSTN, RAPH1, EVL), and T-complex protein ring genes (TCP1, CCT2, CCT3, CCT4, CCT5, CCT6A, CCT6B, CCT7, CCT8). Each category was queried and data analysed independently. For cancer types summary both copy number alterations and mutations tabs were checked. Genes were queried independently for expression analysis between cancer types. For expression cancer specific analysis alteration data was sorted by median. For comparing transcript data the TCGA Pan Cancer Studies aforementioned were loaded into Xenabrowser (https://xenabrowser.net/) and compared with normal tissue expression data through the TCGA TARGET GTEx platform (https://gtexportal.org/home/). Each gene was queried individually in this manner with comparisons drawn between metastatic, primary tumour, normal tissue and solid tissue normal samples.

2.2.16. Confocal imaging and cell counting

Cells were seeded at a density of 50,000 per well in 15 mm diameter 24-well glass bottom imaging plates. Four channels were used during acquisition, excitation and emission wavelengths are listed in table 9. Time intervals used during acquisition varied between experiments. Briefly, for MCF-7 37^{o}C and 41^{o}C runs data was collected in five minutes time intervals and all other imaging was done using 15-minute time points. All images were collected as seven slice Z stacks and maximum intensity projects generated post acquisition. 33 ^{o}C treated lines were imaged at 0.8 zoom and all others at one. Cells in each field of view were counted manually using the Fiji cell counting tool. Percentage change in cell counts were calculated using the following equation where B = cell count at the beginning of treatment and E = cell count at the end of treatment. E/B x 100.

Table 9. Image acquisition fluorophore wavelengths

Fluorophore	Excitation wavelength (λ) (nm)	Emission wavelength (λ) (nm)
mCherry	561	637
mVenus	514	554
CFP	458	521
iRFP670	643	670

2.2.17. Statistics

All statistics were performed using GraphPad Prism version 8.4.3 (471) for Windows, GraphPad Software, San Diego, California USA, www.graphpad.com. Transcriptomic data analysed with One-way ANOVA followed by Dunnett's multiple comparisons test. Cell tracking comparison done through students t-test with normality tested D'Agostino-Pearson test. Standard deviation listed alongside mean values. All data tested to significance level of $P = 0.05$.

3. Results

3.1. Biosensor construction

3.1.1. PiggyBac vector multiple cloning site poly-linker insertion

The PiggyBac transposase system can effectively and stably integrate multiple construct copies into cells without affecting genome integrity. We set out to utilise the system. The current PiggyBac plasmid available to us lacked multiple unique restriction sites. We thus modified our vector through the insertion of a custom multiple cloning site oligonucleotide to facilitate the generation of polycistronic biosensors from multiple construct copies. We built the linker to include multiple unique restriction enzyme cleavage sites (see fig 9A).Our poly-linker was constructed with AgeI and NotI compatible sticky ends for ligation with our PiggyBac vector. We prepared mini-prep cultures transformed with our novel vector and screened the cultures using the restriction enzymes MluI and BamHI. One of six mini prep cultures showed the predicted bands of ~5656 and ~1775 indicating successful ligation (fig. 9B). Figure 9C displays the resultant novel PiggyBac vector with multiple cloning site insert ready to accept biosensor constructs and stably transfect cell lines.

A

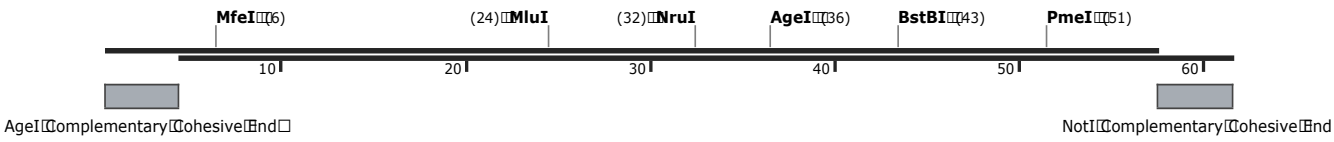

B

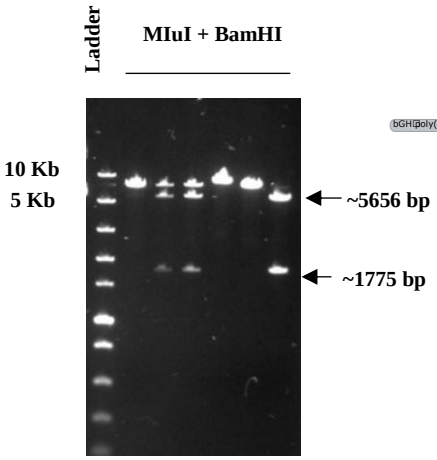

C

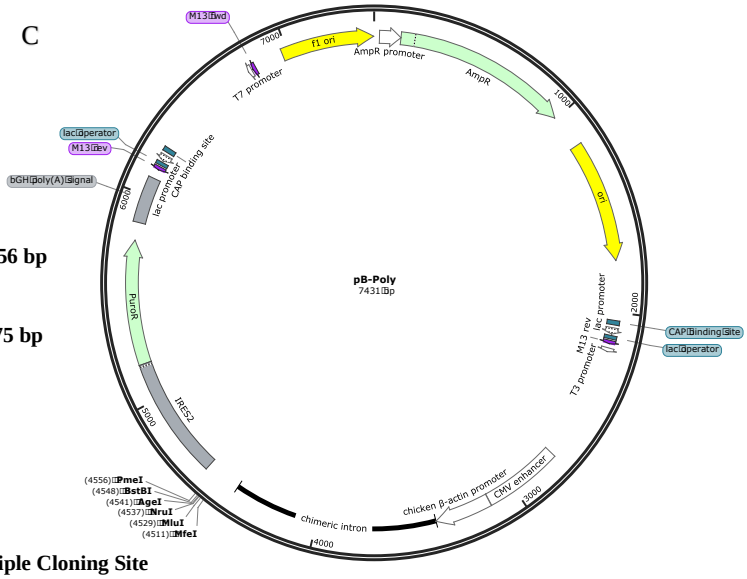

Multiple Cloning Site

Figure 9. PiggyBac vector multiple cloning site insertion. **A)** Schematic of custom double stranded oligonucleotide polylinker sequence with restriction sites and cohesive ends marked. **B)** Gel electrophoresis of poly linker inserted vector MluI and BamHI digestion products. One mini-prep displaying banding pattern of ~5656 and ~1775 confirming successful insertion. **C)** plasmid map of PiggyBac vector displaying inserted multiple cloning site.

3.1.2. H1-Fucci(CA) PiggyBac vector insertion

Fucci(CA) is a cell cycle biosensor with triple colour G1, S and G2 phase discrimination (Sakaue-Sawano *et al.*, 2017). A modified polycistronic Fucci(CA), which includes the H1.0 histone nuclear marker linked to cerulean fluorescent protein (CFP) has previously been constructed in the Mort lab (fig. 10A). To facilitate stable transfection, this construct was inserted into our previously modified PiggyBac vector. This was done via cutting the construct from the vector in which it was housed using MfeI and PmeI restriction enzymes leaving us with the linear construct ready for PiggyBac insertion. To screen for successful insertion, the plasmid was transformed and mini-prepped and triple digested with BamHI, NotI and MluI restriction enzymes. Figure 10B shows the gel electrophoresis banding pattern confirming successful insertion. Our resultant stable expression vector housing the novel cell cycle and nuclear marker biosensor H1-Fucci(CA) is displayed in figure 10C.

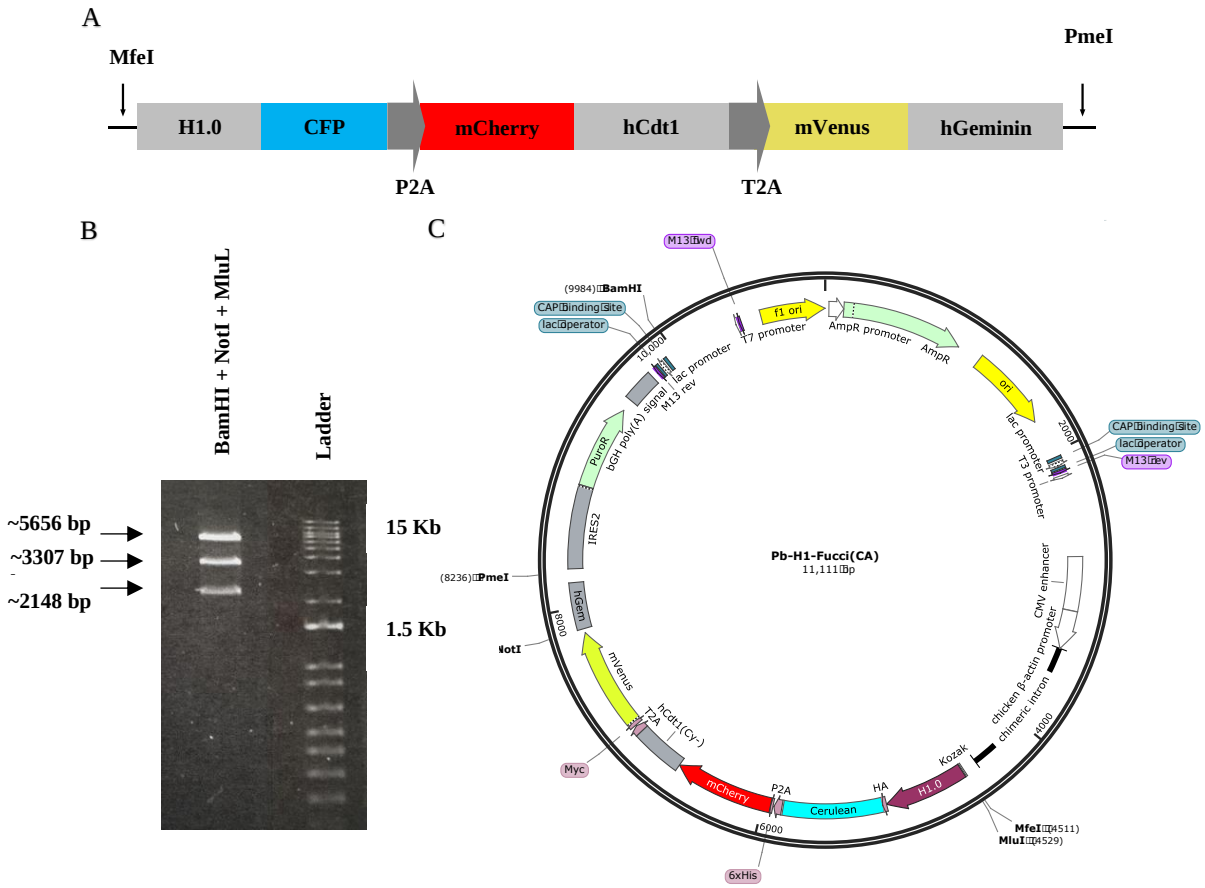

Figure 10. H1-Fucci(CA) PiggyBac vector insertion. A) Schematic of H1-Fucci(CA) biosensor displaying restriction sites used for vector insertion and self-cleaving P2A and T2A sequences **B)** BamHI, NotI and MluI plasmid digestion agarose gel electrophoresis post-cloning displaying expected banding pattern confirming successful insertion. **C)** Plasmid map of Pb-H1-Fucci(CA).

3.1.3. Apoptosis Biosensor Design

Apoptosis is indicated to be a prevalent form of cell death in HT. We therefore set out to extend our H1-Fucci(CA) biosensor by incorporating an apoptosis reporter. Nicholls and colleagues (2011) developed a dark-to-bright GFP apoptosis biosensor. The reporter functions through the linkage of a caspase-7 cleavable recognition site and hydrophobic quenching peptide at the C-terminus of GFP. This peptide quenches GFP fluorescence through disrupting proper chromophore maturation. Once apoptotic caspase cascade is initiated the quenching peptide is cleaved by caspase-7 and GFP is allowed to mature and fluoresce resulting in real time apoptosis monitoring. Our H1-Fucci(CA) biosensor consists of fluorochromes CFP, mCherry, and mVenus. Thus, to facilitate extension of our biosensor and avoid emission and excitation spectral overlap, we set out to utilise the far-red bacterial phytochrome iRFP670 for our apoptosis sensor. We linked this quenching peptide to iRFP670 in order to investigate whether

this would adequately disrupt fluorescence. We used NEBuilder HiFi DNA assembly cloning to insert the quenching peptide at the C-terminus of iRFP670. Primers were designed to amplify the vector and insert with homologous regions to facilitate the HiFi assembly reaction (fig. 11A). Following construction, the vector was transformed, mini-prepped and screened through BamHI digestion. Both our insert and vector contain a single BamHI site (fig. 11C). Agarose gel electrophoresis confirmed successful insertion in all five mini-preps displaying fragments matching the suspected sizes of 4010 and 1052 bp when digested with BamHI (fig. 11B).

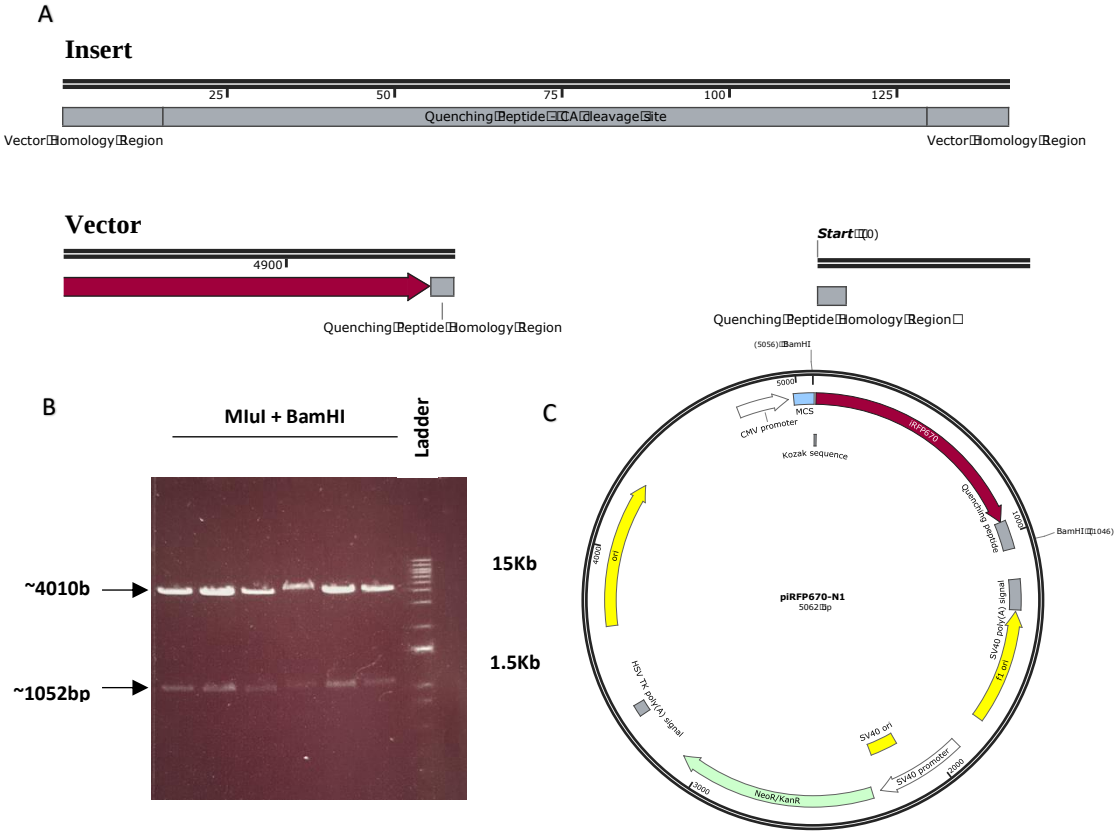

Figure 11. iRFP670 apoptosis biosensor construction. A) PCR amplified linearised iRFP670 vector and quenching peptide insert with extended homologous ends to facilitate HiFi assembly. **B)** BamHI plasmid digestion agarose gel electrophoresis post-cloning displaying expected banding pattern of 4010 and 1052 bp confirming successful insertion. **C)** Plasmid map of iRFP670-quencher apoptosis biosensor.

3.2. Confocal microscopy biosensor validations

3.2.1. MCF-7 H1-Fucci(CA) generation and construct validation

HT is known to be particularly effective in treating breast cancer (Zagar et al., 2010). We therefore set out to use the breast cancer cell line MCF-7 as a model system to investigate thermosensitivity. To determine whether our PiggyBac-H1-Fucci(CA) vector (fig. 10C) functioned as expected we transfected MCF-7 cells with this vector. When imaged, the resultant cells produced stable nuclear (fig. 12D) and phase specific fluorescence (fig. 12B-C), thus validating the expression of our probes and efficiency of our PiggyBac vector system, as well as providing a cellular tool for subsequent cell cycle thermosensitivity investigation.

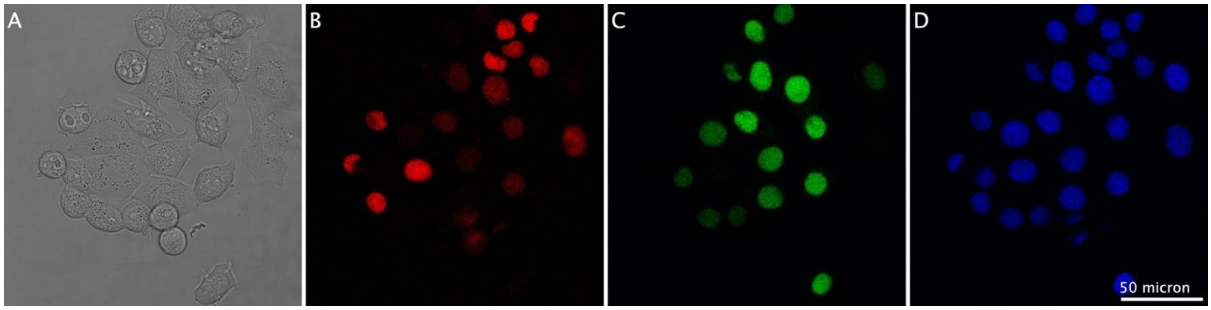

Figure 12. MCF-7 H1-Fucci(CA) (A) Brightfield representation of MCF-7 **(B)** Red channel displaying Cdt-mCherry probe **(C)** Green channel displaying Geminin-mVenus probe (**D)** Blue channel displaying the histone marker H1-CFP. Scale bar 50 µm.

3.2.2. Caspase cleavable quenching peptide fails to disrupt iRFP670 fluorescence

To investigate iRFP670 dark to bright apoptosis biosensor suitability we transiently transfected MCF-7 cells with our iRFP670-Quenching peptide construct (fig. 11C). In addition, we transfected MCF-7 cells with a iRFP670 construct which lacked the quenching peptide in parallel as a negative control. Confocal microscopy indicated the quenching peptide was insufficient in disrupting fluorescence through observable fluorescence in iRFP670 quenching peptide transfected cells (fig. 13A). Thus, the peptide's quenching capacity likely specifically impacts GFP chromophore structure.

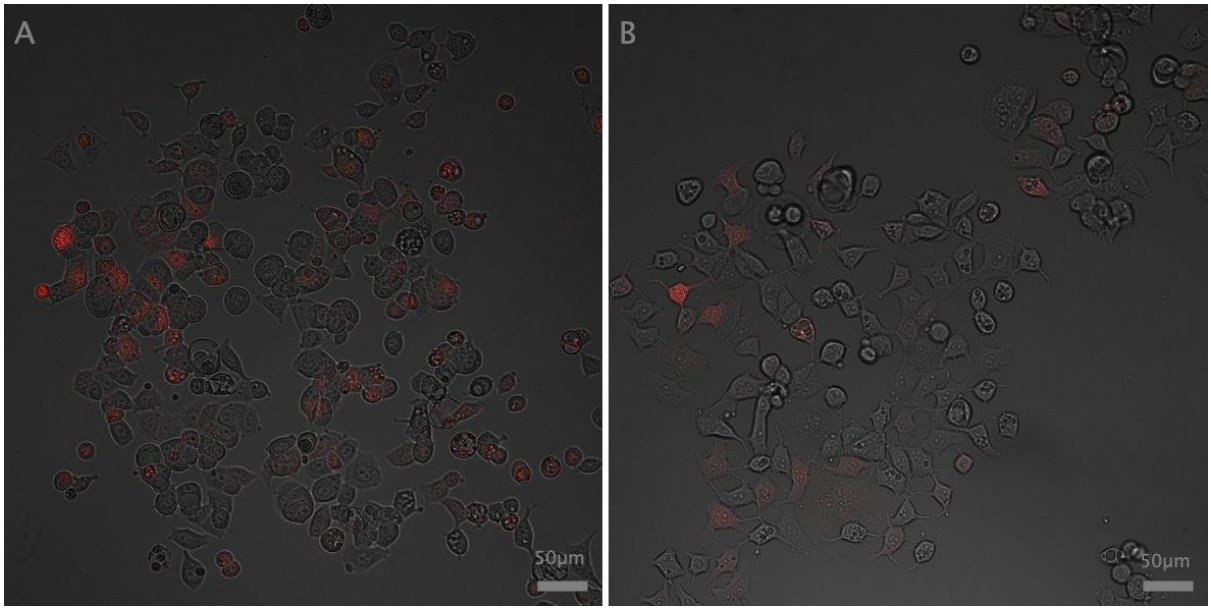

Figure 13. MCF-7 expressing iRFP670-quencher and iRFP670 control A) MCF-7 expressing iRFP670-quencher construct showing fluorescence indicating inefficient quenching. **B)** MCF-7 negative control expressing unmodified iRFP670. Scale bar 50 µm.

3.3. Time lapse confocal microscopy

3.3.1. MCF-7 41 ºC incubation leads to reduced proliferation, endoreplication, and cell death via mitotic catastrophe

Breast cancer is a particular malignancy that is known to respond to HT (Zagar *et al.*, 2010). We therefore set out to investigate the impact of a range of temperatures on the growth and cell cycle phase dynamics of the breast cancer cell line MCF-7. It was intended that we would investigate thermosensitivity by utilising our previously constructed biosensor (fig. 10C) and novel MCF-7-H1-Fucci(CA) cell line (Fig. 12). We were unfortunately limited due to the forced closing of our lab during the coronavirus outbreak. Due to this reduced lab time we were unable to expand individual clones of our MCF-7-H1-Fucci(CA) cell line. Additionally, it was intended that we would transfect a immortalised breast epithelial cell line with our PiggyBac-H1-Fucci(CA) vector (fig. 10C) to act as a normal tissue control for investigating cancer specific thermosensitivity. Due to constrained lab time this was also unfortunately not possible.

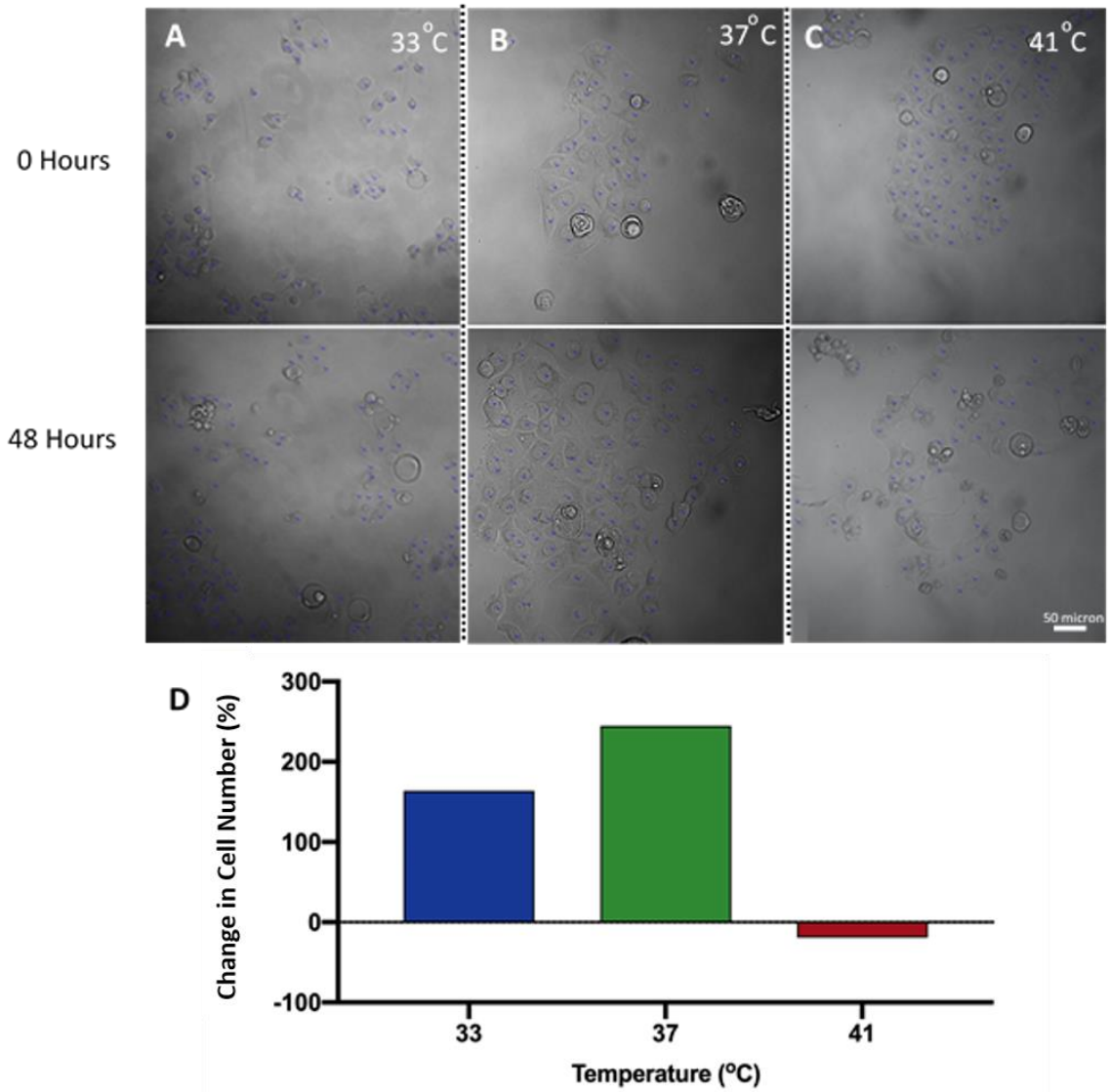

Figure 14 MCF-7 cells decrease in plate number when incubated at 41 °C. *Cells were incubated for 48 hours at 33 °C, 37 °C and 41 °C and imaged. Cell count was quantified by manually counting cells at T=0 and T=48 hours. Percentage change in cell count over time was calculated using the following equation, where B = cell count at the beginning of treatment and E = cell count at the end of treatment. E/B x 100* ***(A-C)*** *Imaging of MCF-7 at varying temperatures including cell counting overlay* ***(D)*** *Percentage change in cell count between* zero *and 48 hours display*ing *an increase of 164% at 33°C, 245% at 37 °C and a decrease of 19% at 41 °C. Scale bar 50 µm.*

As an alternative we utilised a previously constructed MCF-7-Fucci2a cell line for thermosensitivity confocal imaging. Fucci2a functions similarly to Fucci(CA) although is unable to sharply discriminate S phase (Mort *et al.*, 2014b). Cells were plated and incubated at either 33 °C, 37 °C or 41 °C for 48 hours whilst live time-lapse confocal microscopy was simultaneously carried out. For an initial outlook on the impact of these different temperatures on the proliferation of MCF-7 we measured cell count at T=0 and T=48 hours by using the

ImageJ cell counting tool (fig. 14 A-C). As expected, the 37 ºC treatment displayed the largest increase in cell count, showing a 245% increase in cell count at T=48 relative to T=0 (fig. 14D). An increase was also observed at 33 ºC, with cells showing a percentage change increase of 164% (fig. 14D). These data confirm cells grown at 33 ºC demonstrate a reduced replicative capacity when compared with 37 ºC incubation. In contrast, the cells treated at 41 ºC showed a reduction in cell count of 19%. Thus, the hyperthermic range temperature of 41 ºC retards cell viability of MCF-7. We next looked to investigate dynamic cell cycle phase alterations between temperature treatments.

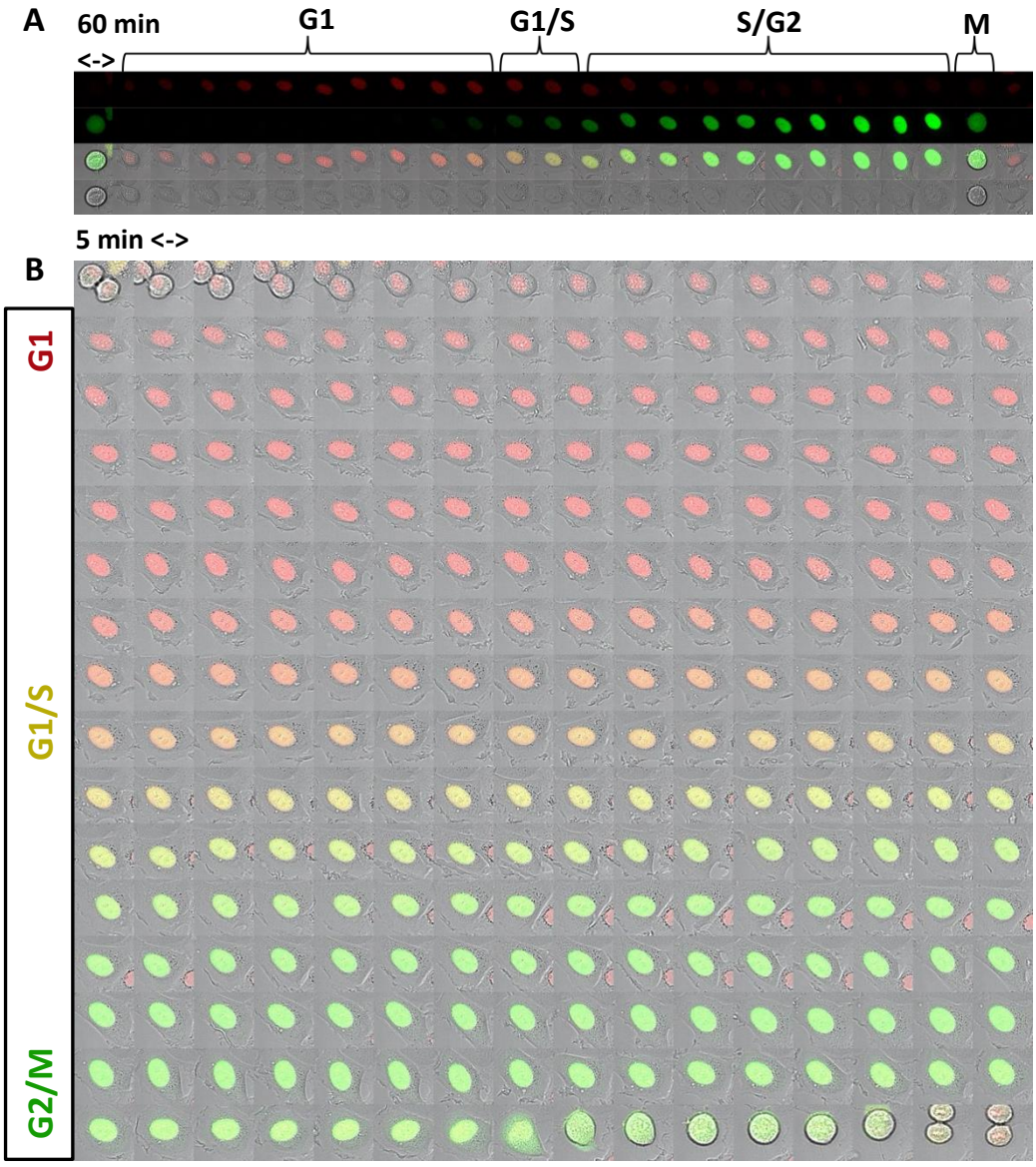

Figure 15. MCF-7 Fucci2a full cell cycle montages displaying phase specific fluorescence (A) Brightfield, red, green and merge montages of full cell cycle from mitosis to mitosis at one hour time points. **(B)** Merge channel montage displaying five minute time point intervals of a complete cell cycle. Scale bar 50 µm.

To demonstrate the cell cycle phase reporting capacity of our MCF-7-Fucci2a cell line we have constructed an individual time step montage of a full cell cycle at 37 ºC. Figure 15A shows a full cell cycle at 1-hour time points and 15B displays individual 5-minute time points of MCF-7 cycling. Both display mCherry (red) G1 fluorescence, mVenus (green) S/G2/M fluorescence, and a brief period of yellow fluorescence due to the presence of both probes conferring G1/S phase.

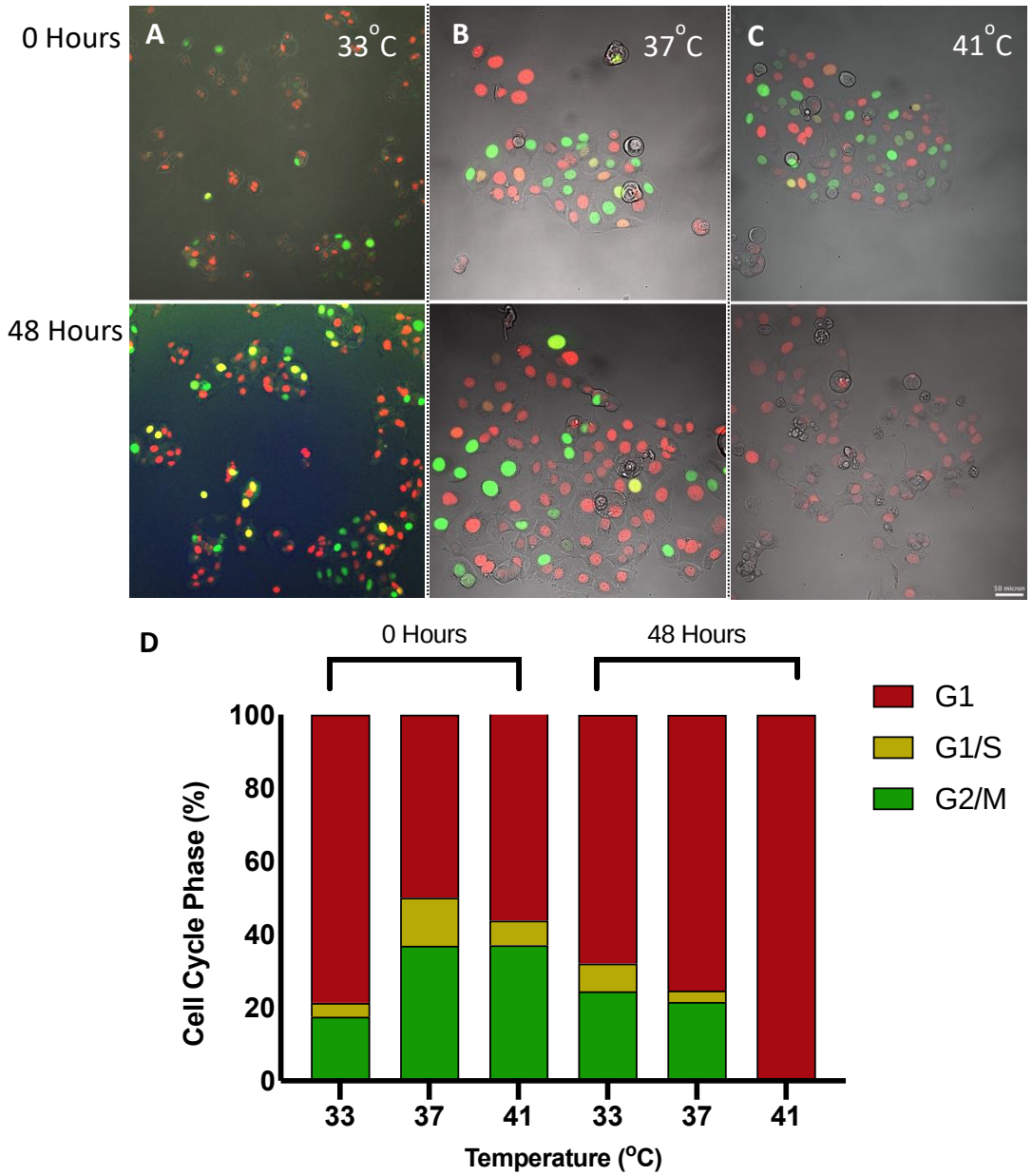

Figure 16. Incubating MCF-7 cells for 48 hours at 41 ºC stalls leads to G1 stalling. MCF-7 Fucci2a total cell cycle phases compared over time between temperature treatments. Cell cycle phases were tallied at T=0 and T=48 hours **(A-C)** Merge channel confocal imaging of different heat treatments displaying T=0 and T=48 hour time points. 33 ºC larger field of view

due to imaging acquired at 0.8 zoom, for further details in methods section **(D)** Cell cycle phases as percentages of total fluorescent cells at both time points showing all cells in 41 ^{o}C treatment stall in G1 after 48 hours. Scale bar 50 µm.

In order to investigate cell cycle phase alterations between temperatures, we utilised a similar pipeline to our cell count analysis (fig. 14). Cells were plated, incubated at either 33 ^{o}C, 37 ^{o}C or 41 ^{o}C and imaged for 48 hours. The ImageJ cell counting tool was then used to quantify the total percentage of cells in a given phase at T=0 and T=48 hours. Figure 16A-C displays confocal Fucci2a imaging at T=0 and T=48 hours for each temperature treatment. We then quantified the total cells in a given phase and plotted as a percentage of total cells (fig. 16D). We observed slight differences in cell cycle phase percentages at T=0, although this is to be expected for homogenous asynchronous cell culture. After 48 hours the 33 ^{o}C and 37 ^{o}C treatments displayed slight changes in cell cycle phase percentages relative to T=0 (Fig. 16D). Conversely, at 41 ^{o}C a striking difference was observed, with all cells stalling in G1. We next set out to investigate differences in MCF-7 cell cycle phase duration between temperature treatments.

To determine whether G1 or G2/M phase duration is impacted by temperature we tracked the intensity of the cell cycle phase specific mCherry and mVenus probes over full individual cell cycles. 10 full cell cycles for each treatment were tracked using a cell tracking ImageJ package developed in the Mort lab. This automated package measures the normalised integrated intensity of each probe during a full cell cycle. By tracking full cell cycles in this way, we were able to quantify the duration of G1 and G2/M phases by monitoring the rise and fall of the individual probes. Figure 17A and B both represent the tracking of one full cell cycle at 37 ^{o}C. This tracking allowed us to quantify G1 and G2/M phases by measuring the lengths of the respective peaks. In line with our previous analysis of counting cells over time (fig. 14), we observed increased G1 and G2/M phase lengths in cells treated at 33 ^{o}C compared with 37 ^{o}C (fig. 17C). The mean G1 and G2/M phase times at 33 ^{o}C were 1095 ± 269 and 1245 ± 237 minutes respectively (n = 10 mitoses for each treatment). Both of these times were significantly longer than the cells treated at 37 ^{o}C (t-test $P < 0.0001$), which showed a duration of 642.5 ± 86.64 and 565 ± 63.68 minutes for G1 and G2/M phases respectively.

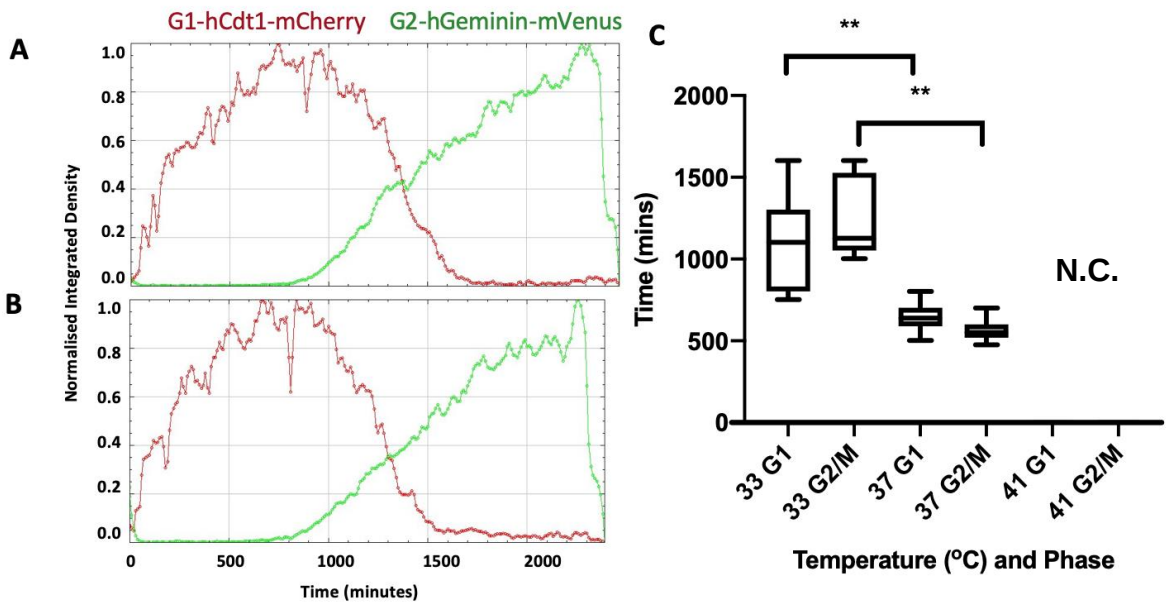

Figure 17. MCF-7 cell cycle phase time tracking (A-B) Relative intensity plots showing mCherry and mVenus peaks. Each plot represents individual MCF-7-Fucci2a cells incubated at 37 ºC. Each figure represents tracking of one full cell cycle. Tracking multiple cells in this way allows for estimation of G1 and S/G2/M phases. **(C)** Quantification of cell cycle phase lengths between temperature treatments. Incubating cells at 33 ºC resulted in a statistically significant increase in G1 and S/G2/M phase lengths relative to 37 ºC (**t-test $P < 0.0001$, normality tested using D'Agostino-Pearson test). 41ºC treatment was unable to be analysed in this way due to the lack of observable full cell cycles (N.C. = Not calculated), Please refer to figure 18 for further details.

We were unable to track cells incubated at 41 ºC in this way due to the lack observable full cell cycles. When tracking these cells however, we observed a number of abnormal events. Due to the observation of reduced cell count over 48 hours (Fig. 14), we assumed the occurrence of cell death in our 41 ºC treatment. Indeed, ~10 cellular death events (Fig. 18C) were observed at 41 ºC. Interestingly, each of these occurrences of cell death occurred during mitosis. Figure 18A displays a montage of MCF-7 full cell cycle at 37 ºC with focusing on mitosis. Nuclear envelope breakdown is the first observable morphological change marking mitotic initiation-

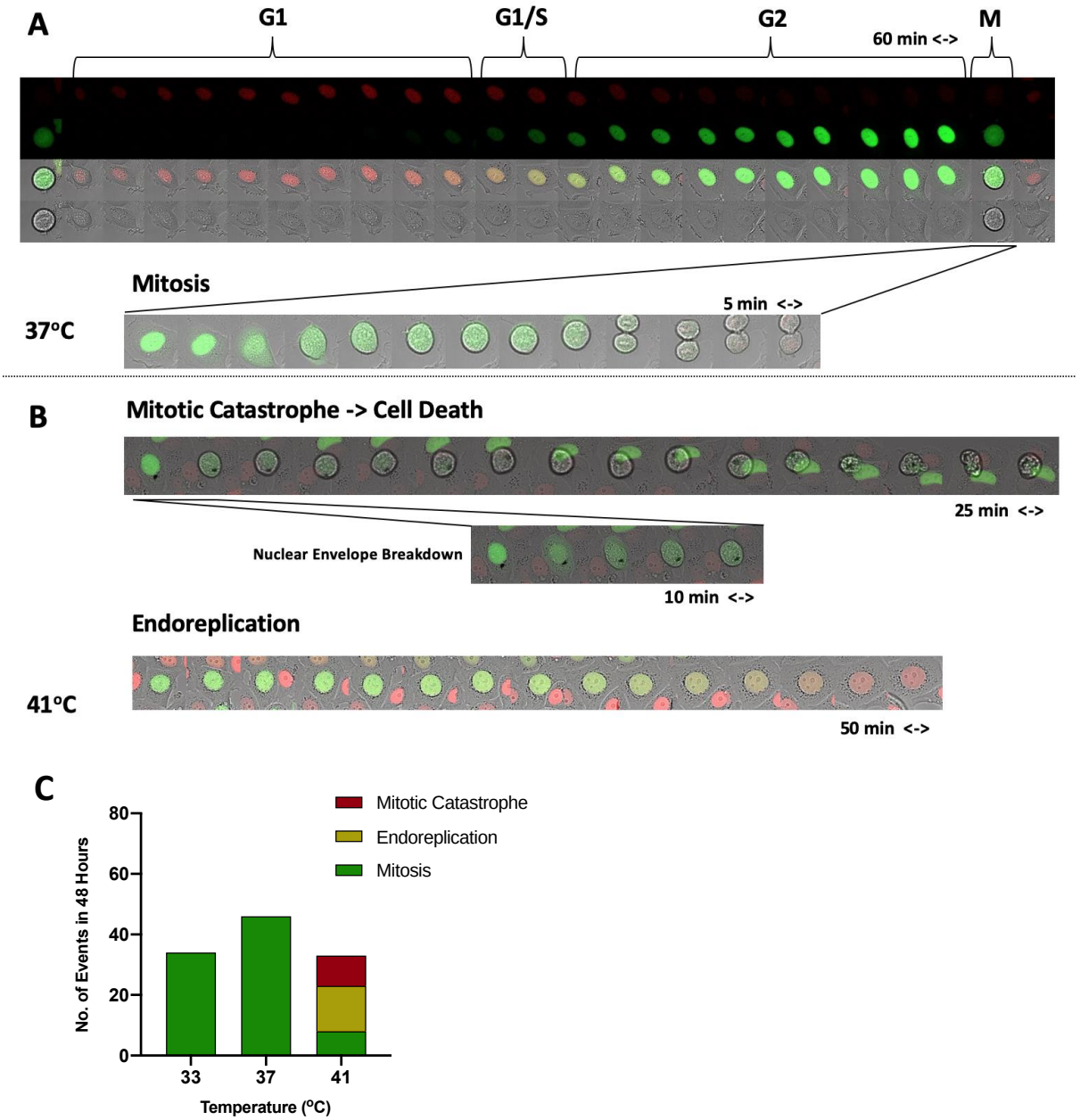

Figure 18. Incubating MCF-7 cells at 41 °C increases endoreplication and cell death via mitotic catastrophe. Cells were incubated at 33 °C, 37 °C or 41 °C and simultaneously imaged for 48 hours. Montage time steps are indicated in figure **(A)** Montage displaying full MCF-7 cell cycle incubated at 37 °C with focusing on mitosis. (**B)** Montages displaying mitotic catastrophe and endoreplication events in cells incubated at 41 °C. In mitotic catastrophe, nuclear envelope breakdown occurs in similar manner to mitosis in 37 °C, followed by observable cell death and apparent membrane blebbing after ~300 minutes (12th time point). Endoreplication event is displayed showing cells transition from G2 back to G1 (without undergoing mitosis) in a duration of ~250 minutes (5 time points). **(C)** Quantification of mitosis, cell death, and endoreplication events in 33 °C, 37 °C and 41 °C treatments. 33 °C and 37 °C treatments displayed 34 and 46 mitoses respectively and 0 endoreplication and mitotic

catastrophe events. The 41 ^{o}C incubated cells displayed 8 mitoses, 15 endoreplication events and 10 mitotic catastrophe events.

-, as is displayed in the 3rd time point of the mitosis cell cycle montage displayed in figure 18A. In cell death at 41 ^{o}C, cells observably gained green fluorescence intensity and rounded marking mitosis, then stalled for ~250 minutes after nuclear envelope breakdown before observably shrivelling and dying (fig. 18B). This behaviour was similar in all occurrences of cell death at this temperature treatment. Thus, we propose the mechanism of cell death in MCF-7 at 41 ^{o}C may occur via mitotic catastrophe. However, further biochemical analysis should be carried out to verify our proposed cell death mechanism. A further interesting behaviour of endoreplication was observed in cells treated at 41 ^{o}C. Endoreplication is the duplication of genomic material in the absence of mitosis. We noted ~15 observable occurrences of cells entering G2, then cycling back into G1, as is displayed in figure 19B. We then tallied each of these events with mitoses in the 41 ^{o}C treatment and contrasted this with events at 33 ^{o}C and 37 ^{o}C (fig. 18C). The impact of this higher temperature treatment on aberrant cellular events and repressed proliferation is substantial. We therefore concluded that 41 ^{o}C treatment of MCF-7 induces both mitotic aberrations resulting in cell death and polyploidy through endoreplication.

3.3.2. Melanocyte cell line Melan-A displays increased G1 phase duration at 33 ^{o}C relative to the melanoma line B16F10

Melanoma is further malignancy known to respond to HT. We therefore set out to investigate cell cycle thermosensitivity of the melanoma model cell line B16F10 and the immortalised melanocyte cell line Melan-A as a normal tissue control. Previous work carried out in the Mort lab led to the development of Fucci2a B16F10 and Melan-A lines. We utilised these lines to interrogate differences in thermosensitivity between melanoma and melanocytes. Due to the aforementioned limited lab time and technical issues with the department confocal, we were unfortunately only able to perform one experiment at 33 ^{o}C.

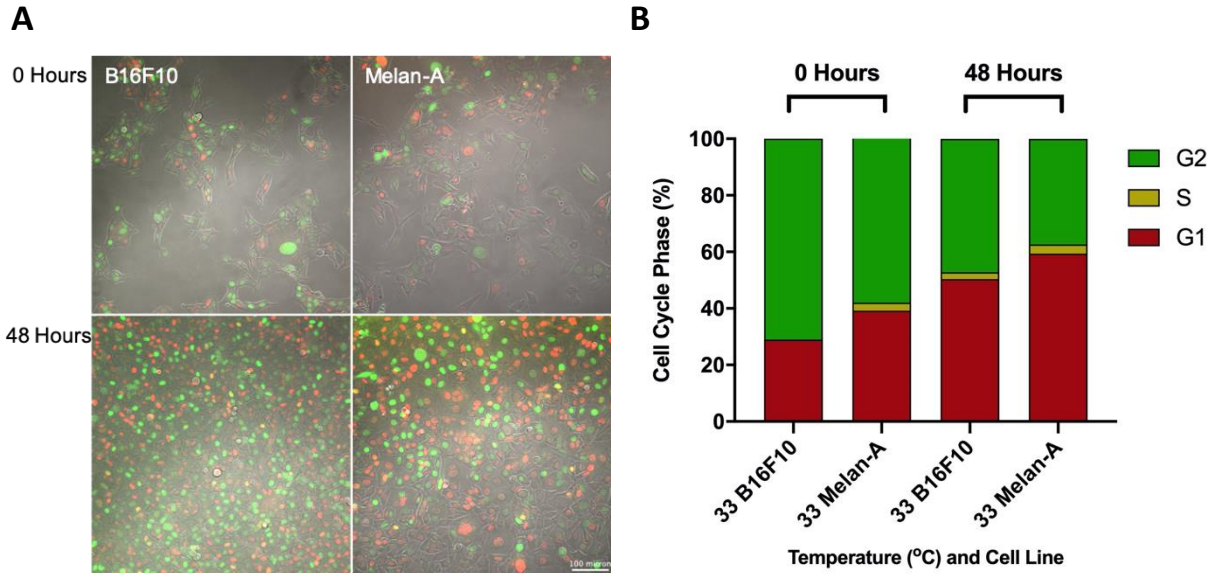

Figure 19. B16F10 and Melan-A display similar cell cycle phase totals at 33 ºC. B16F10-Fucci2a and Melan-A-Fucci2a total cell cycle phases compared over time between temperature treatments. Cell cycle phases were tallied at T=0 and T=48 hours. **(A)** Merge channel confocal imaging of different heat treatments displaying T=0 and T=48 hour time points. Cell cycle phases as percentages of total fluorescent cells at both time points.

Cells were plated, incubated at 33 ºC, and imaged for 48 hours. Figure 19A displays both B16F10 and Melan-A at T=0 and T=48 hours. Firstly, we tallied the total cells in a given phase for each line at T=0 and T=48 hours using the ImageJ cell counting tool (Figure 19B). This analysis revealed no striking differences in total cell cycle percentages at either time point. We did observe a slightly higher percentage of cells in G1 at T=48 hours in each line (Fig 19B). Although this effect is likely due to cells reaching confluency thus more cells arresting in G1 due to contact inhibition.

To determine whether G1 or G2/M phase duration differed between cell lines we tracked 10 full cell cycles for each line. We did this though utilising the aforementioned automated ImageJ cell tracking package developed in the Mort lab. This analysis produces normalised integrated intensities for both probes in each cell line tracked. Examples of these intensities are plotted and displayed in figure 20A-B. Figure 20A shows one full Melan-A cell cycle displaying a longer G1 (red) phase duration relative to both G2/M (green) and B16F10 G1 phases (Fig 20B). We quantified G1 and G2/M phase durations of 10 cells for each line and found a significantly longer G1 phase in the Melan-A cell line. Melan-A G1 phase showed a duration of 885 ± 308 minutes when compared with the B16F10 line time of 565 ± 66 (Normality tested using D'Agostino-Pearson test, t test P = 0.0049)(fig. 20C). Determining whether this

behaviour is a function of temperature or plasticity is difficult however due to our lack of a 37 ^{o}C control.

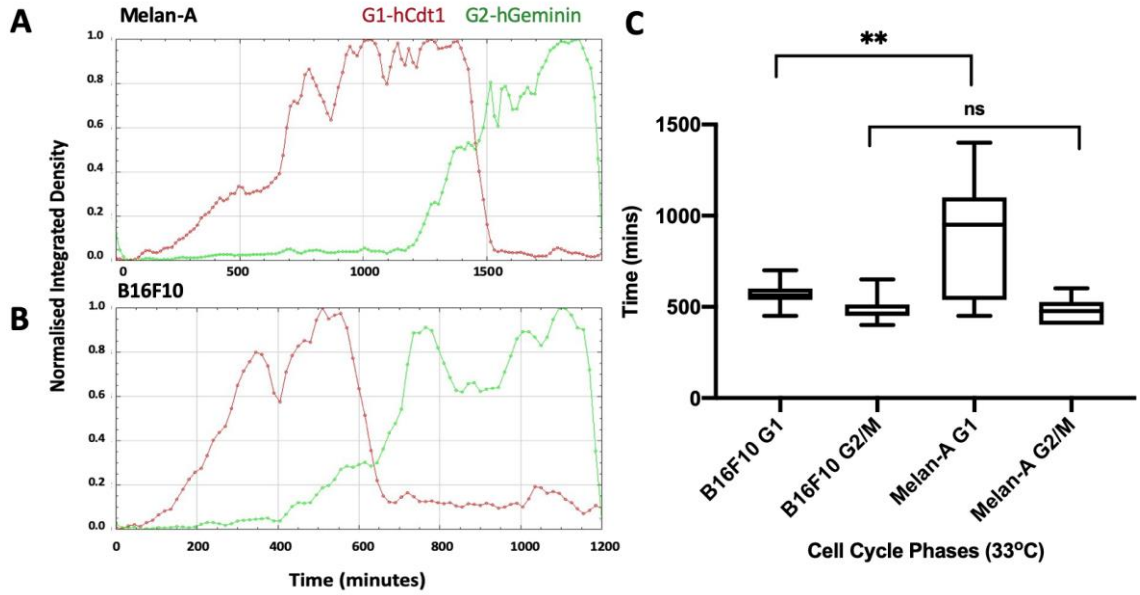

Figure 20. 33 ºC B16F10 and Melan-A cell cycle phase tracking (A-B) Relative intensity plots displaying mCherry and mVenus peaks in one full Melan-A and B16F10 cell cycle respectively. Note observably longer G1 peak fluorescence relative to G2 in Melan-A plot when compared to B16F10. **(C)** Quantification of cell cycle phase lengths. Melan-A cells displayed a statistically significant increase in G1 phase length when compared with B16F10 (n = 10, t-test P < 0.0049, normality tested using D'Agostino-Pearson test). **= Significant, ns = not significant.

3.4. The cBio Cancer Genomics Portal

3.4.1. Identification of cancer genetic alterations in gene groups of interest

In order to investigate whether the genes outlined in table 1 conferred cancer specific thermosensitivity we utilised the open source cancer genomics platform cBioPortal (Cerami *et al.*, 2012). We split our genes of interest into three groups; mitotic regulators, cytoskeletal associated proteins, and T complex protein ring (TRiC) proteins. In order to decipher whether these groups of genes were altered in cancer we queried each group of genes against collective TCGA PanCancer Atlas Studies. Analysing in this way queries each group of proteins against 32 studies each of which consisting of a different cancer type with a total sample count 10967. This analysis showed considerable alterations in each group across multiple cancers (Fig. 22). The Mitotic regulator group displayed a general high mutational

profile trend, most notably in uterine, bladder and melanoma malignancies (Fig 21A). This trend may be an artefact of general mutational burden, as opposed to functional driver mutations. Our cytoskeleton associated protein group displayed a similar trend, although notably uterine carcinosarcoma contained amplification or multiple alterations only (Fig 21B). The TRiC group displayed a trend of high gene amplifications across all cancers except uterine (Fig 21C). Moreover, given the complex's key role in protein folding homeostasis, these amplifications led to us taking an interest in this group of proteins and carrying them forward for transcript expression investigation. We then moved to investigating differences in gene expression of these groups between cancer and normal tissues.

3.4.2. Transcript-level expression analysis

To determine whether these genes differed in expression between cancer and normal tissue we used the Xenabrowser platform to compare the expression of each individual gene of interest in all cancers against the Genotype-Tissue Expression (GTEx) project database (Goldman *et al.*, 2020). GTEx consists of two main data of interest for our analysis, solid tissue normal, which is sampled near to tumour site, and normal tissue, which is taken from cancer free individuals. Using the Xenabrowser platform we compared the metastatic and solid tumour expression data of each our genes of interest against solid tissue normal and normal tissue data. Figure 22 lists two genes from each group which showed the most striking differences in expression. NEK2 displayed the most drastic increase in expression in cancer, with a normalised RNAseq count mean value of 8.1 +/- 2.1 and 8.6 +/- 1.2 for primary and metastatic tissues compared with 3.6 +/- 2.5 for normal tissue ($P < 0.0001$ One-way ANOVA with Dunnett's Post-Hoc test)(fig. 22A1). NEK2 is a mitotic regulatory protein, which as aforementioned, displays a decrease in expression in response to hyperthermia (Amaya *et al.*, 2014). The mitotic regulator NCAPG also displayed an increase in expression in cancer with respective primary and metastatic normalised RNAseq count means of 8.8 +/- 1.8 and 9.7 +/- 1.1 compared with 5.2 +/- 2.0 for the normal control tissue ($P < 0.0001$ One-way ANOVA with Dunnett's Post-Hoc test)(fig. 22A2). Thus, NCAPG may similarly play a role in cancer specific thermosensitivity. Of the cytoskeletal associated proteins we investigated, CFL1 and CFL2 showed the largest differences in expression in cancer. Both of which are actin modulating proteins. Interestingly these genes displayed significant contrasting differences in expression in cancer compared to normal tissue, with CFL1 showing an increase, and CFL2 a decrease ($P < 0.0001$ One-way ANOVA with Dunnett's Post-Hoc test)(Fig. 22A1-2). Furthermore, in line our previous observation of gene amplifications (fig. 21C), we observed a significant increase in expression in cancer in two subunits of the TriC

complex ($P < 0.0001$ One-way ANOVA with Dunnett's Post-Hoc test)(fig. 22 C1-2). These observation's led us to explore alterations of these genes in specific cancer types.

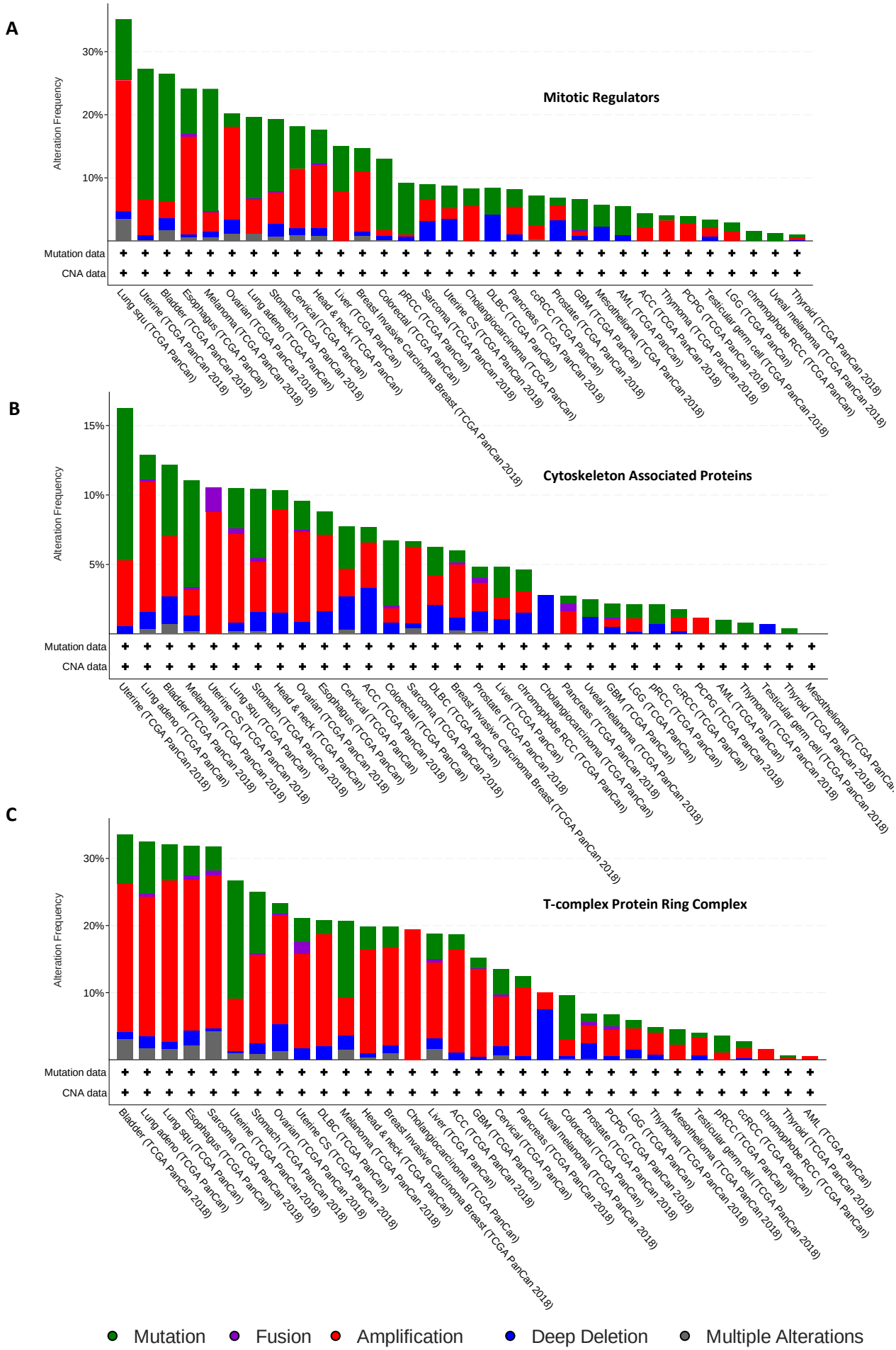
A
Mitotic Regulators
Alteration Frequency
30%
20%
10%
Mutation data
CNA data
Lung squ (TCGA PanCan)
Uterine (TCGA PanCan 2018)
Bladder (TCGA PanCan 2018)
Esophagus (TCGA PanCan)
Melanoma (TCGA PanCan)
Ovarian (TCGA PanCan 2018)
Lung adeno (TCGA PanCan)
Stomach (TCGA PanCan 2018)
Cervical (TCGA PanCan)
Head & neck (TCGA PanCan)
Liver (TCGA PanCan)
Breast Invasive Carcinoma Breast (TCGA PanCan 2018)
Colorectal (TCGA PanCan)
pRCC (TCGA PanCan)
Sarcoma (TCGA PanCan)
Uterine CS (TCGA PanCan 2018)
Cholangiocarcinoma (TCGA PanCan)
DLBC (TCGA PanCan 2018)
Pancreas (TCGA PanCan)
ccRCC (TCGA PanCan 2018)
Prostate (TCGA PanCan)
GBM (TCGA PanCan 2018)
Mesothelioma (TCGA PanCan)
AML (TCGA PanCan 2018)
ACC (TCGA PanCan)
Thymoma (TCGA PanCan 2018)
PCPG (TCGA PanCan 2018)
Testicular germ cell (TCGA PanCan 2018)
LGG (TCGA PanCan)
chromophobe RCC (TCGA PanCan)
Uveal melanoma (TCGA PanCan 2018)
Thyroid (TCGA PanCan 2018)
B
Cytoskeleton Associated Proteins
Alteration Frequency
15%
10%
5%
Mutation data
CNA data
Uterine (TCGA PanCan 2018)
Lung adeno (TCGA PanCan)
Bladder (TCGA PanCan 2018)
Melanoma (TCGA PanCan)
Uterine CS (TCGA PanCan 2018)
Lung squ (TCGA PanCan)
Stomach (TCGA PanCan 2018)
Head & neck (TCGA PanCan)
Ovarian (TCGA PanCan 2018)
Esophagus (TCGA PanCan)
Cervical (TCGA PanCan)
ACC (TCGA PanCan 2018)
Colorectal (TCGA PanCan)
Sarcoma (TCGA PanCan)
DLBC (TCGA PanCan 2018)
Breast Invasive Carcinoma Breast (TCGA PanCan)
Prostate (TCGA PanCan 2018)
Liver (TCGA PanCan)
chromophobe RCC (TCGA PanCan)
Cholangiocarcinoma (TCGA PanCan)
Pancreas (TCGA PanCan)
Uveal melanoma (TCGA PanCan 2018)
GBM (TCGA PanCan)
LGG (TCGA PanCan)
pRCC (TCGA PanCan)
ccRCC (TCGA PanCan)
PCPG (TCGA PanCan)
AML (TCGA PanCan)
Thymoma (TCGA PanCan 2018)
Testicular germ cell (TCGA PanCan 2018)
Thyroid (TCGA PanCan 2018)
Mesothelioma (TCGA PanCa
C
T-complex Protein Ring Complex
Alteration Frequency
30%
20%
10%
Mutation data
CNA data
Bladder (TCGA PanCan 2018)
Lung adeno (TCGA PanCan)
Lung squ (TCGA PanCan)
Esophagus (TCGA PanCan)
Sarcoma (TCGA PanCan)
Uterine (TCGA PanCan 2018)
Stomach (TCGA PanCan 2018)
Ovarian (TCGA PanCan 2018)
Uterine CS (TCGA PanCan 2018)
DLBC (TCGA PanCan 2018)
Melanoma (TCGA PanCan 2018)
Head & neck (TCGA PanCan 2018)
Breast Invasive Carcinoma (TCGA PanCan)
Cholangiocarcinoma (TCGA PanCan)
Liver (TCGA PanCan)
ACC (TCGA PanCan)
GBM (TCGA PanCan 2018)
Cervical (TCGA PanCan)
Pancreas (TCGA PanCan)
Uveal melanoma (TCGA PanCan 2018)
Colorectal (TCGA PanCan)
Prostate (TCGA PanCan 2018)
PCPG (TCGA PanCan)
LGG (TCGA PanCan 2018)
Thymoma (TCGA PanCan)
Mesothelioma (TCGA PanCan 2018)
Testicular germ cell (TCGA PanCan 2018)
pRCC (TCGA PanCan)
ccRCC (TCGA PanCan)
chromophobe RCC (TCGA PanCan)
Thyroid (TCGA PanCan 2018)
AML (TCGA PanCan)
Mutation
Fusion
Amplification
Deep Deletion
Multiple Alterations

Figure 21 Cross cancer alteration summary of genetic changes in groups of genes hypothesised to confer thermosensitivity. All data obtained using cBioPortal comparative cancer genomics. Cohort: TCGA Pan Cancer Atlas studies (32 studies, 10967 samples) **(A)** Mitotic regulators (KIF11, STAG2, NEK2, CHUK, KPNA4, CENPF, NCAPG) displaying general tread of high mutational profiles. **(B)** Cytoskeleton associated proteins (CFL1, CFL2, DSTN, RAPH1, EVL) showing a general trend of gene amplifications **(C)** T-complex Protein Ring Complex proteins (TCP1, CCT2, CCT3, CCT4, CCT5, CCT5, CCT6A, CCT6B, CCT7, CCT8) showing a trend of gene amplifications across cancer types.

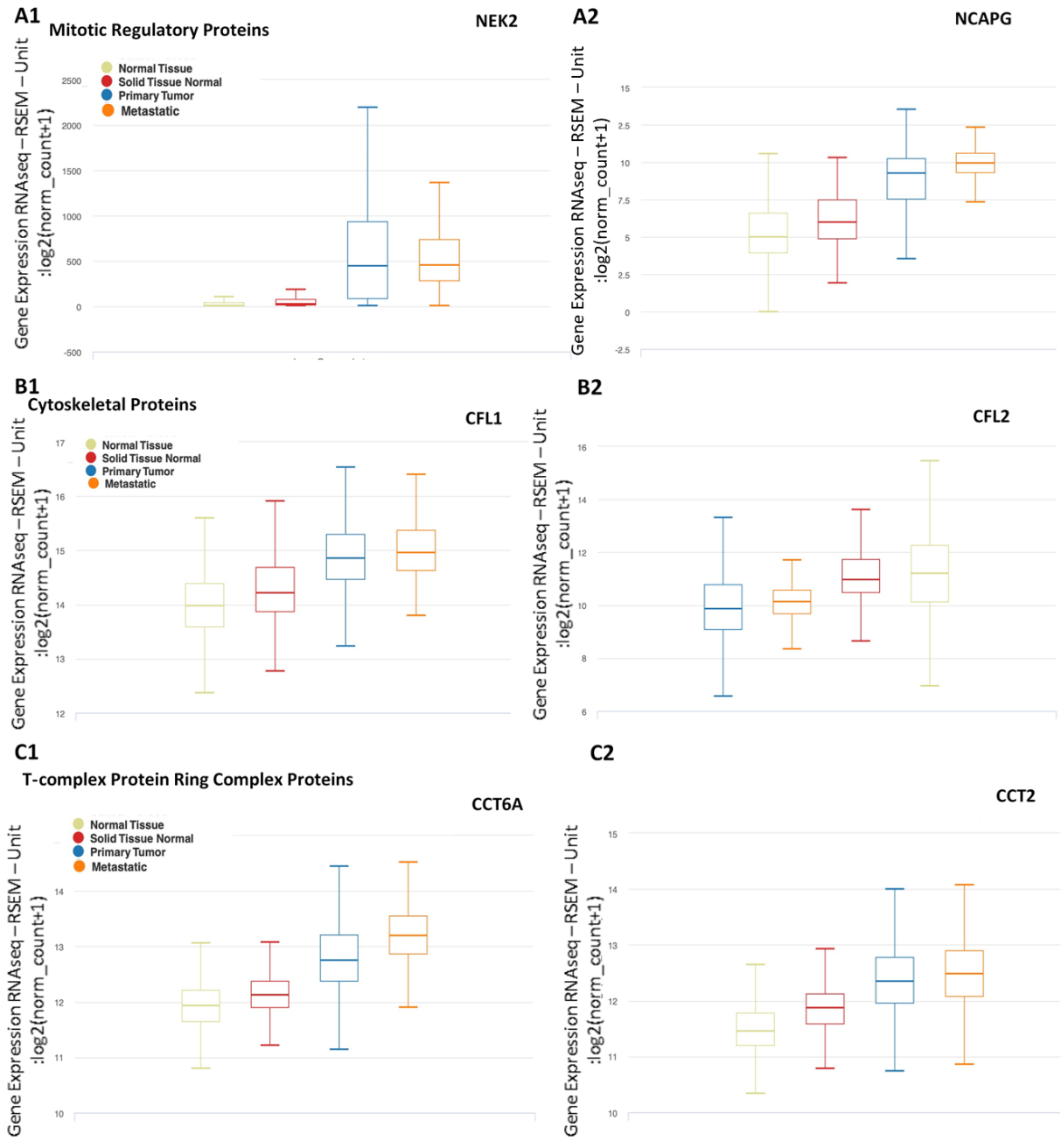

Figure 22. *Tumour vs normal expression of genes hypothesised to confer thermosensitivity. TCGA Pan Cancer Atlas study cohort expression (32 studies, 10967 samples), compared with the Genotype-Tissue Expression (GTEx) data (19131 samples). (A1-A2) Mitotic regulatory proteins NEK2 and NCAPG displaying significant elevated expression when compared with normal tissue. NEK2 showing most drastic increase. (B1-B2) CFL1 and CFL2 actin dynamic stability displayed varied expression in cancer when with normal tissue. CFL1 displayed an increase relative to normal tissue, conversely, CFL2 displayed a decrease. (C1-C2) Both CCT6A and CCT2 displaying increased expression in cancer compared to normal tissue. All*

comparisons of metastatic and primary tumour are significant compared to normal tissue One-way ANOVA with Dunnett's Post-Hoc test (P < 0.0001).

3.4.3. Cancer specific alterations in genes of interest

We then went back to the open source cancer genomics platform cBioPortal to investigate which specific cancer types contain genetic aberrations in our genes of interest. Each gene was queried individually against collective TCGA PanCancer Atlas Studies. This referenced each gene against 32 cancer subtypes from 10967 samples. In the mitotic regulatory proteins investigated NEK2 displayed high amplification and a high number of gene amplifications in breast cancer (Fig. 23). Breast cancer is known to respond to HT, and the treatment of such has been shown to reduce NEK2 expression (Amaya *et al.*, 2014). Our observations support this previously highlighted importance of NEK2 in breast cancer, although further more detailed analysis is required to verify our findings.. The actin modulating genes CFL1 and CFL2 displayed no apparent correlation with cancer types (fig. 24). The TRiC complex subunits CCT6A and CCT2 both showed highest expression in testicular germ cell cancer (fig. 25). Both of which displaying high numbers of gains in copy number. Whether this observation has any biological significance is inconclusive, although supports further investigation into the complexes role in testicular cancer.

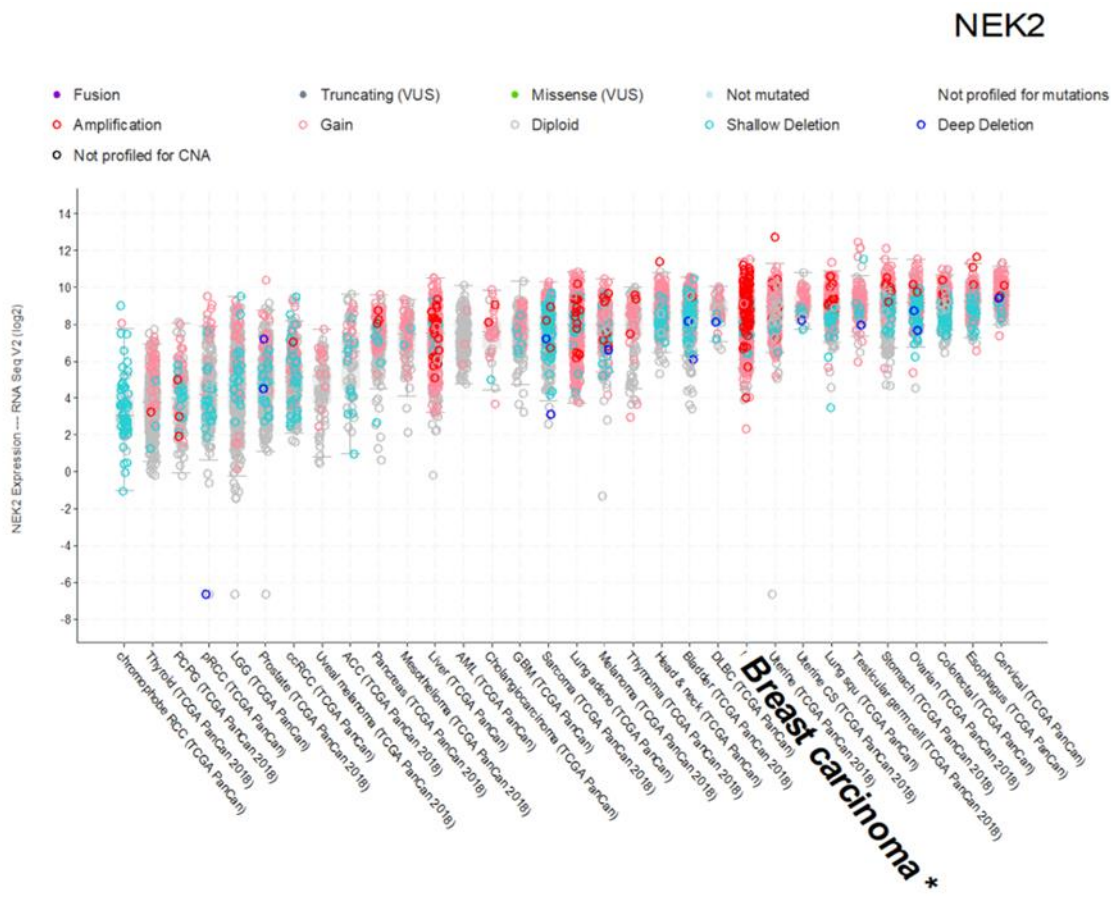
NEK2
Fusion
Truncating (VUS)
Missense (VUS)
Not mutated
Not profiled for mutations
Amplification
Gain
Diploid
Shallow Deletion
Deep Deletion
Not profiled for CNA
NEK2 Expression --- RNA Seq V2 (log2)
Breast carcinoma *

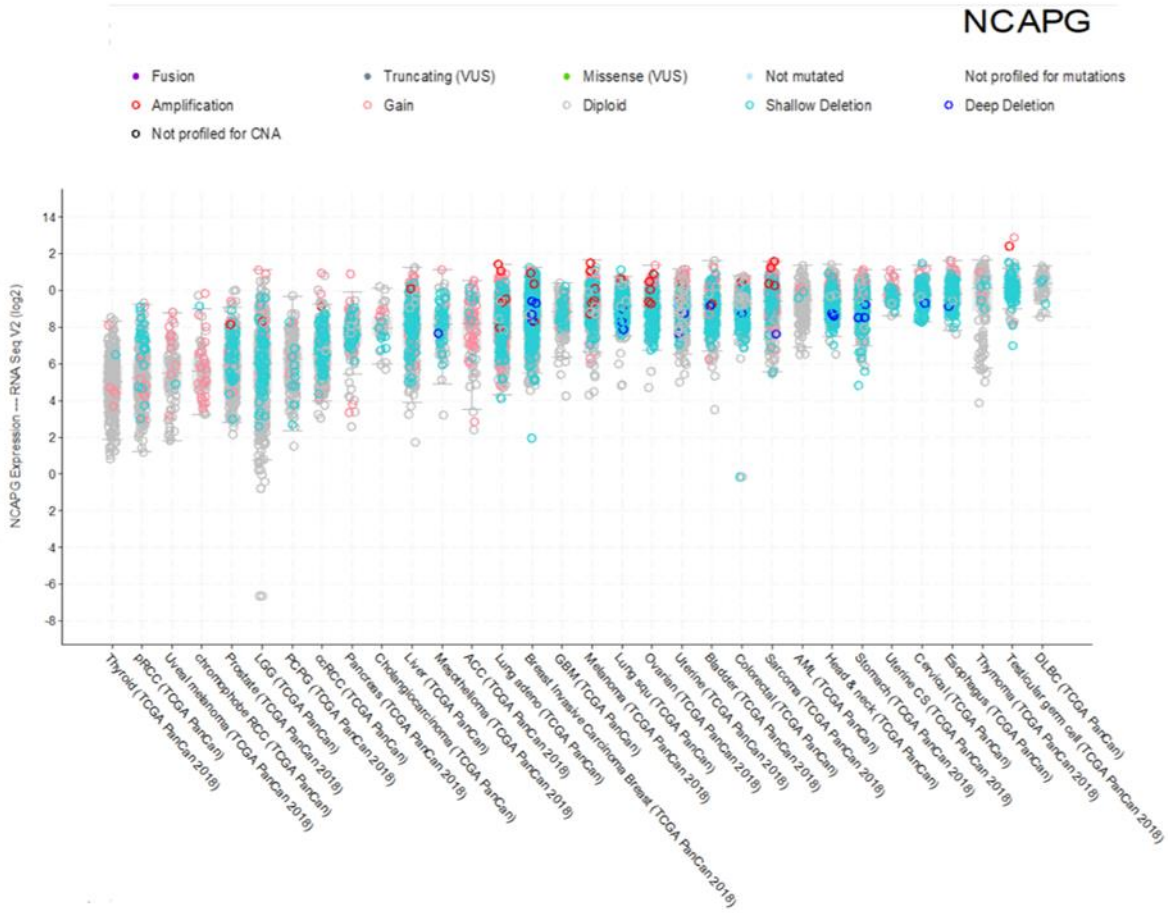
NCAPG
Fusion
Truncating (VUS)
Missense (VUS)
Not mutated
Not profiled for mutations
Amplification
Gain
Diploid
Shallow Deletion
Deep Deletion
Not profiled for CNA
NCAPG Expression --- RNA Seq V2 (log2)

Figure 23. Mitotic regulators NEK2 and NCAPG cancer specific mutations and copy number alterations. each spot-on figure represents a specific alteration. NEK2 showing high expression and gene amplification in breast cancer.

Cytoskeletal Proteins

CFL1

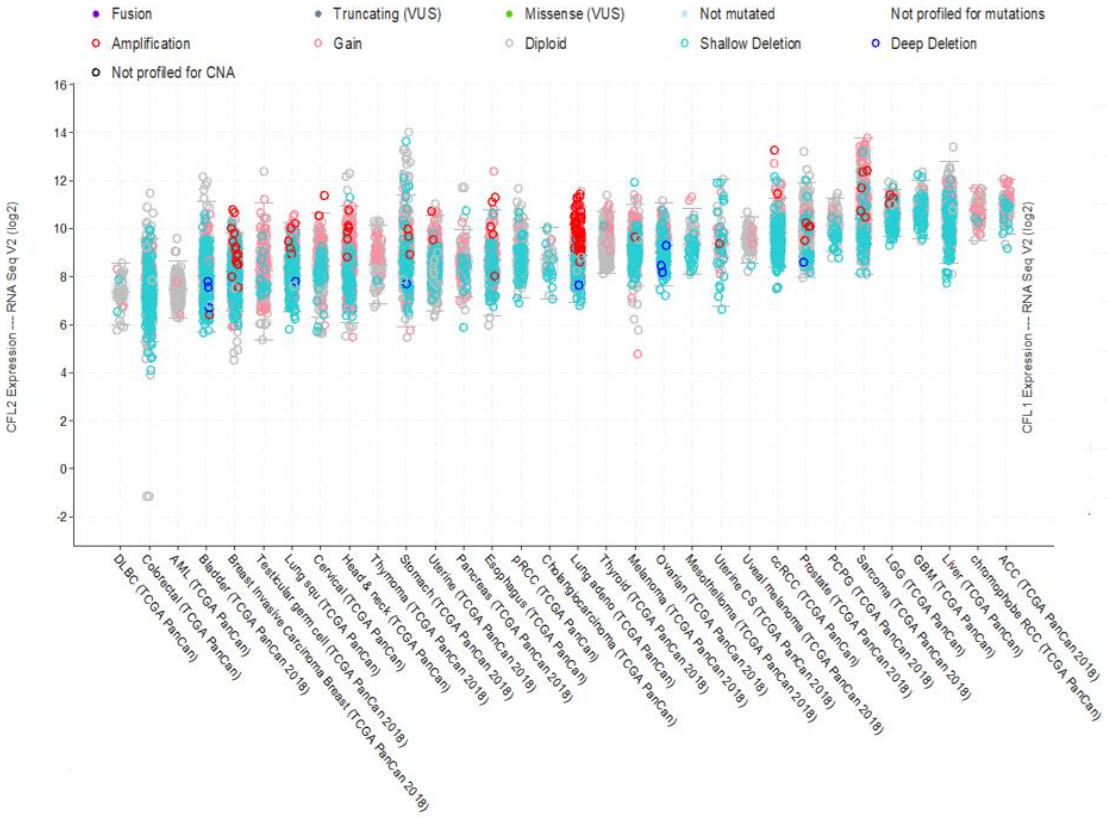

CFL2

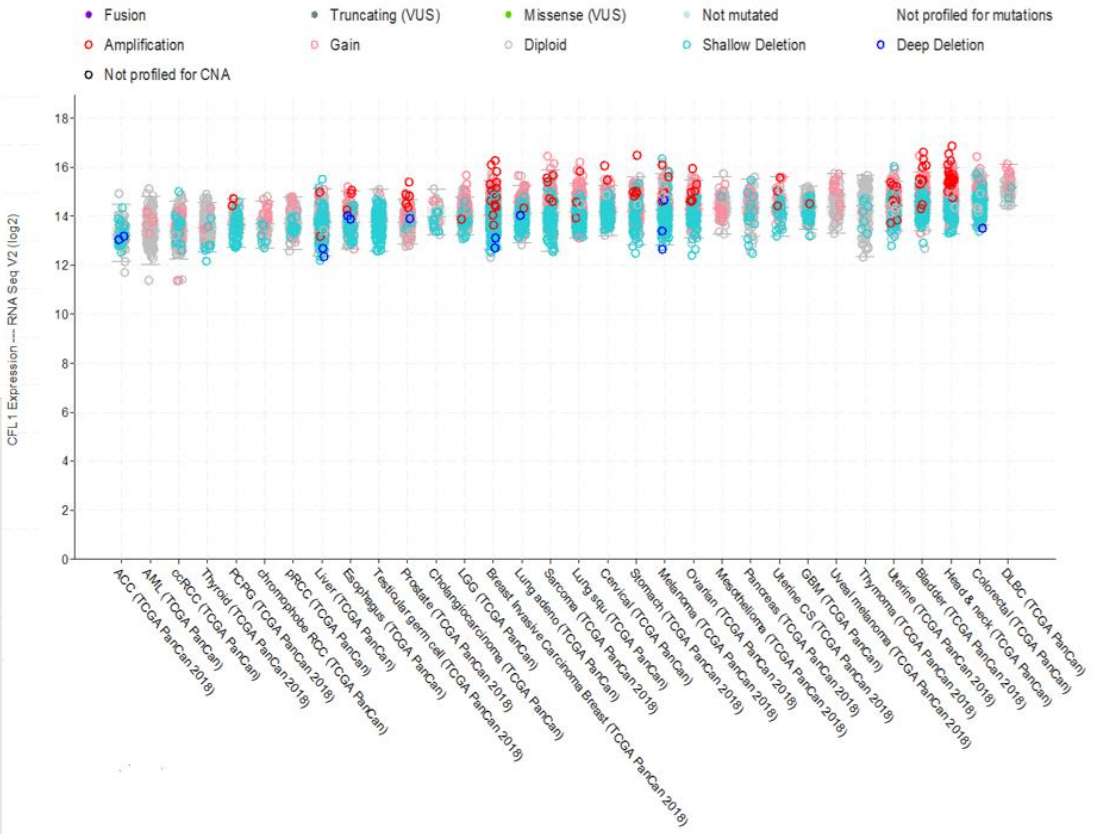

Figure 24. Cancer specific mutation and copy number alterations in cytoskeletal associated proteins CFL1 and CFL2. Each spot-on figure represents a specific alteration.

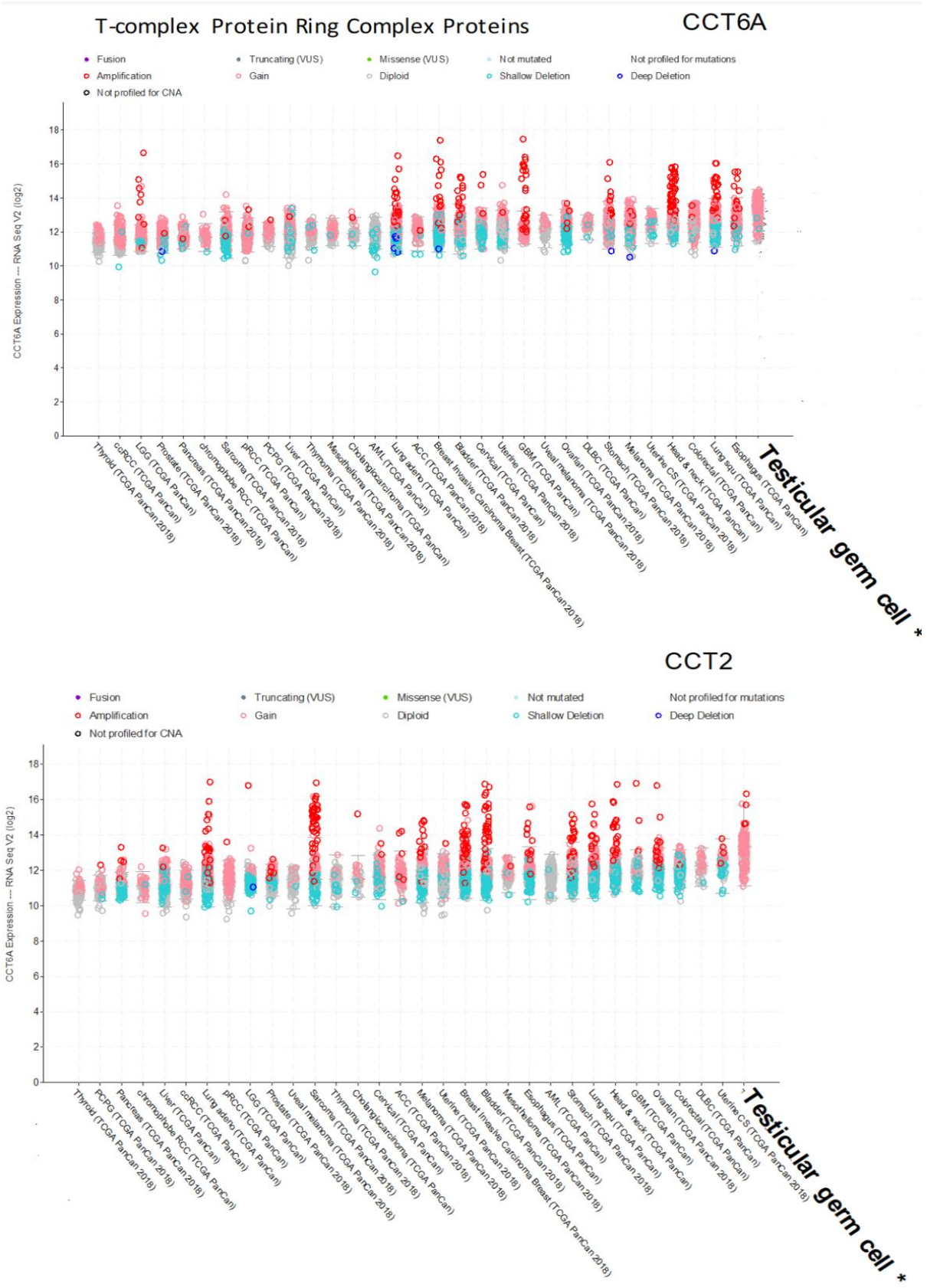

Figure 25. Cancer specific mutation and copy number alterations in T-complex protein ring complex proteins CCT6A and CCT2. Each spot-on figure represents a specific alteration. Both showing highest expression and high gain in copy number in testicular germ cell cancer.

4. Discussion

Interest in HT has undergone a resurgence in recent years due to innovations in methods of application and combination therapies (Datta *et al.*, 2020). Despite this, the cellular and molecular rationale behind HT remains unclear. Fucci is a verified and established tool for the investigation of cell cycle dynamics in cancer (Prasedya *et al.*, 2016; Yano *et al.*, 2014). cBioportal is a powerful open source cancer genomics platform which allows for visualisation and analysis of large-scale genomics data sets (Cerami *et al.*, 2012). These tools complement each other in developing the understanding of cancer, as is demonstrated in recent studies (Hastings *et al.*, 2020; Markovsky *et al.*, 2018). In this investigation, we have applied Fucci alongside cBioPortal based comparative genomics in order to shed light on the mechanisms underpinning HT's efficacy in cancer treatment.

4.1. Biosensor and cell line development

4.1.1. A better multiple cloning site for polycistronic vector approaches

The construction of polycistronic biosensors through the linkage of multiple components depends on multiple specific and novel restriction sites. Our transfection vector initially lacked such sites. In this study, we have constructed and inserted a novel multiple cloning site linker readily able to accept a variety of constructs through restriction cloning. Our vector with unique engineered multiple cloning site (fig. 9C) allows for the easy insertion of DNA consisting of a range of restriction sticky ends. This was demonstrated by the insertion of H1-Fucci(CA) via MluI and BamHI restriction sites (fig. 10). The cloning site includes 6 unique restriction sites, making it a versatile and valuable tool for building polycistronic biosensors from multiple constructs. This is in line with previous work optimising and engineering vector cloning sites to allow for ease of restriction cloning (Staal *et al.*, 2019, 2018).

4.1.2. Developing a robust strategy for batch transformation of Fucci vectors with PiggyBac

Transiently transfected genetic material is often lost during cell division. This approach is hence limited when using transgenetic biosensors to study the cell cycle. The PiggyBac transposase system is able to stably and efficiently genomically integrate constructs. We therefore set out to utilise this system to generate biosensor expressing cell lines to investigate HT in cancer. We have generated a PiggyBac vector housing the polycistronic cell cycle and histone biosensor H1-Fucci(CA)(fig. 10C). Moreover, we have demonstrated this systems

transfection ease and efficiency through the generation of a novel MCF-7 H1-Fucci(CA) expressing cell line (figure 12). This work supports previous reports of PiggyBac constituting an efficient vector in human cell genetic transfer (Wilson *et al.*, 2007; Yusa *et al.*, 2011). Fucci(CA) allows for the accurate discrimination of G1, S, G2/M cell cycle phases (Sakaue-Sawano *et al.*, 2017). Extending Fucci(CA) via the addition of the histone marker H1 linked with CFP expands spatial dynamic interrogation capability through facilitating the simultaneous tracking of chromatin organisation with cell cycle phases (Figure 12D). Furthermore, housing this construct in our PiggyBac vector system allows for future rapid and efficient H1-Fucci(CA) transfection in cell lines of interest, as demonstrated in Figure 12D. Unfortunately, in this study we were unable to utilise these novel tools for cancer cell thermosensitivity investigation. This is due to the coronavirus pandemic forcing the closing of our lab, as it did many others across the world (Vasiliadou, 2020). This limited lab time meant during this study we were unable to select MCF-7-H1-Fucci(CA) clones, or transfect further lines with our PiggyBac-H1-Fucci(CA) construct. For future cancer thermosensitivity investigation these tools will prove invaluable. A clear benefit of this biosensor is the inclusion of the nuclear marker H1. In our MCF-7 thermosensitivity imaging experiments we have shown the main mechanism of cell death in cells treated at 41 ^{o}C to occur via mitotic catastrophe (Figure19B). Simultaneous tracking of the H1 nuclear marker during these events will provide further insight into chromatin organisation during these events. (Wang *et al.*, 2010) demonstrated the surface exposure of H1 in apoptotic cells and nuclear localised H1 in necrotic cells. Thus, tracking the localisation of H1 during cell death may provide insight as to whether apoptosis or necrosis follows mitotic catastrophe in MCF-7 HT response.

4.1.3. Monitoring multiple cell cycle outcomes with a single vector

The impact of HT on cancer cell cycling and cell fate is poorly understood. In particular the mechanism of cell death in response to HT is one of interest. Generating cellular tools able to report in real time on the cell cycle and cell fate will provide insight into these mechanisms. We therefore set out to generate a polycistronic biosensor able to report cell cycle phase dynamics and apoptosis. Nicholls and colleagues (2011) developed a genetically encoded GFP based apoptosis biosensor which functions as a dark to bright reporter. The sensor functions through the incorporation of a quenching peptide at the N-terminus of GFP which disrupts proper chromophore maturation. Linking this peptide to GFP via a caspase-9 recognition motif results in a real-time dark to bright apoptotic biosensor. Identification of other fluorochromes able to function in this system will aid in the design of novel multi-colour biosensor imaging pipelines. iRFP670 is a bright and highly stable far-red fluorochrome which is well tolerated by live cells (Shcherbakova and Verkhusha, 2013). We

linked the aforementioned quenching peptide/caspase-9 recognition motif to the N terminus of iRFP670. Through MCF-7 transient transfection and subsequent time-lapse confocal imaging we found that the peptide is insufficient in quenching iRFP670 fluorescence (Fig. 13A). Thus, iRFP670 is an unsuitable fluorochrome for a biosensor of this sort. Our findings indicate the quenching function of this peptide is unique to GFP and derivatives thereof. This supports a previous study which indicates that the peptide specifically disrupts GFP β-barrel formation and thus chromophore maturation (Nicholls and Hardy, 2013). iRFP670 is a bacterial phytochrome consisting of a bilin chromophore core, a drastically different structure and chemical configuration to GFP (Rockwell *et al.*, 2006; Shcherbakova and Verkhusha, 2013). We conclude these fluorochromes do not respond to quenching via linkage of this peptide. Moving forward in biosensor construction, replacing CFP in our H1 reporter (Fig. 10C) with iRFP670 should function sufficiently as this reporter acts simply by localisation. This will allow for CFP, a derivative of GFP, to be linked to the quenching peptide and thus lead to a functional dark to bright apoptotic biosensor. A polycistronic biosensor capable of discriminating between G1, S and G2/M cell cycle phase state, in addition to, indicating apoptosis and chromatin organisation will be provide invaluable tool for thermosensitivity investigation.

4.2. Thermosensitivity

4.2.1. HT induces mitotic catastrophe and endoreplication in breast cancer

Breast cancer is the second most common form of cancer among women and is estimated to affect at least 1 in 8 women in their lifetime (Rojas and Stucky, 2016). Despite breast cancer research being at the forefront of cancer biology for decades, the disease is often still fatal. In particular, hyper aggressive breast malignancies such as triple negative breast cancer carry with them extremely poor prognostic outcomes (Jitariu *et al.*, 2017). Therefore, there is much effort in the oncology community to develop and harness novel therapeutic strategies to improve breast cancer patient outcome. HT is one such therapy of current high interest. HT has been shown to significantly reduce breast cancer growth and to improve the therapeutic ratio of conventional therapies (Zagar et al., 2010). Not surprisingly therefore, HT is commonly applied in clinic for breast cancer and is the subject of numerous ongoing clinical trials (Datta *et al.*, 2020). Despite HT's wide application, the mechanisms by which HT selectively inhibits tumour growth are poorly understood. In particular, the impact hyperthermia has on cell cycle phase dynamics in cancer remain unclear. Considering HT's common combinatorial application alongside cell cycle phase specific drugs, elucidating the effects of HT on cell cycle dynamics in breast cancer may aid in the design of therapeutic regimens (Otto and Sicinski,

2017). In this study, we employed the breast cancer cell line MCF-7 as a model to investigate the effect of HT cell cycle phase dynamics.

Through utilising the cell cycle biosensor Fucci2a and performing live time-lapse confocal microscopy we observed recurrent cell death in HT treated cells specifically at the point of mitosis. We propose this phenomenon to be mitotic catastrophe induced cell death. Mitotic catastrophe is a pre-stage of cell death which occurs preceding necrosis or apoptosis (Vakifahmetoglu *et al.*, 2008). This finding is consistent with previous reports indicating HT induces mitotic catastrophe in both breast and lung cancer cells (Giovinazzi *et al.*, 2013; Pawlik *et al.*, 2013a). It should be noted that mitotic catastrophe is also induced by microtubule hyper-polymerising and depolymerising drugs, such as taxanes and Vinca alkaloids respectively (Castedo *et al.*, 2004). The induction of mitotic catastrophe by microtubule aberration coupled with HT's induction of mitotic catastrophe support further investigation into cancer specific microtubule molecular alterations as a potential mechanism by which cancer cells are susceptible to HT. This will be further discussed in section 4.2.3.

Furthermore, through our imaging pipeline we found HT induces endoreplication and G1 phase stalling in MCF-7 cells. Endoreplication is defined as the replication of genetic material in the absence of mitosis resulting in polyploidy (Lee *et al.*, 2009). Endoreplication is essential for normal developmental and physiological processes (Fox and Duronio, 2013). An example of such is megakaryocyte endoreplication (Sher *et al.*, 2013). Megakaryocytes are rare cells which can undergo cellular enlargement and endoreplication which can amplify DNA up to 64-fold in order to facilitate platelet biogenesis (Patel *et al.*, 2005). A previous study has confirmed Fucci2 as a reliable indicator of endoreplication through observing Fucci2 probes in megakaryocyte endoreplication cycling (Sakaue-Sawano *et al.*, 2011). Induction of endoreplication and polyploidy in cancer has been similarly observed in response to anti-cancer drugs, the most prevalent and well documented of which being topoisomerase II inhibitors (Cortés and Pastor, 2003). Interestingly, HT has previously been shown to enhance the sensitivity of cancer cells to topoisomerase II targeting drugs, and has been indicated to cause nuclear protein aggregation at the sites of topoisomerase-II DNA interaction (Hirohashi *et al.*, 1995; Kampinga, 1995)(Hirohashi et al., 1995). These reports suggest that an alteration in topoisomerase II function or downstream signalling is a potential causal mechanism for the increased endoreplication events in response to HT seen in figure 19B. Further investigation of this potential causal relationship may aid in the design of HT topoisomerase II inhibitor combinatorial regimens.

As aforementioned we were greatly limited for laboratory time in this study due to the coronavirus pandemic causing the closing of our department. This led to us being unable to perform many experiments which were initially planned. Immortalised cell lines are a powerful tool for studying and comparing neoplastic and normal cell physiology (Boehm and Hahn, 2004). Moving forward, the generation of a Fucci immortalised mammary epithelial cell will be useful for thermosensitivity investigation. As previously stated, whether there are intrinsic cellular differences in sensitivity to HT between normal and cancer cells is unclear and somewhat controversial. The generation of a normal tissue Fucci control for HT treatment and subsequent imaging alongside MCF-7-Fucci2a may offer insight into this unanswered question. In addition, it will also be useful to examine triple negative breast cancer cells lines, such as BT549 or MDA-MB-231, for their responses to HT as triple negative breast cancer has a high therapeutic need. Furthermore, the precise mode of cell death following mitotic catastrophe remains unclear. Pawlik and colleagues (2013) indicated apoptosis to occur following mitotic catastrophe in lung cancer cells treated with HT. This prediction is based only on morphological characteristics however, thus, further investigation is required in order for a more definitive conclusion to be drawn. Whether HT induces apoptosis occurs via intrinsic, extrinsic, or endoplasmic pathways (as reviewed (Ahmed *et al.*, 2015) remains unclear. To interrogate these pathways, the aforementioned dark to bright apoptosis biosensor may provide a useful tool. Given the sensor functions through reporting the catalytic activation of caspase-9, and thus intrinsic apoptosis activation, we propose the sensor may act similarly when replacing the recognition motif to report on the catalytic activation of an alternative pathway. By replacing the caspase-9 recognition motif with the extrinsic pathway specific caspase-8 recognition sequence, one may be able to generate apoptotic pathway specific real-time genetically encoded biosensors. Transfecting these sensors alongside Fucci2a in both normal tissue and MCF-7 cell lines may prove fruitful in uncovering cancer specific thermosensitive cell death mechanisms.

We have demonstrated the induction of mitotic catastrophe, endoreplication, and G1 phase stalling in breast cancer cells in response to HT. These findings coincide with previous reports of mitotic catastrophe based cell death induction (Giovinazzi *et al.*, 2013; Pawlik *et al.*, 2013b). Moreover, to our knowledge we have illustrated for the first time the induction of endoreplication in breast cancer in response to HT alone. However, generating biological replicates for these experiments is required in order to solidify these findings. This work may guide the design of future themosensitivity investigation.

4.2.2. Melanoma

Melanoma is a further malignancy of interest for HT treatment (Mantso *et al.*, 2018). We therefore set out to interrogate the effect of temperature on melanocyte (Melan-A) and melanoma (B16F10) Fucci2a cell lines. We were unfortunately limited to analysing just 33 ^{o}C treatment however, due to the coronavirus pandemic reducing lab time and technical issues with the department's confocal microscope. We had initially intended on investigating a range of temperatures, from 33 ^{o}C up to HT relevant temperature treatment. Our thermosensitivity imaging pipeline has demonstrated its effectiveness through analysing MCF-7 cells. Moving forward, investigating HT range temperature in both melanoma and normal tissue control lines may shed light on intrinsic cellular differences between cancer and normal cell thermosensitivity. We did observe significantly longer G1 phase durations in Melan-A compared with B16F10. Although whether this phenomenon is a function of temperature, or general differences in cell cycling between lines is yet to be resolved. Further experiments using a range of temperatures will shed light on this.

4.2.3. NEK2 is a key player in HT and mitotic catastrophe?

HT is currently the focus of many clinical trials in a range of cancers including ovarian, bladder, breast and neurological malignancies to name just a few (Cowan *et al.*, 2017; Longo *et al.*, 2016; Mahmoudi *et al.*, 2018; Mu *et al.*, 2018). Currently the molecular determinants which sensitise cancer to HT are poorly understood. In addition, specific cancer type responses to HT are underexplored. Identification of the genetic changes and molecular pathways which confer HT response in cancer may facilitate the development of novel therapeutic strategy. Moreover, predicting which specific cancer subclasses may respond to HT could guide the design of future cancer thermosensitivity studies. In this study we utilised the bioinformatic open platforms cBioPortal and Xenabrowser to explore the genetic changes of three categories of genes in cancer which we have hypothesised to be involved cancer thermosensitivity (Goldman *et al.*, 2020; Cerami *et al.*, 2012).

Amaya and colleagues (2014) demonstrated reduced expression of the mitotic regulators KIF11, STAG2, NEK2, CHUK, KPNA4, CENPF and NCAPG in HT treated breast cancer cells. Through cross referencing Pan Cancer Genome atlas studies with Genotype Tissue-expression data we identified NEK2 as being highly differentially expressed in cancer. In particular, we found NEK2 displayed a striking number of gene amplifications in breast invasive carcinoma (fig. 22A1). It should be noted however that this observation lacks statistical investigation due to time constraints, so should be considered speculative. However, the observation is consistent with previous reports of NEK2 being over expressed in a variety

of cancers and in particular in breast cancer (Wang *et al.*, 2011). NEK2 is an oncogenic multifunctional serine/threonine kinase which plays roles in cell cycle control, centrosome amplification, and microtubule stability (Fang and Zhang, 2016). There is currently high interest in targeting NEK2 as a therapeutic approach for breast cancer. Small molecular inhibitors have shown significant anti-cancer activity in vitro and in vivo murine xenograft models (Henise and Taunton, 2011, p.2; Kokuryo *et al.*, 2007, p.2). The efficacy of NEK2 inhibition combined with finding that HT acts to reduce the expression of NEK2 in breast cancer suggests HT's anti breast cancer activity may function through impacting NEK2 signalling. Moreover, NEK2 has been demonstrated to play an essential role in the integrity of centrosome structure and microtubule nucleation activity (Jeong *et al.*, 2007). Aberrant centrosome structure and spindle formation is associated with high rates of mitotic catastrophe (Pihan, 2013). We propose high rates of mitotic catastrophe to occur in MCF-7 cells treated with hyperthermia (fig 19B). This observation alongside these reports indicate HT's anti breast cancer activity may function via reducing NEK2 expression/activity, leading to disruption of centrosome integrity and thus mitotic catastrophe. In further support of NEK2 playing a key role in HT, the cancers we found to most highly express NEK2 (cervical, oesophageal, stomach and ovarian) are each known to respond well to HT (Franckena *et al.*, 2009; Gori *et al.*, 2005; Hulshof *et al.*, 2009; Kaaij *et al.*, 2017). Future directions should include investigating the mechanism of HT reduced NEK2 expression in cancer previously observed (Amaya *et al.*, 2014). NEK2 expression is complex, showing regulation at both the transcriptional and post-transcriptional level (Hames and Fry, 2002). Chromatin immunoprecipitation and proteomic avenues of investigation may prove insightful in elucidating any effects HT has on NEK2 transcriptional regulators or signalling pathways. Additionally, knockdown of NEK2 in breast cancer cells, using siRNA for example, and simultaneously treating these cells with HT may prove fruitful. A combinatorial effect of these perturbations may uncover further mechanistic insight into HT in breast cancer, in addition to, guiding the design of therapies.

4.2.4. TRiC and testicular cancer

Hyperthermia's aberrant effects on microtubules are well established (Coss and Linnemans, 1996). We therefore took interest in the microtubule regulatory TRiC complex. TRiC is a chaperone complex which mediates protein folding in the cytosol, most notably tubulin and actin, as is required for their proper folding (Dunn *et al.*, 2001). We rationalised therefore that cancer genetic alterations in components of this complex in cancer may lead to increased thermosensitivity. Indeed, we found two subunits of this complex CCT6A and CCT2 to show increased expression when cross referencing Pan Cancer Genome atlas studies with Genotype Tissue-expression data (fig. 22C1-C2). When we referenced the expression of

CCT6A and CCT2 against specific cancers we found the highest expression of both genes in testicular germ cell cancer out of all 32 cancer types investigated (fig 23C1-C2). Almost all alterations of CCT6A and CCT2 being gene amplifications. These observations suggest TRiC components as being potentially upregulated in testicular cancer, however, further investigation is needed in order to verify this proposal. Interestingly, a recent study from Guest and colleagues (2015) identified CCT2 and TCP1 (another TRiC subunit) as being necessary for the survival of breast cancer cell line SUM-52. The study further found CCT2 and TCP1 to be determinants of overall survival in breast cancer patients. These data suggest TRiC complex components function as drivers in breast cancer. This supports further investigation into TRiC's potential role in testicular cancer. Exploring potential correlation of components of TRiC with testicular cancer patient survival and in vitro RNAi knock down study represent potential avenues of investigation. Whether this complex contributes to cancer specific thermosensitivity remains inconclusive.

4.3. Conclusion

We here describe the cell fates of the model breast cancer cell line MCF-7 in response to HT. We have constructed a novel cell cycle and chromatin state biosensor transfection vector and demonstrated its functionality through the generation of the MCF-7 H1-Fucci(CA) cell line. Moreover, we have proposed potential molecular mechanisms responsible for cancer cell specific thermosensitivity through interrogating genomic alterations in cBioPortal. This work may guide further investigation into the thermosensitivity of cancer cell cycle dynamics, provide tools for cell cycle study, and has given insight into potential molecular determinants of HT and testicular cancer.

5. Acknowledgements

I would like to express my deep and sincere gratitude to my supervisors Dr. A. Benedetto, Dr. A. Feilding and Dr. R. Mort for giving me the opportunity to undertake this project and for their patience and invaluable guidance. I would also like to extend my thanks to each and every person, student and faculty, in the Biomedical and Life Science department at Lancaster University who advised and helped me during this project. In addition, thank you to North West Cancer Research for funding the project.

6. Reference List

Abe, T. et al. (2013) Visualization of cell cycle in mouse embryos with Fucci2 reporter directed by Rosa26 promoter. *Development (Cambridge, England)*, 140(1), 237–246.

Absher, M. (1973) Hemocytometer counting. In: Elsevier *Tissue culture*. Elsevier.

Ahmed, K. et al. (2015) Hyperthermia: an effective strategy to induce apoptosis in cancer cells. *Apoptosis*, 20(11), 1411–1419.

Alexander, J.L. et al. (2017) Gut microbiota modulation of chemotherapy efficacy and toxicity. *Nature Reviews Gastroenterology & Hepatology*, 14(6), 356–365. Nature Publishing Group.

Amaya, C. et al. (2014) A genomics approach to identify susceptibilities of breast cancer cells to “fever-range” hyperthermia. *BMC Cancer*, 14(1), 81.

Arjona-Sánchez, A. et al. (2018) HIPECT4: multicentre, randomized clinical trial to evaluate safety and efficacy of Hyperthermic intra-peritoneal chemotherapy (HIPEC) with Mitomycin C used during surgery for treatment of locally advanced colorectal carcinoma. *BMC cancer*, 18(1), 1–8. BioMed Central.

Banerjee, R. & Kamrava, M. (2014) Brachytherapy in the treatment of cervical cancer: a review. *International Journal of Women’s Health*, 6, 555–564.

Bartee, L. et al. (2017) The Eukaryotic Cell Cycle. *Principles of Biology: Biology 211, 212, and 213*. Open Oregon Educational Resources.

Baskar, R. et al. (2012) Cancer and Radiation Therapy: Current Advances and Future Directions. *International Journal of Medical Sciences*, 9(3), 193–199.

Basto, R. et al. (2008) Centrosome Amplification Can Initiate Tumorigenesis in Flies. *Cell*, 133(6), 1032–1042.

Baumann, M. et al. (2016) Radiation oncology in the era of precision medicine. *Nature Reviews Cancer*, 16(4), 234–249. Nature Publishing Group.

Beere, H.M. (2004) `The stress of dying’: the role of heat shock proteins in the regulation of apoptosis. *Journal of Cell Science*, 117(13), 2641–2651. The Company of Biologists Ltd.

Behrouzkia, Z. et al. (2016) Hyperthermia: How Can It Be Used? *Oman Medical Journal*, 31(2), 89–97.

Belzile, J.-P. et al. (2010) HIV-1 Vpr induces the K48-linked polyubiquitination and proteasomal degradation of target cellular proteins to activate ATR and promote G2 arrest. *Journal of virology*, 84(7), 3320–3330. Am Soc Microbiol.

Bensimon, A. et al. (2010) ATM-Dependent and -Independent Dynamics of the Nuclear Phosphoproteome After DNA Damage. *Science Signaling*, 3(151), rs3–rs3. American Association for the Advancement of Science.

Berndsen, C.E. & Wolberger, C. (2014) New insights into ubiquitin E3 ligase mechanism. *Nature structural & molecular biology*, 21(4), 301. Nature Publishing Group.

Bertoli, C. et al. (2013) Control of cell cycle transcription during G1 and S phases. *Nature Reviews Molecular Cell Biology*, 14(8), 518–528. Nature Publishing Group.

Bharadwaj, R. & Yu, H. (2004) The spindle checkpoint, aneuploidy, and cancer. *Oncogene*, 23(11), 2016–2027. Nature Publishing Group.

Bianconi, E. et al. (2013) An estimation of the number of cells in the human body. *Annals of Human Biology*, 40(6), 463–471. Taylor & Francis.

Biesterfeld, S. et al. (2011) Feulgen Staining Remains the Gold Standard for Precise DNA Image Cytometry. *Anticancer Research*, 31(1), 53–58. International Institute of Anticancer Research.

Blagosklonny, M.V. & Pardee, A.B. (2002) The Restriction Point of the Cell Cycle. *Cell Cycle*, 1(2), 102–109. Taylor & Francis.

Blanchoin, L. et al. (2014) Actin Dynamics, Architecture, and Mechanics in Cell Motility. *Physiological Reviews*, 94(1), 235–263. American Physiological Society.

Blasina, A. et al. (1999) A human homologue of the checkpoint kinase Cds1 directly inhibits Cdc25 phosphatase. *Current Biology*, 9(1), 1–10. Elsevier.

Boehm, J.S. & Hahn, W.C. (2004) Immortalized cells as experimental models to study cancer. *Cytotechnology*, 45(1–2), 47–59.

Bolomey, J.-C. et al. (1995) *Thermoradiotherapy and Thermochemotherapy: Biology, Physiology, Physics*. Springer Science & Business Media.

Borg, N.A. & Dixit, V.M. (2017) Ubiquitin in Cell-Cycle Regulation and Dysregulation in Cancer. *Annual Review of Cancer Biology*, 1(1), 59–77.

Brade, A.M. et al. (2003) Heat-directed suicide gene therapy for breast cancer. *Cancer Gene Therapy*, 10(4), 294–301. Nature Publishing Group.

Brookes, P. (1990) The early history of the biological alkylating agents, 1918–1968. *Mutation Research/Fundamental and Molecular Mechanisms of Mutagenesis*, 233(1), 3–14.

Brookes, P. & Lawley, P. (1961) The reaction of mono- and di-functional alkylating agents with nucleic acids. *Biochemical Journal*, 80(3), 496–503.

Brouhard, G.J. & Rice, L.M. (2018) Microtubule dynamics: an interplay of biochemistry and mechanics. *Nature Reviews Molecular Cell Biology*, 19(7), 451–463. Nature Publishing Group.

Brown, A.L. et al. (1999) A human Cds1-related kinase that functions downstream of ATM protein in the cellular response to DNA damage. *Proceedings of the National Academy of Sciences*, 96(7), 3745–3750. National Academy of Sciences.

Brunton, L.L. et al. (2006) Antineoplastic agents. *Goodman and Gilmans The Pharmacological Basis of Therapeutics, 11th edition, McGrow–Hill Companies, USA*, 1315–1405.

Bryan, A.K. et al. (2010) Measurement of mass, density, and volume during the cell cycle of yeast. *Proceedings of the National Academy of Sciences*, 107(3), 999–1004. National Academy of Sciences.

Bukhari, A.B. et al. (2019) Inhibiting Wee1 and ATR kinases produces tumor-selective synthetic lethality and suppresses metastasis. *The Journal of Clinical Investigation*, 129(3), 1329–1344. American Society for Clinical Investigation.

Burridge, K. et al. (1990) Actin—membrane interaction in focal adhesions. *Cell Differentiation and Development*, 32(3), 337–342.

Cappadocia, L. & Lima, C.D. (2018) Ubiquitin-like Protein Conjugation: Structures, Chemistry, and Mechanism. *Chemical Reviews*, 118(3), 889–918. American Chemical Society.

Castedo, M. et al. (2004) Cell death by mitotic catastrophe: a molecular definition. *Oncogene*, 23(16), 2825–2837. Nature Publishing Group.

Cerami, E. et al. (2012) The cBio Cancer Genomics Portal: An Open Platform for Exploring Multidimensional Cancer Genomics Data. *Cancer Discovery*, 2(5), 401–404. American Association for Cancer Research.

Champoux, J.J. (2001) DNA Topoisomerases: Structure, Function, and Mechanism. *Annual Review of Biochemistry*, 70(1), 369–413.

Chi, X.-Z. et al. (2017) Runx3 plays a critical role in restriction-point and defense against cellular transformation. *Oncogene*, 36(50), 6884–6894. Nature Publishing Group.

Chieco, P. & Derenzini, M. (1999) The Feulgen reaction 75 years on. *Histochemistry and Cell Biology*, 111(5), 345–358.

Cleveland, D.W. et al. (2003) Centromeres and Kinetochores: From Epigenetics to Mitotic Checkpoint Signaling. *Cell*, 112(4), 407–421.

Condeelis, J. & Pollard, J.W. (2006) Macrophages: Obligate Partners for Tumor Cell Migration, Invasion, and Metastasis. *Cell*, 124(2), 263–266.

Cooper, G.M. (2000a) Intermediate Filaments. *The Cell: A Molecular Approach. 2nd edition*. Sinauer Associates. [Accessed: 21 May 2020].

Cooper, G.M. (2000b) The Events of M Phase. *The Cell: A Molecular Approach. 2nd edition*. Sinauer Associates. [Accessed: 16 May 2020].

Cortés, F. & Pastor, N. (2003) Induction of endoreduplication by topoisomerase II catalytic inhibitors. *Mutagenesis*, 18(2), 105–112. Oxford Academic.

Coss, R.A. & Linnemans, W.A.M. (1996) The effects of hyperthermia on the cytoskeleton: a review. *International Journal of Hyperthermia*, 12(2), 173–196. Taylor & Francis.

Cowan, R.A. et al. (2017) Current status and future prospects of hyperthermic intraoperative intraperitoneal chemotherapy (HIPEC) clinical trials in ovarian cancer. *International Journal of Hyperthermia*, 33(5), 548–553. Taylor & Francis.

Cuadrado, M. et al. (2009) p27Kip1 Stabilization Is Essential for the Maintenance of Cell Cycle Arrest in Response to DNA Damage. *Cancer Research*, 69(22), 8726–8732. American Association for Cancer Research.

Datta, N.R. et al. (2015) Local hyperthermia combined with radiotherapy and-/or chemotherapy: Recent advances and promises for the future. *Cancer Treatment Reviews*, 41(9), 742–753.

Datta, N.R. et al. (2020) Integrating Loco-Regional Hyperthermia Into the Current Oncology Practice: SWOT and TOWS Analyses. *Frontiers in Oncology*, 10. Frontiers. [Accessed: 8 September 2020].

Davis, P.K. et al. (2001) Biological methods for cell-cycle synchronization of mammalian cells. *BioTechniques*, 30(6), 1322–1326, 1328, 1330–1331.

De Ruysscher, D. et al. (2019) Radiotherapy toxicity. *Nature Reviews Disease Primers*, 5(1), 1–20. Nature Publishing Group.

DelSal, G. et al. (1996) Cell Cycle and Cancer: Critical Events at the G1 Restriction Point. *Critical Reviews™ in Oncogenesis*, 7(1–2). Begel House Inc. [Accessed: 10 August 2020].

Deol, K.K. et al. (2019) Enzymatic Logic of Ubiquitin Chain Assembly. *Frontiers in Physiology*, 10. [Accessed: 10 August 2020].

Deshaies, R.J. & Joazeiro, C.A.P. (2009) RING Domain E3 Ubiquitin Ligases. *Annual Review of Biochemistry*, 78(1), 399–434.

Dewey, W.C. et al. (1971) Heat-induced lethality and chromosomal damage in synchronized Chinese hamster cells treated with 5-bromodeoxyuridine. *International Journal of Radiation Biology and Related Studies in Physics, Chemistry and Medicine*, 20(6), 505–520. Taylor & Francis.

Diamantis, A. et al. (2008) The contribution of Maria Sklodowska-Curie and Pierre Curie to Nuclear and Medical Physics. A hundred and ten years after the discovery of radium. *Hellenic Journal of Nuclear Medicine*, 11(1), 33–38.

Dickson, J.A. & Calderwood, S.K. (1980) Temperature Range and Selective Sensitivity of Tumors to Hyperthermia: A Critical Review. *Annals of the New York Academy of Sciences*, 335(1), 180–205.

Do, K. et al. (2013) Wee1 kinase as a target for cancer therapy. *Cell Cycle*, 12(19), 3159–3164.

Donjerkovic, D. & Scott, D.W. (2000) Regulation of the G1 phase of the mammalian cell cycle. *Cell Research*, 10(1), 1–16. Nature Publishing Group.

Dunn, A.Y. et al. (2001) Review: Cellular Substrates of the Eukaryotic Chaperonin TRiC/CCT. *Journal of Structural Biology*, 135(2), 176–184.

Dunn, J.M. et al. (1988) Identification of germline and somatic mutations affecting the retinoblastoma gene. *Science*, 241(4874), 1797–1800. American Association for the Advancement of Science.

Eissing, N. et al. (2014) Easy performance of 6-color confocal immunofluorescence with 4-laser line microscopes. *Immunology Letters*, 161(1), 1–5.

Emil Frei, I.I.I. & Eder, J.P. (2003) Combination Chemotherapy. *Holland-Frei Cancer Medicine. 6th edition*. BC Decker. [Accessed: 6 August 2020].

Engelborghs, Y. et al. (1976) Effect of temperature and pressure on polymerisation equilibrium of neuronal microtubules. *Nature*, 259(5545), 686–689. Nature Publishing Group.

Erlandsson, F. et al. (2000) A Detailed Analysis of Cyclin A Accumulation at the G1/S Border in Normal and Transformed Cells. *Experimental Cell Research*, 259(1), 86–95.

Ettinger, A. & Wittmann, T. (2014) Fluorescence Live Cell Imaging. *Methods in cell biology*, 123, 77–94.

Falzone, L. et al. (2018) Evolution of Cancer Pharmacological Treatments at the Turn of the Third Millennium. *Frontiers in Pharmacology*, 9. Frontiers. [Accessed: 4 August 2020].

Fang, Y. & Zhang, X. (2016) Targeting NEK2 as a promising therapeutic approach for cancer treatment. *Cell Cycle*, 15(7), 895–907. Taylor & Francis.

Ferlay, J. et al. (2019) Estimating the global cancer incidence and mortality in 2018: GLOBOCAN sources and methods. *International Journal of Cancer*, 144(8), 1941–1953.

Fletcher, D.A. & Mullins, R.D. (2010) Cell mechanics and the cytoskeleton. *Nature*, 463(7280), 485–492.

Ford, M.J. et al. (2018) A Cell/Cilia Cycle Biosensor for Single-Cell Kinetics Reveals Persistence of Cilia after G1/S Transition Is a General Property in Cells and Mice. *Developmental Cell*, 47(4), 509-523.e5.

Forgacs, G. et al. (2004) Role of the cytoskeleton in signaling networks. *Journal of Cell Science*, 117(Pt 13), 2769–2775.

Fox, D.T. & Duronio, R.J. (2013) Endoreplication and polyploidy: insights into development and disease. *Development*, 140(1), 3–12. Oxford University Press for The Company of Biologists Limited.

Franckena, M. et al. (2009) Hyperthermia dose-effect relationship in 420 patients with cervical cancer treated with combined radiotherapy and hyperthermia. *European Journal of Cancer*, 45(11), 1969–1978.

Freeman, M.L. et al. (1977) Effect of pH on Hyperthermic Cell Survival: Brief Communication. *JNCI: Journal of the National Cancer Institute*, 58(6), 1837–1839. Oxford Academic.

Frey, B. et al. (2012) Old and new facts about hyperthermia-induced modulations of the immune system. *International Journal of Hyperthermia*, 28(6), 528–542. Taylor & Francis.

Fujimoto-Ouchi, K. et al. (2007) Antitumor activity of trastuzumab in combination with chemotherapy in human gastric cancer xenograft models. *Cancer chemotherapy and pharmacology*, 59(6), 795–805. Springer.

Fujita, T. et al. (2008a) Dissection of the APCCdh1-Skp2 Cascade in Breast Cancer. *Clinical Cancer Research*, 14(7), 1966–1975. American Association for Cancer Research.

Fujita, T. et al. (2008b) Regulation of Skp2-p27 Axis by the Cdh1/Anaphase-Promoting Complex Pathway in Colorectal Tumorigenesis. *The American Journal of Pathology*, 173(1), 217–228.

Furrukh, M. (2013) Tobacco Smoking and Lung Cancer. *Sultan Qaboos University Medical Journal*, 13(3), 345–358.

Furusawa, Y. et al. (2012) Inhibition of checkpoint kinase 1 abrogates G2/M checkpoint activation and promotes apoptosis under heat stress. *Apoptosis*, 17(1), 102–112.

Ganem, N.J. et al. (2009) A mechanism linking extra centrosomes to chromosomal instability. *Nature*, 460(7252), 278–282. Nature Publishing Group.

Gas, P. (2017) Essential Facts on the History of Hyperthermia and their Connections with Electromedicine. *arXiv:1710.00652 [physics, q-bio]*. [Accessed: 4 June 2020].

Gavet, O. & Pines, J. (2010) Activation of cyclin B1–Cdk1 synchronizes events in the nucleus and the cytoplasm at mitosis. *Journal of Cell Biology*, 189(2), 247–259. The Rockefeller University Press.

Gianfaldoni, S. et al. (2017) An Overview on Radiotherapy: From Its History to Its Current Applications in Dermatology. *Open Access Macedonian Journal of Medical Sciences*, 5(4), 521–525.

Gilman, A. (1963) The initial clinical trial of nitrogen mustard. *The American Journal of Surgery*, 105(5), 574–578. Elsevier.

Giovinazzi, S. et al. (2013) Targeting mitotic exit with hyperthermia or APC/C inhibition to increase paclitaxel efficacy. *Cell Cycle*, 12(16), 2598–2607.

Giustini, A.J. et al. (2010) MAGNETIC NANOPARTICLE HYPERTHERMIA IN CANCER TREATMENT. *Nano LIFE*, 1(01n02). [Accessed: 6 June 2020].

Godinho, S.A. et al. (2014) Oncogene-like induction of cellular invasion from centrosome amplification. *Nature*, 510(7503), 167–171. Nature Publishing Group.

Goldman, M.J. et al. (2020) Visualizing and interpreting cancer genomics data via the Xena platform. *Nature Biotechnology*, 38(6), 675–678. Nature Publishing Group.

Goodman, M.D. et al. (2016) Chemotherapy for intraperitoneal use: a review of hyperthermic intraperitoneal chemotherapy and early post-operative intraperitoneal chemotherapy. *Journal of Gastrointestinal Oncology*, 7(1), 45–57.

Gori, J. et al. (2005) Intraperitoneal hyperthermic chemotherapy in ovarian cancer. *International Journal of Gynecologic Cancer*, 15(2). BMJ Specialist Journals. [Accessed: 10 September 2020].

Gratzner, H.G. et al. (1975) The use of antibody specific for bromodeoxyuridine for the immunofluorescent determination of DNA replication in single cells and chromosomes. *Experimental Cell Research*, 95(1), 88–94.

Greenwald, E.C. et al. (2018) Genetically Encoded Fluorescent Biosensors Illuminate the Spatiotemporal Regulation of Signaling Networks. *Chemical Reviews*, 118(24), 11707–11794. American Chemical Society.

Grzanka, D. et al. (2008) Hyperthermia-induced reorganization of microtubules and microfilaments and cell killing in CHO AA8 cell line. *Neoplasma*, 55(5), 409–415.

Guest, S.T. et al. (2015) Two members of the TRiC chaperonin complex, CCT2 and TCP1 are essential for survival of breast cancer cells and are linked to driving oncogenes. *Experimental Cell Research*, 332(2), 223–235.

Habash, R.W.Y. et al. (2006a) Thermal Therapy, Part 1: An Introduction to Thermal Therapy. *Critical Reviews™ in Biomedical Engineering*, 34(6), 459–489.

Habash, R.W.Y. et al. (2006b) Thermal Therapy, Part 2: Hyperthermia Techniques. *Critical Reviews™ in Biomedical Engineering*, 34(6). Begel House Inc. [Accessed: 2 July 2020].

Hames, R.S. & Fry, A.M. (2002) Alternative splice variants of the human centrosome kinase Nek2 exhibit distinct patterns of expression in mitosis. *Biochemical Journal*, 361(1), 77–85. Portland Press.

Hanahan, D. & Weinberg, R.A. (2011) Hallmarks of Cancer: The Next Generation. *Cell*, 144(5), 646–674. Elsevier.

Hanks, S. et al. (2004) Constitutional aneuploidy and cancer predisposition caused by biallelic mutations in BUB1B. *Nature Genetics*, 36(11), 1159–1161. Nature Publishing Group.

Hansen, S.D. & Mullins, R.D. (2015) Lamellipodin promotes actin assembly by clustering Ena/VASP proteins and tethering them to actin filaments. *eLife*, 4, e06585. eLife Sciences Publications, Ltd.

Harper, J.W. et al. (2002) The anaphase-promoting complex: it's not just for mitosis any more. *Genes & Development*, 16(17), 2179–2206.

Hastings, J.F. et al. (2020) Analysis of pulsed cisplatin signalling dynamics identifies effectors of resistance in lung adenocarcinoma. *eLife*, 9, e53367. eLife Sciences Publications, Ltd.

Heald, R. & McKeon, F. (1990) Mutations of phosphorylation sites in lamin A that prevent nuclear lamina disassembly in mitosis. *Cell*, 61(4), 579–589.

Hedayatnasab, Z. et al. (2017) Review on magnetic nanoparticles for magnetic nanofluid hyperthermia application. *Materials & Design*, 123, 174–196.

Hedigan, K. (2010) Herbal medicine reduces chemotherapy toxicity. *Nature Reviews Drug Discovery*, 9(10), 765–765. Nature Publishing Group.

Henise, J.C. & Taunton, J. (2011) Irreversible Nek2 kinase inhibitors with cellular activity. *Journal of medicinal chemistry*, 54(12), 4133–4146. ACS Publications.

Herrmann, H. et al. (2002) Functional complexity of intermediate filament cytoskeletons: From structure to assembly to gene ablation. In: Academic Press *International Review of Cytology*. [Online]. Academic Press. Available at: doi:10.1016/S0074-7696(05)23003-6 [Accessed: 21 May 2020].

Hildebrandt, B. & Wust, P. (2007) The Biologic Rationale of Hyperthermia. In: Ceelen, W.P. (ed.) *Peritoneal Carcinomatosis: A Multidisciplinary Approach*. [Online]. Boston, MA: Springer US. Available at: doi:10.1007/978-0-387-48993-3_10 [Accessed: 5 July 2020].

Hirohashi, Y. et al. (1995) Biomodulation by Hyperthermia of Topoisomerase II-Targeting Drugs in Human Colorectal Cancer Cells. *Japanese Journal of Cancer Research : Gann*, 86(11), 1097–1105.

Hoadley, K.A. et al. (2018) Cell-of-origin patterns dominate the molecular classification of 10,000 tumors from 33 types of cancer. *Cell*, 173(2), 291–304. Elsevier.

Hoffmann, I. et al. (1994) Activation of the phosphatase activity of human cdc25A by a cdk2-cyclin E dependent phosphorylation at the G1/S transition. *The EMBO journal*, 13(18), 4302–4310.

Hohmann, T. & Dehghani, F. (2019) The Cytoskeleton—A Complex Interacting Meshwork. *Cells*, 8(4). [Accessed: 10 August 2020].

Hoppe, T. (2005) Multiubiquitylation by E4 enzymes: 'one size' doesn't fit all. *Trends in Biochemical Sciences*, 30(4), 183–187.

Horsman, M.R. & Overgaard, J. (2007) Hyperthermia: a Potent Enhancer of Radiotherapy. *Clinical Oncology*, 19(6), 418–426.

Houtgraaf, J.H. et al. (2006) A concise review of DNA damage checkpoints and repair in mammalian cells. *Cardiovascular Revascularization Medicine*, 7(3), 165–172.

Hu, Q. et al. (2016) Recent Advances of Cocktail Chemotherapy by Combination Drug Delivery Systems. *Advanced drug delivery reviews*, 98, 19–34.

Huang, C.-Y. et al. (2017) A review on the effects of current chemotherapy drugs and natural agents in treating non–small cell lung cancer. *Biomedicine*, 7(4). EDP Sciences.

Huang, S. & Ingber, D.E. (2002) A Discrete Cell Cycle Checkpoint in Late G1 That Is Cytoskeleton-Dependent and MAP Kinase (Erk)-Independent. *Experimental Cell Research*, 275(2), 255–264.

Hulshof, M.C.C.M. et al. (2009) Preoperative chemoradiation combined with regional hyperthermia for patients with resectable esophageal cancer. *International Journal of Hyperthermia*, 25(1), 79–85. Taylor & Francis.

Humphreys, B.D. (2015) Cutting to the chase: taking the pulse of label-retaining cells in kidney. *American Journal of Physiology - Renal Physiology*, 308(1), F29–F30.

Ibrahim, N. et al. (2012) Molecular targeted therapies for cancer: sorafenib mono-therapy and its combination with other therapies (review). *Oncology Reports*, 27(5), 1303–1311.

Jackson, S.P. & Bartek, J. (2009) The DNA-damage response in human biology and disease. *Nature*, 461(7267), 1071–1078. Nature Publishing Group.

Jensen, E.C. (2013) Overview of Live-Cell Imaging: Requirements and Methods Used. *The Anatomical Record*, 296(1), 1–8.

Jeong, Y. et al. (2007) Characterization of NIP2/centrobin, a novel substrate of Nek2, and its potential role in microtubule stabilization. *Journal of Cell Science*, 120(12), 2106–2116. The Company of Biologists Ltd.

Jia, D. & Liu, J. (2010) Current devices for high-performance whole-body hyperthermia therapy. *Expert Review of Medical Devices*, 7(3), 407–423. Taylor & Francis.

Jitariu, A.-A. et al. (2017) Triple negative breast cancer: the kiss of death. *Oncotarget*, 8(28), 46652–46662.

Job, D. et al. (2003) Microtubule nucleation. *Current Opinion in Cell Biology*, 15(1), 111–117.

Jongmans, W. et al. (1997) Nijmegen breakage syndrome cells fail to induce the p53-mediated DNA damage response following exposure to ionizing radiation. *Molecular and Cellular Biology*, 17(9), 5016–5022. American Society for Microbiology Journals.

Kaaij, R.T. van der et al. (2017) Treatment of Peritoneal Dissemination in Stomach Cancer Patients With Cytoreductive Surgery and Hyperthermic Intraperitoneal Chemotherapy (HIPEC): Rationale and Design of the PERISCOPE Study. *JMIR Research Protocols*, 6(7), e136.

Kampinga, H.H. (1995) Hyperthermia, thermotolerance and topoisomerase II inhibitors. *British Journal of Cancer*, 72(2), 333–338.

Kaneko, K. & Yomo, T. (1994) Cell division, differentiation and dynamic clustering. *Physica D: Nonlinear Phenomena*, 75(1), 89–102.

Kang, C.-D. & Kim, S.-H. (2016) Effects of Regional Hyperthermia with Moderate Temperature on Cancer Treatment. 생명과학회지, 26(9), 1088–1096.

Khanna, A. (2015) DNA Damage in Cancer Therapeutics: A Boon or a Curse? *Cancer Research*, 75(11), 2133–2138. American Association for Cancer Research.

Kim, B.M. et al. (2015) Therapeutic Implications for Overcoming Radiation Resistance in Cancer Therapy. *International Journal of Molecular Sciences*, 16(11), 26880–26913.

Kim, K.H. & Sederstrom, J.M. (2015) Assaying cell cycle status using flow cytometry. *Current protocols in molecular biology / edited by Frederick M. Ausubel ... [et al.]*, 111, 28.6.1-28.6.11.

Kim, S.-T. et al. (1999) Substrate Specificities and Identification of Putative Substrates of ATM Kinase Family Members. *Journal of Biological Chemistry*, 274(53), 37538–37543. American Society for Biochemistry and Molecular Biology.

Kittaneh, M. et al. (2013) Molecular Profiling for Breast Cancer: A Comprehensive Review. *Biomarkers in Cancer*, 5, BIC.S9455. SAGE Publications Ltd STM.

Klymkowsky, M.W. (2019) Filaments and phenotypes: cellular roles and orphan effects associated with mutations in cytoplasmic intermediate filament proteins. *F1000Research*, 8. [Accessed: 10 August 2020].

Knox, S.S. (2010) From 'omics' to complex disease: a systems biology approach to gene-environment interactions in cancer. *Cancer Cell International*, 10, 11.

Kodera, N. & Ando, T. (2014) The path to visualization of walking myosin V by high-speed atomic force microscopy. *Biophysical Reviews*, 6(3), 237–260.

Kokuryo, T. et al. (2007) Nek2 as an effective target for inhibition of tumorigenic growth and peritoneal dissemination of cholangiocarcinoma. *Cancer Research*, 67(20), 9637–9642. AACR.

Koole, S. et al. (2020) Primary cytoreductive surgery with or without hyperthermic intraperitoneal chemotherapy (HIPEC) for FIGO stage III epithelial ovarian cancer: OVHIPEC-2, a phase III randomized clinical trial. *International Journal of Gynecologic Cancer*, 30(6). BMJ Specialist Journals.

Kramer, E.R. et al. (2000) Mitotic Regulation of the APC Activator Proteins CDC20 and CDH1. *Molecular Biology of the Cell*, 11(5), 1555–1569. American Society for Cell Biology (mboc).

Lamouille, S. et al. (2014) Molecular mechanisms of epithelial–mesenchymal transition. *Nature Reviews Molecular Cell Biology*, 15(3), 178–196. Nature Publishing Group.

Latt, S.A. (1974) DETECTION OF DNA SYNTHESIS IN INTERPHASE NUCLEI BY FLUORESCENCE MICROSCOPY. *The Journal of Cell Biology*, 62(2), 546–550.

Lavoie, J.N. et al. (1996) Cyclin D1 Expression Is Regulated Positively by the p42/p44MAPK and Negatively by the p38/HOGMAPK Pathway. *Journal of Biological Chemistry*, 271(34), 20608–20616. American Society for Biochemistry and Molecular Biology.

Lee, H.O. et al. (2009) Endoreplication: polyploidy with purpose. *Genes & Development*, 23(21), 2461–2477.

Levine, M.S. et al. (2017) Centrosome Amplification Is Sufficient to Promote Spontaneous Tumorigenesis in Mammals. *Developmental Cell*, 40(3), 313-322.e5.

Levitsky, D.I. et al. (2008) Thermal unfolding and aggregation of actin. *The FEBS Journal*, 275(17), 4280–4295.

Lind, M.J. (2008) Principles of cytotoxic chemotherapy. *Medicine*, 36(1), 19–23.

Lindahl, T. & Barnes, D.E. (2000) Repair of Endogenous DNA Damage. *Cold Spring Harbor Symposia on Quantitative Biology*, 65, 127–134. Cold Spring Harbor Laboratory Press.

Little, M.P. (2010) Cancer models, genomic instability and somatic cellular Darwinian evolution. *Biology Direct*, 5(1), 19.

Liu, B. et al. (2015) Protecting the normal in order to better kill the cancer. *Cancer Medicine*, 4(9), 1394–1403.

Liu, Q. et al. (2000) Chk1 is an essential kinase that is regulated by Atr and required for the G2/M DNA damage checkpoint. *Genes & Development*, 14(12), 1448–1459.

Lohez, O.D. et al. (2003) Arrest of mammalian fibroblasts in G1 in response to actin inhibition is dependent on retinoblastoma pocket proteins but not on p53. *Journal of Cell Biology*, 161(1), 67–77. The Rockefeller University Press.

Longo, T.A. et al. (2016) A systematic review of regional hyperthermia therapy in bladder cancer. *International Journal of Hyperthermia*, 32(4), 381–389. Taylor & Francis.

Lundberg, A.S. & Weinberg, R.A. (1998) Functional inactivation of the retinoblastoma protein requires sequential modification by at least two distinct cyclin-cdk complexes. *Molecular and cellular biology*, 18(2), 753–761. Am Soc Microbiol.

Maccarini, P.F. et al. (2004) *Optimization of a dual concentric conductor antenna for superficial hyperthermia applications*. In: The 26th Annual International Conference of the IEEE Engineering in Medicine and Biology Society. Sep, 2004. Available at: doi:10.1109/IEMBS.2004.1403725

Mahmoudi, K. et al. (2018) Magnetic hyperthermia therapy for the treatment of glioblastoma: a review of the therapy's history, efficacy and application in humans. *International Journal of Hyperthermia*, 34(8), 1316–1328. Taylor & Francis.

Majka, J. & Burgers, P.M.J. (2004) The PCNA–RFC Families of DNA Clamps and Clamp Loaders. In: Academic Press *Progress in Nucleic Acid Research and Molecular Biology*. [Online]. Academic Press. Available at: doi:10.1016/S0079-6603(04)78006-X [Accessed: 7 May 2020].

Malumbres, M. & Barbacid, M. (2001) To cycle or not to cycle: a critical decision in cancer. *Nature Reviews Cancer*, 1(3), 222–231. Nature Publishing Group.

Malumbres, M. & Barbacid, M. (2009) Cell cycle, CDKs and cancer: a changing paradigm. *Nature Reviews Cancer*, 9(3), 153–166. Nature Publishing Group.

Manchado, E. et al. (2010) Targeting Mitotic Exit Leads to Tumor Regression In Vivo: Modulation by Cdk1, Mastl, and the PP2A/B55α,δ Phosphatase. *Cancer Cell*, 18(6), 641–654.

Mantso, T. et al. (2018) Hyperthermia induces therapeutic effectiveness and potentiates adjuvant therapy with non-targeted and targeted drugs in an in vitro model of human malignant melanoma. *Scientific Reports*, 8(1), 10724.

Maréchal, A. & Zou, L. (2013) DNA Damage Sensing by the ATM and ATR Kinases. *Cold Spring Harbor Perspectives in Biology*, 5(9). [Accessed: 25 May 2020].

Markovsky, E. et al. (2018) Phosphorylation state of Ser165 in α-tubulin is a toggle switch that controls proliferating human breast tumors. *Cellular Signalling*, 52, 74–82.

Masui, K. et al. (2013) A tale of two approaches: complementary mechanisms of cytotoxic and targeted therapy resistance may inform next-generation cancer treatments. *Carcinogenesis*, 34(4), 725–738.

Matheson, C.J. et al. (2016) Targeting WEE1 Kinase in Cancer. *Trends in Pharmacological Sciences*, 37(10), 872–881. Elsevier.

Matsuoka, S. et al. (1998) Linkage of ATM to Cell Cycle Regulation by the Chk2 Protein Kinase. *Science*, 282(5395), 1893–1897. American Association for the Advancement of Science.

McGarry, T.J. & Kirschner, M.W. (1998) Geminin, an Inhibitor of DNA Replication, Is Degraded during Mitosis. *Cell*, 93(6), 1043–1053.

McGowan, C.H. & Russell, P. (2004) The DNA damage response: sensing and signaling. *Current Opinion in Cell Biology*, 16(6), 629–633.

McHugh, B. & Heck, M.M. (2003) Regulation of chromosome condensation and segregation. *Current Opinion in Genetics & Development*, 13(2), 185–190.

McKinley, K.L. & Cheeseman, I.M. (2016) The molecular basis for centromere identity and function. *Nature Reviews Molecular Cell Biology*, 17(1), 16–29. Nature Publishing Group.

McKinnon, K.M. (2018) Flow Cytometry: An Overview. *Current protocols in immunology*, 120, 5.1.1-5.1.11.

Mei, Z. et al. (2012) *Counting leukocytes from whole blood using a lab-on-a-chip Coulter counter*. In: 2012 Annual International Conference of the IEEE Engineering in Medicine and Biology Society. Aug, 2012. Available at: doi:10.1109/EMBC.2012.6347429

Melchionna, R. et al. (2000) Threonine 68 is required for radiation-induced phosphorylation and activation of Cds1. *Nature Cell Biology*, 2(10), 762–765. Nature Publishing Group.

Metcalf, J.L. et al. (2014) K63-ubiquitylation of VHL by SOCS1 mediates DNA double-strand break repair. *Oncogene*, 33(8), 1055–1065. Nature Publishing Group.

Mitchison, T.J. (2012) The proliferation rate paradox in antimitotic chemotherapy. *Molecular Biology of the Cell*, 23(1), 1–6. American Society for Cell Biology (mboc).

Morgan, D.O. (1995) Principles of CDK regulation. *Nature*, 374(6518), 131–134. Nature Publishing Group.

Morgan, D.O. (1997) CYCLIN-DEPENDENT KINASES: Engines, Clocks, and Microprocessors. *Annual Review of Cell and Developmental Biology*, 13(1), 261–291.

Morgan, D.O. & Roberts, J.M. (2002) Oscillation sensation. *Nature*, 418(6897), 495–496. Nature Publishing Group.

Morise, H. et al. (1974) Intermolecular energy transfer in the bioluminescent system of Aequorea. *Biochemistry*, 13(12), 2656–2662.

Mort, R.L. et al. (2014a) Fucci2a: A bicistronic cell cycle reporter that allows Cre mediated tissue specific expression in mice. *Cell Cycle*, 13(17), 2681–2696. Taylor & Francis.

Mort, R.L. et al. (2014b) Fucci2a: A bicistronic cell cycle reporter that allows Cre mediated tissue specific expression in mice. *Cell Cycle*, 13(17), 2681–2696.

Morten, B.C. et al. (2016) Comparison of Three Different Methods for Determining Cell Proliferation in Breast Cancer Cell Lines. *Journal of Visualized Experiments : JoVE*, (115). [Accessed: 17 July 2020].

Mu, C. et al. (2018) Chemotherapy Sensitizes Therapy-Resistant Cells to Mild Hyperthermia by Suppressing Heat Shock Protein 27 Expression in Triple-Negative Breast Cancer. *Clinical Cancer Research*, 24(19), 4900–4912. American Association for Cancer Research.

Muir, B. & Nunney, L. (2015) The expression of tumour suppressors and proto-oncogenes in tissues susceptible to their hereditary cancers. *British Journal of Cancer*, 113(2), 345–353. Nature Publishing Group.

Murray, A. (1993) *The cell cycle: an introduction*.

Murshid, A. et al. (2011) Heat shock proteins and cancer vaccines: developments in the past decade and chaperoning in the decade to come. *Expert Review of Vaccines*, 10(11), 1553–1568. Taylor & Francis.

Musacchio, A. & Hardwick, K.G. (2002) The spindle checkpoint: structural insights into dynamic signalling. *Nature Reviews Molecular Cell Biology*, 3(10), 731–741. Nature Publishing Group.

Musgrove, E.A. (2006) Cyclins: Roles in mitogenic signaling and oncogenic transformation. *Growth Factors*, 24(1), 13–19. Taylor & Francis.

Musgrove, E.A. et al. (2011) Cyclin D as a therapeutic target in cancer. *Nature Reviews Cancer*, 11(8), 558–572. Nature Publishing Group.

Nagy, J.A. et al. (2009) Why are tumour blood vessels abnormal and why is it important to know? *British Journal of Cancer*, 100(6), 865–869. Nature Publishing Group.

Nakayama, K.I. & Nakayama, K. (2005) *Regulation of the cell cycle by SCF-type ubiquitin ligases*. In: Elsevier, 2005. Elsevier.

Nicholls, S.B. et al. (2011) Mechanism of a Genetically Encoded Dark-to-Bright Reporter for Caspase Activity. *Journal of Biological Chemistry*, 286(28), 24977–24986. American Society for Biochemistry and Molecular Biology.

Nicholls, S.B. & Hardy, J.A. (2013) Structural basis of fluorescence quenching in caspase activatable-GFP. *Protein Science : A Publication of the Protein Society*, 22(3), 247–257.

North, A.J. (2006) Seeing is believing? A beginners' guide to practical pitfalls in image acquisition. *The Journal of Cell Biology*, 172(1), 9–18.

Nurgali, K. et al. (2018) Editorial: Adverse Effects of Cancer Chemotherapy: Anything New to Improve Tolerance and Reduce Sequelae? *Frontiers in Pharmacology*, 9. [Accessed: 6 August 2020].

Nurse, P. (2000) A Long Twentieth Century of the Cell Cycle and Beyond. *Cell*, 100(1), 71–78. Elsevier.

O., B. et al. (2009) Lysine 269 is essential for cyclin D1 ubiquitylation by the SCFFbx4/αB-crystallin ligase and subsequent proteasome-dependent degradation. *Oncogene*, 28(49), 4317–4325.

O'Connell, M.J. et al. (1997) Chk1 is a wee1 kinase in the G2 DNA damage checkpoint inhibiting cdc2 by Y15 phosphorylation. *The EMBO journal*, 16(3), 545–554.

Ohguri, T. et al. (2018) Relationships between thermal dose parameters and the efficacy of definitive chemoradiotherapy plus regional hyperthermia in the treatment of locally advanced cervical cancer: data from a multicentre randomised clinical trial. *International Journal of Hyperthermia*, 34(4), 461–468. Taylor & Francis.

Ohnishi, K. (2016) Thermo-Tolerance. In: Kokura, S. et al. (eds.) *Hyperthermic Oncology from Bench to Bedside*. [Online]. Singapore: Springer. Available at: doi:10.1007/978-981-10-0719-4_7 [Accessed: 5 July 2020].

Ondracka, A. et al. (2018) Decoupling of Nuclear Division Cycles and Cell Size during the Coenocytic Growth of the Ichthyosporean Sphaeroforma arctica. *Current Biology*, 28(12), 1964-1969.e2.

Ormerod, M.G. & Imrie, P.R. (1990) Flow Cytometry. In: Walker, J.M. et al. (eds.) *Animal Cell Culture* Methods in Molecular Biology. [Online]. Totowa, NJ: Humana Press. Available at: doi:10.1385/0-89603-150-0:543 [Accessed: 27 July 2020].

Otto, T. & Sicinski, P. (2017) Cell cycle proteins as promising targets in cancer therapy. *Nature Reviews Cancer*, 17(2), 93–115.

Overlack, K. et al. (2014) When Mad met Bub. *EMBO Reports*, 15(4), 326–328.

Pagano, M. et al. (1992) Cyclin A is required at two points in the human cell cycle. *The EMBO journal*, 11(3), 961–971. John Wiley & Sons, Ltd.

Pardee, A.B. (1974) A restriction point for control of normal animal cell proliferation. *Proceedings of the National Academy of Sciences of the United States of America*, 71(4), 1286–1290.

Patel, S.R. et al. (2005) The biogenesis of platelets from megakaryocyte proplatelets. *Journal of Clinical Investigation*, 115(12), 3348–3354.

Pawlik, A. et al. (2013a) Hyperthermia induces cytoskeletal alterations and mitotic catastrophe in p53-deficient H1299 lung cancer cells. *Acta Histochemica*, 115(1), 8–15.

Pawlik, A. et al. (2013b) Hyperthermia induces cytoskeletal alterations and mitotic catastrophe in p53-deficient H1299 lung cancer cells. *Acta Histochemica*, 115(1), 8–15.

Payrastre, B. et al. (1991) Phosphoinositide kinase, diacylglycerol kinase, and phospholipase C activities associated to the cytoskeleton: effect of epidermal growth factor. *Journal of Cell Biology*, 115(1), 121–128. The Rockefeller University Press.

Peter, M. et al. (1990) In vitro disassembly of the nuclear lamina and M phase-specific phosphorylation of lamins by cdc2 kinase. *Cell*, 61(4), 591–602. Elsevier.

Petersen, B.O. et al. (2000) Cell cycle– and cell growth–regulated proteolysis of mammalian CDC6 is dependent on APC–CDH1. *Genes & Development*, 14(18), 2330–2343.

Pickart, C.M. (2001) Mechanisms Underlying Ubiquitination. *Annual Review of Biochemistry*, 70(1), 503–533.

Pihan, G.A. (2013) Centrosome Dysfunction Contributes to Chromosome Instability, Chromoanagenesis, and Genome Reprograming in Cancer. *Frontiers in Oncology*, 3. [Accessed: 9 September 2020].

Pommier, Y. (2013) Drugging Topoisomerases: Lessons and Challenges. *ACS Chemical Biology*, 8(1), 82–95. American Chemical Society.

Porter, A.T. et al. (1995) Brachytherapy for prostate cancer. *CA: A Cancer Journal for Clinicians*, 45(3), 165–178. American Cancer Society.

Potten, C.S. & Loeffler, M. (1990) Stem cells: attributes, cycles, spirals, pitfalls and uncertainties. Lessons for and from the crypt. *Development*, 110(4), 1001–1020. The Company of Biologists Ltd.

Prasedya, E.S. et al. (2016) Carrageenan delays cell cycle progression in human cancer cells in vitro demonstrated by FUCCI imaging. *BMC Complementary and Alternative Medicine*, 16(1), 270.

Prasher, D.C. et al. (1992) Primary structure of the Aequorea victoria green-fluorescent protein. *Gene*, 111(2), 229–233.

Price, K.M. et al. (2016) Proliferation by Many Other Names: Monitoring Cell Cycle Progression and Cell Division by Flow Cytometry. *Cytometry. Part A : the journal of the International Society for Analytical Cytology*, 89(3), 233–235.

Pritchard, J.R. et al. (2012) Understanding resistance to combination chemotherapy. *Drug Resistance Updates*, 15(5), 249–257.

Quaresma, M. et al. (2015) 40-year trends in an index of survival for all cancers combined and survival adjusted for age and sex for each cancer in England and Wales, 1971-2011: a population-based study. *Lancet (London, England)*, 385(9974), 1206–1218.

Quintá, H.R. et al. (2011) Management of cytoskeleton architecture by molecular chaperones and immunophilins. *Cellular Signalling*, 23(12), 1907–1920.

Rajagopalan, H. & Lengauer, C. (2004) Aneuploidy and cancer. *Nature*, 432(7015), 338–341. Nature Publishing Group.

Ralhan, R. & Kaur, J. (2007) Alkylating agents and cancer therapy. *Expert Opinion on Therapeutic Patents*, 17(9), 1061–1075. Taylor & Francis.

Reichl, E.M. et al. (2008) Interactions between myosin and actin crosslinkers control cytokinesis contractility dynamics and mechanics. *Current biology: CB*, 18(7), 471–480.

Riihimäki, M. et al. (2013) Comparison of survival of patients with metastases from known versus unknown primaries: survival in metastatic cancer. *BMC Cancer*, 13, 36.

Ringborg, U. et al. (2003) The Swedish Council on Technology Assessment in Health Care (SBU) systematic overview of radiotherapy for cancer including a prospective survey of radiotherapy practice in Sweden 2001--summary and conclusions. *Acta Oncologica (Stockholm, Sweden)*, 42(5–6), 357–365.

Rockwell, N.C. et al. (2006) PHYTOCHOME STRUCTURE AND SIGNALING MECHANISMS. *Annual review of plant biology*, 57, 837–858.

Rockwell, S. et al. (2009) Hypoxia and radiation therapy: Past history, ongoing research, and future promise. *Current molecular medicine*, 9(4), 442–458.

ROJAS, K. & STUCKEY, A. (2016) Breast Cancer Epidemiology and Risk Factors. *Clinical Obstetrics and Gynecology*, 59(4), 651–672.

Romar, G.A. et al. (2016) Research Techniques Made Simple: Techniques to Assess Cell Proliferation. *Journal of Investigative Dermatology*, 136(1), e1–e7.

Roostalu, J. & Surrey, T. (2017) Microtubule nucleation: beyond the template. *Nature Reviews Molecular Cell Biology*, 18(11), 702–710. Nature Publishing Group.

Rubin, S.M. (2013) Deciphering the retinoblastoma protein phosphorylation code. *Trends in Biochemical Sciences*, 38(1), 12–19.

Ryan, S.D. et al. (2012) Up-regulation of the mitotic checkpoint component Mad1 causes chromosomal instability and resistance to microtubule poisons. *Proceedings of the National Academy of Sciences*, 109(33), E2205–E2214. National Academy of Sciences.

Sacristan, C. et al. (2018) Dynamic kinetochore size regulation promotes microtubule capture and chromosome biorientation in mitosis. *Nature Cell Biology*, 20(7), 800–810. Nature Publishing Group.

Sage, J. et al. (2000) Targeted disruption of the three Rb-related genes leads to loss of G1 control and immortalization. *Genes & Development*, 14(23), 3037–3050.

Sakaue-Sawano, A. et al. (2008) Visualizing Spatiotemporal Dynamics of Multicellular Cell-Cycle Progression. *Cell*, 132(3), 487–498.

Sakaue-Sawano, A. et al. (2011) Drug-induced cell cycle modulation leading to cell-cycle arrest, nuclear mis-segregation, or endoreplication. *BMC Cell Biology*, 12(1), 2.

Sakaue-Sawano, A. et al. (2017) Genetically encoded tools for optical dissection of the mammalian cell cycle. *Molecular cell*, 68(3), 626–640. Elsevier.

Salmon, E.D. et al. (1994) High resolution multimode digital imaging system for mitosis studies in vivo and in vitro. *The Biological Bulletin*, 187(2), 231–232. Marine Biological Laboratory.

Sankari, S.L. et al. (2012) Apoptosis in cancer-an update. *Asian Pac J Cancer Prev*, 13(10), 4873–4878.

Santra, M.K. et al. (2009) F-box protein FBXO31 mediates cyclin D1 degradation to induce G1 arrest after DNA damage. *Nature*, 459(7247), 722–725. Nature Publishing Group.

Savitsky, K. et al. (1995) A single ataxia telangiectasia gene with a product similar to PI-3 kinase. *Science*, 268(5218), 1749–1753. American Association for the Advancement of Science.

Schiff, H. (1866) Eine neue Reihe organischer Diamine; *Justus Liebigs Annalen der Chemie*, 140(1), 92–137. John Wiley & Sons, Ltd.

Schorl, C. & Sedivy, J.M. (2007) Analysis of Cell Cycle Phases and Progression in Cultured Mammalian Cells. *Methods (San Diego, Calif.)*, 41(2), 143–150.

Sergent-Tanguy, S. et al. (2003) Fluorescent activated cell sorting (FACS): a rapid and reliable method to estimate the number of neurons in a mixed population. *Journal of Neuroscience Methods*, 129(1), 73–79.

Sever, R. & Brugge, J.S. (2015) Signal Transduction in Cancer. *Cold Spring Harbor Perspectives in Medicine*, 5(4). [Accessed: 3 July 2020].

Seyfried, T.N. & Huysentruyt, L.C. (2013) On the Origin of Cancer Metastasis. *Critical reviews in oncogenesis*, 18(1–2), 43–73.

Shamovsky, I. & Nudler, E. (2008) New insights into the mechanism of heat shock response activation. *Cellular and Molecular Life Sciences*, 65(6), 855–861.

Shan, J. et al. (2009) Suppression of Cancer Cell Growth by Promoting Cyclin D1 Degradation. *Molecular Cell*, 36(3), 469–476.

Shcherbakova, D.M. & Verkhusha, V.V. (2013) Near-infrared fluorescent proteins for multicolor in vivo imaging. *Nature methods*, 10(8), 751–754.

Sher, N. et al. (2013) Fundamental differences in endoreplication in mammals and Drosophila revealed by analysis of endocycling and endomitotic cells. *Proceedings of the National Academy of Sciences of the United States of America*, 110(23), 9368–9373.

Smith, A. (2020) *Economic burden of cancer costs UK £7.6bn a year*. PharmaTimes Media Limited. Available at: http://www.pharmatimes.com/news/economic_burden_of_cancer_costs_uk_7.6bn_a_year_1321994 [Accessed: 9 April 2020].

Song, C.W. et al. (2001) Improvement of Tumor Oxygenation by Mild Hyperthermia. *Radiation Research*, 155(4), 515–528. Allen Press.

Sørensen, C.S. et al. (2003) Chk1 regulates the S phase checkpoint by coupling the physiological turnover and ionizing radiation-induced accelerated proteolysis of Cdc25A. *Cancer Cell*, 3(3), 247–258.

Staal, J. et al. (2018) *Engineering a Minimal 1185 Bp Cloning Vector from a Puc18 Plasmid Backbone with an Extended Multiple Cloning Site*.

Staal, J. et al. (2019) Engineering a minimal cloning vector from a pUC18 plasmid backbone with an extended multiple cloning site. *BioTechniques*, 66(6), 254–259. Future Science.

Swaney, D.L. et al. (2013) Global analysis of phosphorylation and ubiquitylation cross-talk in protein degradation. *Nature Methods*, 10(7), 676–682. Nature Publishing Group.

Tang, L. et al. (2018) Role of metabolism in cancer cell radioresistance and radiosensitization methods. *Journal of Experimental & Clinical Cancer Research : CR*, 37. [Accessed: 11 August 2020].

Thorn, K. (2017) Genetically encoded fluorescent tags. *Molecular Biology of the Cell*, 28(7), 848–857.

Thornton, B.R. & Toczyski, D.P. (2003) Securin and B-cyclin/CDK are the only essential targets of the APC. *Nature Cell Biology*, 5(12), 1090–1094. Nature Publishing Group.

Tohme, S. et al. (2017) Surgery for Cancer: A Trigger for Metastases. *Cancer Research*, 77(7), 1548–1552. American Association for Cancer Research.

Toraya-Brown, S. et al. (2013) Phagocytes mediate targeting of iron oxide nanoparticles to tumors for cancer therapy. *Integrative Biology*, 5(1), 159–171. Oxford Academic.

Toufektchan, E. & Toledo, F. (2018) The Guardian of the Genome Revisited: p53 Downregulates Genes Required for Telomere Maintenance, DNA Repair, and Centromere Structure. *Cancers*, 10(5). [Accessed: 7 May 2020].

Umar, A. et al. (1996) Requirement for PCNA in DNA Mismatch Repair at a Step Preceding DNA Resynthesis. *Cell*, 87(1), 65–73.

Umar, A. & Kunkel, T.A. (1997) DNA-replication fidelity, mismatch repair and genome instability in cancer cells. In: Christen, P. & Hofmann, E. (eds.) *EJB Reviews 1996* EJB Reviews. [Online]. Berlin, Heidelberg: Springer. Available at: doi:10.1007/978-3-642-60659-5_9 [Accessed: 7 May 2020].

Vakifahmetoglu, H. et al. (2008) Death through a tragedy: mitotic catastrophe. *Cell Death & Differentiation*, 15(7), 1153–1162. Nature Publishing Group.

Vasiliadou, R. (2020) Virtual laboratories during coronavirus (COVID-19) pandemic. *Biochemistry and Molecular Biology Education*. Wiley Online Library.

Vembadi, A. et al. (2019) Cell cytometry: review and perspective on biotechnological advances. *Frontiers in Bioengineering and Biotechnology*, 7. Frontiers Media SA.

Vermeulen, K. et al. (2003) The cell cycle: a review of regulation, deregulation and therapeutic targets in cancer. *Cell Proliferation*, 36(3), 131–149.

Voellmy, R. (1994) Transduction of the stress signal and mechanisms of transcriptional regulation of heat shock/stress protein gene expression in higher eukaryotes. *Critical Reviews in Eukaryotic Gene Expression*, 4(4), 357–401.

Vorsanova, S.G. et al. (2010) Human interphase chromosomes: a review of available molecular cytogenetic technologies. *Molecular Cytogenetics*, 3(1), 1.

Walczak, C.E. et al. (2010) Mechanisms of chromosome behaviour during mitosis. *Nature Reviews Molecular Cell Biology*, 11(2), 91–102. Nature Publishing Group.

Walter, H.S. & Ahmed, S. (2018) Targeted therapies in cancer. *Surgery (Oxford)*, 36(3), 122–127.

Wang, K. et al. (2010) In vivo imaging of tumor apoptosis using histone H1-targeting peptide. *Journal of Controlled Release*, 148(3), 283–291.

Wang, S. et al. (2011) Abnormal expression of Nek2 and β-catenin in breast carcinoma: clinicopathological correlations. *Histopathology*, 59(4), 631–642.

Watmough, D.J. & Ross, W.M. (1986) Hyperthermia: Clinical and scientific aspects. *Blackie and Son, Glasgow*.

Weaver, B.A. (2014) How Taxol/paclitaxel kills cancer cells. *Molecular Biology of the Cell*, 25(18), 2677–2681.

Wilson, M.H. et al. (2007) PiggyBac Transposon-mediated Gene Transfer in Human Cells. *Molecular Therapy*, 15(1), 139–145.

Wordeman, L. (2010) How Kinesin Motor Proteins Drive Mitotic Spindle Function: Lessons from Molecular Assays. *Seminars in cell & developmental biology*, 21(3), 260–268.

Wright, P. et al. (2019) Differential expression of cyclin-dependent kinases in the adult human retina in relation to CDK inhibitor retinotoxicity. *Archives of Toxicology*, 93(3), 659–671.

Yano, S. et al. (2014) Selective methioninase-induced trap of cancer cells in S/G2 phase visualized by FUCCI imaging confers chemosensitivity. *Oncotarget*, 5(18), 8729–8736.

Yu, H. (2002) Regulation of APC–Cdc20 by the spindle checkpoint. *Current Opinion in Cell Biology*, 14(6), 706–714.

Yusa, K. et al. (2011) A hyperactive piggyBac transposase for mammalian applications. *Proceedings of the National Academy of Sciences*, 108(4), 1531–1536. National Acad Sciences.

Zagar, T.M. et al. (2010) Hyperthermia for locally advanced breast cancer. *International journal of hyperthermia : the official journal of European Society for Hyperthermic Oncology, North American Hyperthermia Group*, 26(7), 618–624.

van der Zee, J. (2002) Heating the patient: a promising approach? *Annals of Oncology*, 13(8), 1173–1184.

Zhou, B.-B.S. & Elledge, S.J. (2000) The DNA damage response: putting checkpoints in perspective. *Nature*, 408(6811), 433–439. Nature Publishing Group.

Zhu, S. et al. (2015) Culture at a Higher Temperature Mildly Inhibits Cancer Cell Growth but Enhances Chemotherapeutic Effects by Inhibiting Cell-Cell Collaboration. *PLOS ONE*, 10(10), e0137042.